

000
001
002
003
004
005
006
007
008
009
010
011
012
013
014
015
016
017
018
019
020
021
022
023
024
025
026
027
028
029
030
031
032
033
034
035
036
037
038
039
040
041
042
043
044
045
046
047
048
049
050
051
052
053

DECOUPLED Q-CHUNKING

Anonymous authors

Paper under double-blind review

ABSTRACT

Bootstrapping bias problem is a long-standing challenge in temporal-difference (TD) methods in off-policy reinforcement learning (RL). Multi-step return backups can alleviate this issue but require delicate importance sampling to correct their off-policy bias. Recent work has proposed to use chunked critics, which estimate the value of short action sequences (“chunks”) rather than individual actions, enabling unbiased multi-step backup. However, extracting policies from chunked critics is challenging: policies must output the entire action chunk open-loop, which can be sub-optimal in environments that require policy reactivity and also challenging to model especially when the chunk length grows. Our key insight is to decouple the chunk length of the critic from that of the policy, allowing the policy to operate over shorter action chunks. We propose a novel algorithm that achieves this by optimizing the policy against a distilled critic for partial action chunks, constructed by optimistically backing up from the original chunked critic to approximate the maximum value achievable when a partial action chunk is extended to a complete one. This design retains the benefits of multi-step value propagation while sidestepping both the open-loop sub-optimality and the difficulty of learning policies over long action chunks. We evaluate our method on challenging, long-horizon offline goal-conditioned benchmarks and **show** that it reliably outperforms prior methods.

1 INTRODUCTION

A reinforcement learning (RL) agent can in principle solve any task with a well-defined reward function, but training an RL agent from scratch can be sample inefficient. In many practical problems, we have access to an offline dataset of trajectories that serves as a great prior to accelerate learning. Temporal-difference (TD)-based RL algorithms, which learn a value network to perform approximate dynamic programming via value backups, are particularly suitable in this setting because they are designed to handle off-policy data. A well-known yet long-lasting bottleneck, however, is the bootstrapping bias problem (Jaakkola et al., 1993; Sutton et al., 1998; De Asis et al., 2018; Park et al., 2025)—as the value network regresses towards its own estimates, any error compounds across time steps, making accurate value propagation challenging especially in long-horizon, sparse reward tasks.

Multi-step return backups (such as n -step return (Sutton et al., 1998)) can alleviate bootstrapping bias by effectively reducing the time horizon, but naïvely applying them can result in another form of bias that causes the value estimates to be overly conservative/pessimistic. While it is possible to correct such systematic biases with importance sampling (Munos et al., 2016), they often require additional heuristics and truncations to balance a delicate scale between bias and variance which is often tricky to tune. Recent works (Seo & Abbeel, 2024; Li et al., 2025a; Tian et al., 2025; Li et al., 2025b) leverage chunked value functions, which estimate the value of short action sequences (“chunks”) rather than a single action. This formulation allows n -step return backup without the pessimistic bias (under the open-loop consistency condition, which we will formalize in Section 4). However, directly optimizing a policy over full action chunks is difficult, particularly as the chunk size grows, and it is still unclear how to best extract a policy from a chunked critic.

In this work, we develop a simple, novel technique to address this challenge. We train a policy to predict a shorter, partial action chunk using the chunked critic that takes in longer, complete action chunks. The key idea enabling this approach is a ‘distilled’ chunked critic with a chunk size that matches the policy: it optimistically regresses to the original chunked critic to approximate the maximum value that the partial action chunk can achieve after being extended into a full action chunk. Conceptually, while optimization is still performed for the longer, complete action chunks, the policy

network is only trained to output the partial action chunk of an optimized complete action chunk. This way, the policy only needs to predict a much shorter action chunk (e.g., in the extreme case, only one action), which often admits a much simpler distribution, while enjoying the value learning benefits from the use of chunked critics.

Our main contributions are two-fold. On the theoretical side, we provide a formal analysis of Q-learning with action chunking, identifying the open-loop value learning bias and characterizing the conditions under which action chunking critic backup is preferable over n -step return backup with a single-step critic. On the empirical side, we propose a novel technique, **Decoupled Q-chunking (DQC)**, that addresses the policy learning challenge in action chunking Q-learning by decoupling the policy chunk size from the critic chunk size. DQC trains a policy to only predict a partial action chunk, significantly reducing the policy learning challenge, while retaining the value learning benefits of the chunked critic. We instantiate this technique as a practical offline RL algorithm that outperforms the previous state-of-the-art method on the hardest set of environments in OGBench (Park et al., 2024a), a challenging, long-horizon goal-conditioned RL benchmark.

2 RELATED WORK

Offline and offline-to-online reinforcement learning methods assume access to an offline dataset to learn a policy without interactions with the environment (offline) (Kumar et al., 2020; Kostrikov et al., 2021; Tarasov et al., 2024) or with as little online interaction with the environment as possible (offline-to-online) (Lee et al., 2022; Ball et al., 2023; Nakamoto et al., 2024). TD-based RL algorithms have been a popular choice for these problem settings as they naturally handle off-policy data while requiring no on-policy rollouts, and they also exhibit good online sample-efficiency (Chen et al., 2021; D’Oro et al., 2022). A large body of literature in these areas has been focusing on tackling the distribution shift challenge by appropriately constraining the policies with respect to the prior offline data, and most of them use the standard 1-step TD backup for Q-learning, which has been known to suffer from the bootstrapping bias problem in the RL literature (Jaakkola et al., 1993; Sutton et al., 1998). To tackle this, recent work (Jeong et al., 2022; Park & Lee, 2024; Park et al., 2025; Li et al., 2025b) has shown that multi-step return backups are effective for improving offline/offline-to-online Q-learning agents. These methods either use a standard single-step critic network (Park et al., 2025) that suffers from the off-policy bias, or use a ‘chunked,’ multi-step critic network (Li et al., 2025b) that does not have such bias but poses a huge policy learning challenge when the chunk size is too large. Our method brings the best of both worlds—it uses action chunking to avoid the off-policy bias while simultaneously avoiding the policy learning challenge by extracting a simpler policy that predicts a shorter action chunk from the full-chunk-sized critic.

Multi-step return backups are computed with multi-step off-policy rewards that can lead to systematic value underestimation (Sutton et al., 1998; Peng & Williams, 1994; Konidaris et al., 2011; Thomas et al., 2015), and there has been a rich literature (Precup et al., 2000; Munos et al., 2016; Rowland et al., 2020) dedicated to fix these biases via importance sampling (Kloek & Van Dijk, 1978) with truncation (Ionides, 2008). These approaches often require a careful balance between bias and variance that can be tricky to tune. More recently, Seo & Abbeel (2024); Li et al. (2025a); Tian et al. (2025); Li et al. (2025b) group temporally extended sequences of actions as chunks and directly estimate the value of an action chunk rather than a single action. Such a formulation allows the value backup to operate directly in the chunk space, which allows multi-step return backup without the systematic biases from the sub-optimal off-policy data. Despite their empirical success, we still lack a good theoretical understanding of the convergence of TD-learning with ‘chunked’ critics, as well as when it should be favored over more traditional multi-step returns. Our work lays out the theoretical foundation for Q-learning with critic chunking, and identifies an important yet subtle, often overlooked bias in the TD-backup. We quantify such bias and provide the condition under which TD backup using critic chunking is guaranteed to perform better than the standard n -step return backup with a single-step critic.

See additional discussions for related work in hierarchical reinforcement learning in Appendix I.

3 PRELIMINARIES

Reinforcement learning can be formalized as a Markov decision process, $\mathcal{M} = (\mathcal{S}, \mathcal{A}, T, r, \rho, \gamma)$, where \mathcal{S} is the state space, \mathcal{A} is the action space, $T : \mathcal{S} \times \mathcal{A} \rightarrow \Delta_{\mathcal{A}}$ is the transition kernel that defines the next state distribution conditioned on the current state and the current action (e.g., $s' \sim T(\cdot | s, a)$), $r : \mathcal{S} \times \mathcal{A} \rightarrow [0, 1]$ is the reward function, $\rho \in \Delta_{\mathcal{S}}$ is the initial state distribution,

108 and $\gamma \in [0, 1]$ is the discount factor. We also assume we have access to a prior offline dataset
 109 $D = \{(s_0^i, a_0^i, r_0^i, s_1^i, a_1^i, r_1^i, \dots, s_H^i)\}_{i=1}^{|D|}$ where the goal is to learn a policy, $\pi : \mathcal{S} \rightarrow \Delta_{\mathcal{A}}$ that
 110 maximizes its return, $\eta(\pi) = \mathbb{E}_{s_{t+1} \sim T(\cdot|s_t, a_t), a_t \sim \pi(\cdot|s_t), s_0 \sim \rho} [\sum_{t=0}^{\infty} \gamma^t r(s_t, a_t)]$, the cumulative
 111 discounted sum of rewards that the policy receives in expectation.
 112

113 **Temporal difference learning.** Modern value-based reinforcement learning methods often learn a
 114 critic network, $Q : \mathcal{S} \times \mathcal{A} \rightarrow \mathbb{R}$ to approximate the maximum discounted cumulative reward starting
 115 from state s and action a , and the critic is often trained using the temporal-difference (TD) loss:

$$116 \quad L(\phi) = \mathbb{E}_{s, a, s' \sim \mathcal{D}} [(Q_{\phi}(s, a) - r(s, a) - \gamma \bar{Q}(s', a'^*))^2], \quad (1)$$

117 where \bar{Q} is the target critic that is set to the same critic with its parameters set to an exponential
 118 moving average of ϕ , and $a'^* = \arg \max_{a'} Q(s', a')$ (often approximated by a policy π_{θ}).
 119

120 **Implicit value learning with implicit maximization loss function.** Instead of using $Q(s', a'^*) \sim$
 121 $\pi_{\theta}(s')$ as the TD target, we can use what we refer to as an *implicit maximization* loss function f_{imp}
 122 to learn a value function $V_{\xi}(s)$ that approximates the maximum value $Q(s, a^*)$ (Kostrikov et al.,
 2021; Hansen-Estruch et al., 2023):
 123

$$124 \quad L(\xi) = \mathbb{E}_{s, a \sim \mathcal{D}} [f_{\text{imp}}^{\kappa}(\bar{Q}(s, a) - V_{\xi}(s))]. \quad (2)$$

125 Two popular choices of f_{imp}^{κ} are (1) expectile: $f_{\text{expectile}}^{\kappa}(c) = |\kappa - \mathbb{I}_{c < 0}|c^2$, and (2) quantile:
 126 $f_{\text{quantile}}^{\kappa}(c) = |\kappa - \mathbb{I}_{c < 0}|c|$, for any real value $\kappa \in [0.5, 1)$. At the optimum of $L(\xi)$, $V_{\xi}(s)$
 127 approximates the κ -expectile/quantile of the distribution of the critic values evaluated at $Q(s, a)$,
 128 induced by the data distribution \mathcal{D} . With this implicit maximization technique, we no longer need to
 129 explicitly find the action a that maximizes $Q(s, a)$ and can use $V_{\xi}(s)$ as the backup target:
 130

$$130 \quad L(\phi) = \mathbb{E}_{s, a, s' \sim \mathcal{D}} [(Q_{\phi}(s, a) - r(s, a) - \gamma V_{\xi}(s'))^2]. \quad (3)$$

131 **Multi-step return backup.** TD learning can sometimes struggle with long-horizon tasks due to
 132 the well-known bootstrapping bias problem, where regressing the value network towards its own
 133 potentially inaccurate value estimates amplifies the value estimation errors further. To tackle this
 134 challenge, we can instead sample a trajectory segment, $(s_t, a_t, s_{t+1}, \dots, a_{t+n-1}, s_{t+n})$, to construct
 135 an n -step return backup target from states h steps ahead:
 136

$$137 \quad L_{\text{ns}}(\phi) = \mathbb{E}_{s_t, a_t, \dots, s_{t+n}} [(Q_{\phi}(s_t, a_t) - R_{t:t+n} - \gamma^n \bar{Q}(s_{t+n}, a_{t+n}^*))^2], \quad (4)$$

138 where $a_{t+n}^* = \arg \max_{a_{t+n}} Q(s_{t+n}, a_{t+n})$, $R_{t:t+n} := \sum_{t'=t}^{t+n-1} \gamma^{t'-t} r(s_{t'}, a_{t'})$. The n -step return
 139 value estimate of reduces the effective horizon by a factor of n , alleviating the bootstrapping bias
 140 problem. However, such value estimate is always biased towards the off-policy data distribution, and
 141 is also commonly referred to as the *uncorrected n-step return estimator* (Fedus et al., 2020; Kozuno
 142 et al., 2021). While there are ways to correct this value estimator via importance sampling (Precup
 143 et al., 2000; Munos et al., 2016; Rowland et al., 2020), they require additional tricks (e.g., importance
 144 ratio truncation) for numerical stability and re-introduce biases into the estimator, ultimately resulting
 145 in a delicate trade-off between variances and biases that must be carefully balanced.
 146

147 **Action chunking critic.** Alternatively, one may learn an action chunking critic to estimate the
 148 value of a short sequence of actions, $a_{t:t+h} := (a_t, a_{t+1}, \dots, a_{t+h-1})$ (or an *action chunk*) instead:
 149 $Q(s_t, a_{t:t+h})$ (Seo & Abbeel, 2024; Li et al., 2025a; Tian et al., 2025; Li et al., 2025b). The TD
 150 backup loss for such a critic is naturally multi-step:
 151

$$151 \quad L_{\text{QC}}(\phi) = \mathbb{E}_{s_{t+h+1}, a_{t:t+h}} [(Q_{\phi}(s_t, a_{t:t+h}) - R_{t:t+h} - \gamma^h \bar{Q}(s_{t+h}, a_{t+h:t+2h}^*))^2], \quad (5)$$

152 where again $a_{t+h:t+2h}^* = \arg \max_{a_{t+h:t+2h}} Q(s_{t+h}, a_{t+h:t+2h})$. On the one hand, unlike n -step
 153 return estimate for single-action critic that is pessimistic, the n -step return estimate (with $n = h$)
 154 for the action chunking critic is *unbiased* as long as the action chunk $a_{t:t+h}$ is *independent* of the
 155 intermediate states $s_{t+1:t+h+1}$, while enjoying the reduction in effective horizon (Li et al., 2025a;b).
 156 On the other hand, action chunking critic implicitly imposes a constraint on the policy that the actions
 157 are predicted and executed in chunks. As a result, the policy extracted from the action chunking critic
 158 needs to predict the entire action chunk all at once, posing a big learning challenge, especially for
 159 environments with complex transition dynamics.
 160

161 In the following two sections, we offer theoretical insights that characterize the conditions when using
 162 action chunking critic is more preferable over n -step return backup with a single critic (Section 4), and
 163 develop a practical method that tackles the action chunking policy extraction challenge (Section 5).
 164

162 4 WHEN SHOULD WE USE ACTION CHUNKING FOR Q-LEARNING?
163

164 In this section, we build a theoretical foundation for Q-learning with action chunking critic functions.
 165 We start by formalizing the setup of our analysis in Section 4.1, quantifying the value estimation bias
 166 incurred from backing up on non-action chunking data (Theorem 4.4) and the optimality of action
 167 chunking policy (Theorem 4.6) in Section 4.2. Using these result, we derive the condition under which
 168 we prefer action chunking Q-learning over the standard n -step return learning in Section 4.3. We
 169 also include some examples in which the condition holds in Appendix F.5 in the hope of facilitating
 170 theoretical analysis of action chunking policy learning in future work.
 171

172 4.1 ASSUMPTIONS
173

174 To build the foundation of our analysis, we start by describing the trajectory data distribution that we
 175 use for Q-learning and the trajectory distribution induced by an open-loop action chunking policy. In
 176 particular, we assume that the trajectory data distribution obeys the transition dynamics T :
 177

178 **Assumption 4.1** (Data Distribution Obeys Dynamics). $\mathcal{D} \in \Delta_{\mathcal{T}}$ is a trajectory distribution generated
 179 by rolling out a behavior policy from a distribution of $s_t \sim \mu$. The behavior policy can be non-
 180 Markovian (i.e., $\pi_{\beta}(a_{t+k} \mid s_{t+k+1}, a_{t+k})$). Each subsequent state is generated obeying the
 181 dynamics of the MDP \mathcal{M} : $s_{t+k+1} \sim T(\cdot \mid s_{t+k}, a_{t+k}), \forall k \in \{0, 1, \dots, h-1\}$. The resulting
 182 trajectory is $\{s_t, s_{t+1}, \dots, s_{t+h}, a_t, a_{t+1}, \dots, a_{t+h}\} \in \mathcal{T} = \mathcal{S}^h \times \mathcal{A}^h$.
 183

184 Next, we formally define the open-loop trajectory distribution that we would obtain if we take the
 185 same actions in the data and roll them out open-loop in the environment.
 186

187 **Definition 4.2** (Open-loop Trajectory). From any trajectory distribution \mathcal{D} , we can extract an open-
 188 loop policy with a horizon of h by marginalizing out all intermediate states. We use $\pi_{\mathcal{D}}^{\circ} : \mathcal{S} \rightarrow \Delta_{\mathcal{A}^h}$
 189 to denote such policy which is formally defined as:
 190

$$\pi_{\mathcal{D}}^{\circ}(a_{t:t+h} \mid s_t) := P_{\mathcal{D}}(a_{t:t+h} \mid s_t). \quad (6)$$

191 By using this open-loop policy to roll-out trajectories in the MDP \mathcal{M} , it induces a trajectory
 192 distribution $P_{\mathcal{D}}^{\circ} \in \Delta_{\mathcal{S}^{h+1}, \mathcal{A}^h}$ that is generally different from \mathcal{D} . We can decompose this open-loop
 193 policy step-by-step with the following factorization $\pi_{\mathcal{D}}^{\circ}(a_{t:t+k} \mid s_t) = \prod_{k=0}^{h-1} \pi_{\mathcal{D}}^{\circ}(a_{t+k} \mid s_t, a_{t:t+k})$
 194 which allows us to define the induced trajectory distribution $P_{\mathcal{D}}^{\circ}$ recursively (for $k \in \{1, 2, \dots, h\}$):
 195

$$P_{\mathcal{D}}^{\circ}(s_{t+k}, a_{t:t+k} \mid s_t) := \quad (7)$$

$$P_{\mathcal{D}}^{\circ}(s_{t+k-1}, a_{t:t+k-1} \mid s_t) T(s_{t+k} \mid s_{t+k-1}, a_{t+k-1}) \pi_{\mathcal{D}}^{\circ}(a_{t+k} \mid s_t, a_{t:t+k}). \quad (8)$$

196 4.2 OPEN-LOOP VALUE BIAS OF ACTION CHUNKING Q-LEARNING
197

198 As what we have elucidated in our definition above, replaying the actions from the trajectory data
 199 distribution $P_{\mathcal{D}}$ in an open-loop manner, in general, can result in a different trajectory distribution,
 200 $P_{\mathcal{D}}^{\circ}$. This discrepancy between $P_{\mathcal{D}}^{\circ}$ and $P_{\mathcal{D}}$ has not been carefully analyzed by prior work (e.g., Q-
 201 chunking (Li et al., 2025b)) but can play a huge role in the optimal policy that action chunking Q-
 202 learning converges to. This is because TD-backup is only unbiased when it is done under the open-
 203 loop trajectory distribution $P_{\mathcal{D}}^{\circ}$. Naively running TD-backup on $P_{\mathcal{D}}$ (as done in Li et al. (2025b))
 204 may lead to a biased Q-target. We now formalize the discrepancy and analyze such bias.
 205

206 **Definition 4.3** (Open-Loop Consistency). \mathcal{D} is ε_h -open-loop consistent if for every $s_t \in \mathcal{S}, h' \in \{1, \dots, h\}$, as long as $s_t \in \mathcal{S}$ has non-zero probability in the data (i.e., $P_{\mathcal{D}}(s_t) > 0$),
 207

$$D_{\text{TV}}(P_{\mathcal{D}}^{\circ}(s_{t+h'}, a_{t+h'} \mid s_t) \parallel P_{\mathcal{D}}(s_{t+h'}, a_{t+h'} \mid s_t)) \leq \varepsilon_h, \forall h' \in \{1, 2, \dots, h-1\}, \quad (9)$$

$$D_{\text{TV}}(P_{\mathcal{D}}^{\circ}(s_{t+h} \mid s_t) \parallel P_{\mathcal{D}}(s_{t+h} \mid s_t)) \leq \varepsilon_h. \quad (10)$$

208 We say \mathcal{D} is strongly ε_h -open-loop consistent if additionally for $h' \in \{1, 2, \dots, h\}$, for every
 209 $a_{t:t+h} \in \mathcal{A}^h$ with non-zero probability in the data (i.e., $P_{\mathcal{D}}(a_{t:t+h}, s_t) > 0$),
 210

$$D_{\text{TV}}(T(s_{t+h'} \mid s_t, a_{t:t+h'}) \parallel P_{\mathcal{D}}(s_{t+h'} \mid s_t, a_{t:t+h})) \leq \varepsilon_h. \quad (11)$$

211 Intuitively, \mathcal{D} is ε -open-loop consistent if, when executing the same sequence of actions from it open-
 212 loop from s_t , the resulting marginal distribution of the state-action h steps into the future (i.e., s_{t+h})
 213 deviates from the corresponding distribution in the dataset by at most ε in total variation distance.
 214 The strong version (Equation (11)) requires the total variation distance bound to hold for every action
 215

sequence in the support, whereas the weak version (Equation (9)) only requires the bound to hold in expectation. Having *weak* open-loop consistency of \mathcal{D} is sufficient to show that *behavior* value iteration of an action chunking critic results in a *nominal* value function with a bounded bias from the true value of the open-loop policy $\pi_{\mathcal{D}}^{\circ}$:

Theorem 4.4 (Bias of Action Chunking Critic). *Let $\hat{V}_{\text{ac}} : \mathcal{S} \rightarrow [0, 1/(1-\gamma)]$ be a solution of*

$$\hat{V}_{\text{ac}}(s_t) = \mathbb{E}_{s_{t+1:t+h+1}, a_{t:t+h} \sim P_{\mathcal{D}}(\cdot|s_t)} \left[R_{t:t+h} + \gamma^h \hat{V}_{\text{ac}}(s_{t+h}) \right], \quad (12)$$

with $R_{t:t+h} = \sum_{t'=t}^{t+h} \gamma^{t'-t} r(s_{t'}, a_{t'})$ and V_{ac} is the true value of $\pi_{\mathcal{D}}^{\circ} : s_t \mapsto P_{\mathcal{D}}(a_{t:t+h} | s_t)$. If \mathcal{D} is ε_h -open-loop consistent, then under $\text{supp}(\mathcal{D})$,

$$\|V_{\text{ac}} - \hat{V}_{\text{ac}}\|_{\infty} \leq \frac{\varepsilon_h \gamma}{(1 - (1 - \varepsilon_h) \gamma^h)(1 - \gamma)} \leq \frac{\varepsilon_h}{(1 - \gamma^h)(1 - \gamma)}. \quad (13)$$

The proof of Theorem 4.4 is available in Appendix G.2. We also show this bound is tight in Appendix F.1. A direct consequence of this result is that the true value of the optimal action chunking policy is close to that of the optimal closed-loop policy:

Corollary 4.5 (Optimal Action Chunking Policy). *Let $\pi^* : \mathcal{S} \rightarrow \Delta_{\mathcal{A}}$ be an optimal policy in \mathcal{M} and \mathcal{D}^* be the data collected by π^* . If \mathcal{D}^* is ε_h -open-loop consistent, then under $\text{supp}(\mathcal{D}^*)$,*

$$\|V_{\text{ac}}^* - V^*\|_{\infty} \leq \|\tilde{V}_{\text{ac}} - V^*\|_{\infty} \leq \frac{\varepsilon_h \gamma}{(1 - (1 - \varepsilon_h) \gamma^h)(1 - \gamma)} \leq \frac{\varepsilon_h}{(1 - \gamma^h)(1 - \gamma)}, \quad (14)$$

where V^ is the value of the optimal policy π^* , V_{ac}^* is the true value of the optimal action chunking policy, and \tilde{V}_{ac} is the true value of the action chunking policy from cloning the data \mathcal{D}^* :*

$$\tilde{\pi}_{\text{ac}}(a_{t:t+h} | s_t) : s_t \mapsto P_{\mathcal{D}^*}(\cdot | s_t). \quad (15)$$

We again show that this bound is tight in Appendix F.2. The proof of Corollary 4.5 (available in Appendix G.4) builds on the observation that the nominal (biased) value of the action chunking critic obtained from behavior value iteration on an optimal data \mathcal{D}^* (i.e., the data collected from an optimal policy π^*) recovers the value of the optimal policy. This allows us to use Theorem 4.4 to show that the value of the action chunking policy obtained by behavior cloning on such optimal data is close to the nominal (biased) value of its critic, and thus close to the optimal value of the closed-loop policy.

Next, we analyze the performance of the action chunking policy obtained by Q-learning. In particular, we analyze the Q-function obtained as a solution of the following equation under $\text{supp}(\mathcal{D})$:

$$\hat{Q}_{\text{ac}}^+(s_t, a_{t:t+h}) = \mathbb{E}_{s_{t+1:t+h+1} \sim P_{\mathcal{D}}(\cdot|s_t, a_{t:t+h})} \left[R_{t:t+h} + \gamma^h \max_{a_{t+h:t+2h}} \hat{Q}_{\text{ac}}^+(s_{t+h}, a_{t+h:t+2h}) \right]. \quad (16)$$

The corresponding action chunking policy is

$$\pi_{\text{ac}}^+ : s_t \mapsto \arg \max_{a_{t:t+h}} \hat{Q}_{\text{ac}}^+(s_t, a_{t:t+h}). \quad (17)$$

It turns out that with the weak version of the open-loop consistent condition, the worst case performance of the action chunking policy may be arbitrarily low (see an example in Appendix H). Fortunately, as long as the data \mathcal{D} satisfies the strongly open-loop consistency (Equation (11)), we can show that the learned policy π_{ac}^+ is provably near-optimal by combining all the results above together:

Theorem 4.6 (Q-Learning with Action Chunking Policy on Off-policy Data). *If \mathcal{D} is strongly ε_h -open-loop consistent and $\text{supp}(\mathcal{D}) \supseteq \text{supp}(\mathcal{D}^*)$, with \mathcal{D}^* being the data distribution of an arbitrary optimal policy π^* under \mathcal{M} , then the following bound holds under $\text{supp}(\mathcal{D}^*)$:*

$$\|V_{\text{ac}}^+ - V^*\|_{\infty} \leq \frac{\varepsilon_h \gamma}{1 - \gamma} \left[\frac{2}{1 - (1 - 2\varepsilon_h) \gamma^h} + \frac{1}{1 - (1 - \varepsilon_h) \gamma^h} \right] \leq \frac{3\varepsilon_h}{(1 - \gamma)(1 - \gamma^h)}. \quad (18)$$

where V^* is the value of an optimal policy under \mathcal{M} .

This bound is also tight (as shown in Appendix F.3). The implication of Theorem 4.6 (proof available in Appendix G.6) is that as long as \mathcal{D} satisfies the strongly open-loop consistency condition and contains the behavior in \mathcal{D}^* , Q-learning with action chunking is guaranteed to converge to a near-optimal action chunking policy regardless of how sub-optimal the data \mathcal{D} might be. As we will show in the following section, this is in contrast to n -step return policy where its performance depends on the sub-optimality of the data.

270 4.3 COMPARING TO n -STEP RETURN Q-LEARNING
271

272 We now characterize the condition when action chunking Q-learning should be preferred over the
273 standard n -step return backup. We start by introducing a notion of sub-optimality of the data \mathcal{D} :

274 **Definition 4.7** (Sub-optimal data). \mathcal{D} is δ_n -suboptimal for backup horizon length $n \in \mathbb{N}^+$ if

$$275 \quad Q^*(s_t, a_t) - \mathbb{E}_{P_{\mathcal{D}}(\cdot|s_t, a_t)} [R_{t:t+n} + \gamma^n V^*(s_{t+n})] \geq \delta_n, \forall s_t \in \mathcal{S}, a_t \in \mathcal{A}. \quad (19)$$

276 Intuitively, δ_n captures how much worse the n -step return policy can get compared to the optimal
277 policy incurred by the backup bias. Under such condition, we can show that the action chunking
278 policy is provably better than the n -step return policy as long as δ_n is large.
279

280 **Theorem 4.8.** Let \mathcal{D} be strongly ε_h -open-consistent, δ_n -suboptimal, and $\text{supp}(\mathcal{D}) \supseteq \text{supp}(\mathcal{D}^*)$. Let
281 π_n^* be the optimal n -step return policy learned from \mathcal{D} , as the solution of

$$282 \quad Q_n^*(s_t, a_t) = \mathbb{E}_{P_{\mathcal{D}}} [R_{t:t+n} + \gamma^n Q_n^*(s_{t+n}, \pi_n^*(s_{t+n}))], \quad \pi_n^*: s_t \mapsto \arg \max_{a_t} Q_n^*(s_t, a_t). \quad (20)$$

283 As long as $\delta_n > \frac{3\varepsilon_h(1-\gamma^n)}{(1-\gamma)(1-\gamma^h)}$, then from all $s \in \text{supp}(\mathcal{D}^*)$, the action chunking policy, π_{ac}^+ (Equation
284 (17)), is better than the n -step return policy, π_n (Equation (20)) (i.e., $V_{\text{ac}}^+(s) > V_n^*(s)$).

285 The proof of Theorem 4.8 is available in Appendix G.9. Notably, for $n = h$, the condition on δ_n and
286 ε_h reduces to $\delta_n > 3\varepsilon_h H$ with effective horizon H (i.e., $H = 1/(1-\gamma)$). As long as \mathcal{D} is more than
287 $O(\varepsilon_h H)$ sub-optimal, the action chunking policy performs provably better than n -step return policy.
288

289 4.4 CLOSED-LOOP EXECUTION OF ACTION CHUNKING POLICY

290 Under the same strongly ε_h -open-loop consistency assumption, we can guarantee that closed-loop
291 execution of the action chunking policy is also near-optimal. This is based on the intuition that in order
292 for action chunking policy to be near-optimal, the first action in the chunk cannot be too sub-optimal:
293

294 **Proposition 4.9** (Optimality of Closed-loop Execution of Action Chunking Policy). Let V^* be the
295 value of the one-step policy, π^* , defined as the closed-loop execution of the action chunking policy
296 π_{ac}^+ learned from \mathcal{D} . That is, for each $s_t \in \text{supp}(P_{\mathcal{D}}(s_t))$,

$$297 \quad \pi^*(s_t) = a_t^+, \quad \text{where } a_{t:t+h}^+ = \pi_{\text{ac}}^+(s_t). \quad (21)$$

298 If we assume \mathcal{D} and \mathcal{D}^* are both strongly ε_h -open-loop consistent and $\text{supp}(P_{\mathcal{D}}(s_t, a_{t:t+h})) \supseteq$
299 $\text{supp}(P_{\mathcal{D}^*}(s_t, a_{t:t+h}))$, then under $\text{supp}(\mathcal{D}^*)$,

$$300 \quad \|V^* - V^*\|_{\infty} \leq \frac{\varepsilon_h \gamma}{(1-\gamma)^2} \left[\frac{2}{1 - (1-2\varepsilon_h)\gamma^h} + \frac{1}{1 - (1-\varepsilon_h)\gamma^h} \right] \leq \frac{3\varepsilon_h}{(1-\gamma)^2(1-\gamma^h)}. \quad (22)$$

301 The proof is available in Appendix G.8. This result demonstrates that closed-loop execution is also
302 near-optimal as long as the action chunking policy is near-optimal, though we might have to pay up to
303 a horizon factor H (i.e., $1/(1-\gamma)$) in sub-optimality gap in the worst case. Can we do better than this?
304

305 In practical applications, the data distributions that we are dealing with often have more structures.
306 For example, it is common to have a dataset consisting of multiple sources where each data source is
307 collected by either human expert or scripted policy that exhibits a somewhat predictable behavior
308 (e.g., after a robot arm picks up a cube, it will always move up rather than dropping it right away).
309 We formalize this kind of structure as the notion of optimality variability:
310

311 **Definition 4.10** (Optimality Variability). We say \mathcal{D} exhibits ϑ_h -variability in optimality conditioned
312 on an event X if

$$313 \quad \max_{\text{supp}(P_{\mathcal{D}}(\cdot|X))} [R_{t:t+h} + \gamma^h V^*(s_{t+h})] - \min_{\text{supp}(P_{\mathcal{D}}(\cdot|X))} [R_{t:t+h} + \gamma^h V^*(s_{t+h})] \leq \vartheta_h. \quad (23)$$

314 See more discussion of this the definition in Appendix J. We can now formalize our results as follows:
315

316 **Theorem 4.11** (Closed-loop AC Policy under Bounded OV). Let \mathcal{D}^* be the data distribution col-
317 lected by an optimal policy. Assume \mathcal{D} can be decomposed into a mixture of data distributions
318 $\{\mathcal{D}^*, \mathcal{D}_1, \mathcal{D}_2, \dots, \mathcal{D}_N\}$ such that each data distribution component satisfies Assumption 4.1 and for
319 some $\vartheta_h^L, \vartheta_h^G \geq 0$, they satisfy the following two conditions:
320

321 **1. Locally bounded optimality variability condition:** every \mathcal{D}_i (including \mathcal{D}^*) exhibits ϑ_h^L -bounded
322 variability in optimality conditioned on s_t, a_t for all $(s_t, a_t) \in \text{supp}(P_{\mathcal{D}_i}(s_t, a_t))$, and
323

324 **2. Globally bounded optimality variability condition:** \mathcal{D} as a whole exhibits ϑ_h^G -variability in
 325 optimality conditioned on $s_t, a_{t:t+h}$ for all $(s_t, a_{t:t+h}) \in \text{supp}(P_{\mathcal{D}}(s_t, a_{t:t+h}))$.
 326

327 Then for all $s_t \in \text{supp}(P_{\mathcal{D}^*}(s_t))$,

$$328 \quad V^*(s_t) - V^{\bullet}(s_t) \leq \frac{\vartheta_h^L}{1-\gamma} + \frac{\vartheta_h^G + \gamma^h \min(\vartheta_h^L, \vartheta_h^G)}{(1-\gamma)(1-\gamma^h)} \leq \vartheta_h^L H + 2\vartheta_h^G H \bar{H} \quad (24)$$

331 This bound is also tight up to the exact value (as shown in Appendix F.4). It is worth noting that
 332 although the global optimality variability condition looks similar to the strong open-loop consistency
 333 condition, they have completely different properties. For instance, a nearly strong open-loop consistent
 334 data distribution \mathcal{D} can have unbounded global optimality variability and a data distribution that
 335 exhibits zero optimality variability can also have large open-loop inconsistency. The implication of
 336 this is that even when the closed-loop execution of an action chunking policy is near-optimal, the same
 337 action chunking policy executed in chunks can be very sub-optimal (formalized in Appendix F.4).
 338 Furthermore, executing the first action of the original action chunk also brings practical benefits: it
 339 removes the need to explicitly train a policy to predict the full action chunk all at once, which is hard
 340 when the chunk size grows big. Can we develop a practical method that realizes such potential?

341 5 DECOUPLED Q-CHUNKING

343 We propose a new algorithm that enjoys the benefits of value backup speedup of Q-chunking while
 344 avoiding the difficulty of learning an open-loop action chunking policy with a large chunk size.

345 Our core idea is to decouple the chunk size of the critic from that of the policy. In particular, we train a
 346 policy $\pi(a_{t:t+h_a} | s_t)$ to output an action chunk (with a size of $h_a \ll h$) with the following objective:

$$347 \quad L(\pi) := -\mathbb{E}_{a_{t:t+h_a} \sim \pi(\cdot | s_t)} [Q_{\phi}(s, [a_{t:t+h_a}, a_{t+h_a:t+h}^*])], \quad (25)$$

349 where $[a_{t:t+h_a}, a_{t+h_a:t+h}^*]$ represents the concatenation of two partial action chunks (size h_a and size
 350 $h - h_a$) into a full action chunk $a_{t:t+h}$ of size h , and $a_{t+h_a:t+h}^*$ is the best ‘second-half’ of the action
 351 chunk that maximizes the critic value under Q_{ϕ} :

$$352 \quad a_{t+h_a:t+h}^* := \arg \max_{a_{t+h_a:t+h}} Q_{\phi}(s, [a_{t:t+h_a}, a_{t+h_a:t+h}]). \quad (26)$$

354 Essentially, we want our policy to predict the partial action chunk (of size h_a) within an optimal
 355 action chunk of size h , rather than the entire optimal action chunk. This lowers the policy expressivity
 356 requirement and hence the learning challenges associated with it with $h_a < h$.

357 However, directly optimizing this objective (Equation (25)) does not lead to a novel algorithm because
 358 taking the maximization over $a_{t+h_a:t+h}$ seemingly requires us to learn a policy of the original chunk
 359 size anyways. To address this issue, we learn a separate partial critic Q_{ψ}^P , which only takes in the
 360 partial action chunk (of size h_a) as input, to approximate the maximum value this partial action chunk
 361 can achieve when it is extended to the full action chunk (of size h):

$$362 \quad Q_{\psi}^P(s, a_{t:t+h_a}) \approx Q_{\phi}(s, [a_{t:t+h_a}, a_{t+h_a:t+h}^*]) \quad (27)$$

364 To train Q_{ψ}^P , we can use an *implicit maximization* loss function (as described in Equation (2)):

$$366 \quad L(\psi) := f_{\text{imp}}^{\kappa_d}(\bar{Q}_{\phi}(s_t, a_{t:t+h}) - Q_{\psi}^P(s_t, a_{t:t+h})), \quad (28)$$

367 where $s_t, a_{t:t+h}$ are sampled from \mathcal{D} . As a result, the partial critic, Q_{ψ}^P , is distilled from
 368 the original critic via an optimistic regression, where its optimum $Q_{\psi}^P(s, a_{t:t+h_a})$ approximates
 369 $Q_{\phi}(s, [a_{t:t+h_a}, a_{t+h_a:t+h}^*])$ in Equation (25), conveniently removing the need for training a policy to
 370 predict the whole optimal action chunk entirely. This allows us to simplify the policy objective as
 371

$$372 \quad L(\pi) := -\mathbb{E}_{a_{t:t+h_a} \sim \pi(\cdot | s_t)} [Q_{\psi}^P(s, a_{t:t+h_a})]. \quad (29)$$

374 In summary, DQC trains a policy to predict a partial chunk, $a_{t:t+h_a}$ (of size h_a), by hill climbing the
 375 value of a partial critic $Q_{\psi}^P(s, a_{t:t+h_a})$ that is distilled from the original chunked critic $Q_{\phi}(s, a_{t:t+h})$
 376 via an implicit maximization loss. This allows our policy to fully leverage the chunked critic Q_{ϕ}
 377 (and thus the value speedup benefits associated with Q-chunking) without the need to predict the full
 378 action chunk (of size h), mitigating the learning challenge of an action chunking policy.

378 **Algorithm 1** Decoupled Q-chunking (DQC).

379 **Given:** $D, Q_\phi(s_t, a_{t:t+h}), Q_\psi^P(s_t, a_{t:t+h_a}), V_\xi(s_t), \pi_\beta(a_{t:t+h_a} | s_t)$ 380 **1. Agent Update:**381 $(s_{t:t+h+1}, a_{t:t+h}, r_{t:t+h}) \sim D.$ \triangleright sample trajectory chunk from the offline dataset382 Optimize Q_ϕ with $L(\phi) = \left(Q_\phi(s_t, a_{t:t+h}) - \sum_{k=0}^{h-1} \gamma^k r_{t+k} - \gamma^h \bar{V}_\xi(s_{t+h}) \right)^2.$ 383 Optimize Q_ψ^P with $L(\psi) = f_{\text{expectile}}^{\kappa_d} (\bar{Q}_\phi(s_t, a_{t:t+h}) - Q_\psi^P(s_t, a_{t:t+h_a})).$ 384 Optimize V_ξ with $L(\xi) = f_{\text{quantile}}^{\kappa_b} (\bar{Q}_\psi^P(s_t, a_{t:t+h_a}^\beta) - V_\xi(s_t)), a_{t:t+h_a}^\beta \sim \pi_\beta(\cdot | s_t)$ 385 **2. Policy Extration:**386 $a_{t:t+h_a}^1, a_{t:t+h_a}^2, \dots, a_{t:t+h_a}^N \sim \pi_\beta(\cdot | s_t)$ \triangleright sample N actions from behavior policy387 $a_{t:t+h_a}^* \leftarrow \arg \max_{\{a_{t:t+h_a}^i\}_{i=1}^N} Q_\psi^P(s_t, a_{t:t+h_a}^i)$ \triangleright take the action with the highest Q -value

391 **Practical considerations for offline RL.** Finally, we describe several implementation details that
392 we find to work well in the offline RL setting, which our experiments primarily focus on. Our
393 implementation draws inspirations from a prior method, IDQL (Hansen-Estruch et al., 2023).394 We first train a behavior cloning flow policy π_β using a standard flow-matching objective (Liu et al.,
395 2022) on the offline dataset D . Then, we approximate the policy optimization objective in DQC
396 (Equation (29)) using best-of- N sampling without explicitly modeling π :

397
$$a_{t:t+h_a}^* \leftarrow \arg \max_{\{a_{t:t+h_a}^i\}_{i=1}^N} Q_\psi^P(s_t, a_{t:t+h_a}^i), \quad \text{where } a_{t:t+h_a}^1, \dots, a_{t:t+h_a}^N \sim \pi_\beta(\cdot | s_t). \quad (30)$$

400 where $a_{t:t+h_a}^*$ is output of the policy that we extract from Q_ψ^P for state s_t . Essentially, this sampling
401 procedure is a test-time approximation of the objective in Equation (29), where it outputs action
402 (chunk) that maximizes Q_ψ^P , subject to the behavior prior, as modeled by π_β .403 For TD learning of Q_ϕ , directly computing the TD backup target from either Q_ϕ or Q_ψ^P is computationally
404 expensive, as either requires samples from the current policy, which is approximated via the best-
405 of- N sampling procedure as described above. Instead, we use the implicit value backup (Kostrikov
406 et al., 2021) (i.e., as described in Equation (2)) to approximate the target:

407
$$L(\xi) = f_{\text{quantile}}^{\kappa_b} (\bar{Q}_\psi^P(s_t, a_{t:t+h_a}^\beta) - V_\xi(s_t)), \quad a_{t:t+h_a}^\beta \sim \pi_\beta(\cdot | s_t) \quad (31)$$

408 where we pick the quantile regression loss as the implicit maximization loss function. This is
409 because the Q-value obtained from best-of- N sampling can be seen as the largest order statistic of
410 a random batch (of size N) of the behavior Q-values (i.e., $\{Q(s, a^i)\}_{i=1}^N, a^i \sim \pi_\beta(\cdot | s)$). Such
411 statistic estimates the behavior Q-value distribution's $\frac{N}{1-N}$ -quantile, which is the same as $V_\xi(s)$ at
412 the optimum of $L(\xi)$ if we set $\kappa_b = \frac{N}{1-N}$. In practice, we use a larger κ_b for numerical stability.413 Finally, we pick the expectile regression loss for training the distilled partial critic Q_ψ^P because prior
414 work has found it to work the best among all implicit maximization loss functions (Hansen-Estruch
415 et al., 2023). A summary of the algorithm is available in Algorithm 1.416

6 EXPERIMENTAL SETUP

417 We conduct experiments to evaluate the benefits of decoupling the policy chunk size and the critic
418 chunk size on OGBench (Park et al., 2024a)—a challenging long-horizon, goal-conditioned offline
419 RL benchmark consisting of a diverse set of environments (from manipulation to locomotion). In
420 particular, we use the more difficult environments introduced by Park et al. (2025) (Figure 6), where
421 multi-step return backups are crucial. These environments require highly complex, long-horizon
422 reasoning, and serve as an ideal testbed for our algorithm, which improves upon n -step returns and
423 Q-chunking. We now describe our main comparisons, starting with direct ablation baselines:424 **DQC-naïve** is a naïve attempt at decoupling the critic chunk size from the policy chunk size, where
425 it takes the QC policy to predict full action chunks of size h but only execute the first h_a actions.426 **QC** (Li et al., 2025b) uses a single critic that has the same chunk length as that of the policy (i.e.,
427 $h = h_a$). This baseline tests whether having *decoupled* chunk sizes is important.

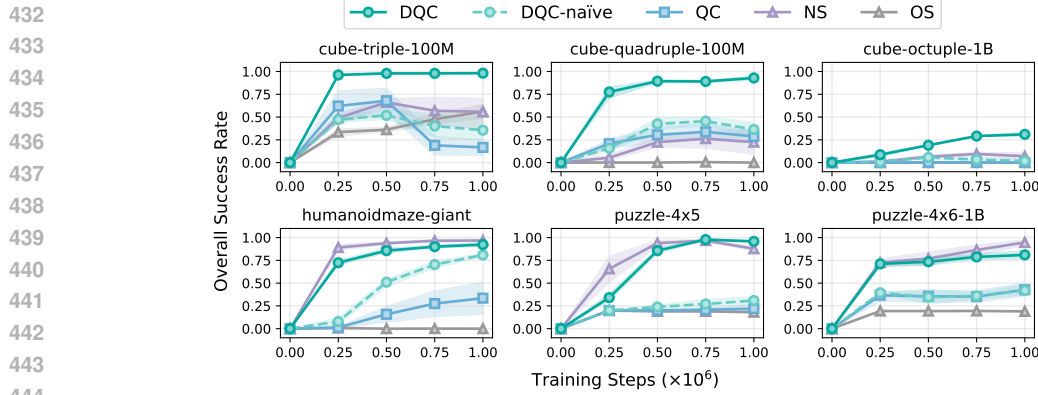


Figure 1: **Offline goal-conditioned RL results.** Our method (**DQC**) uses a *decoupled* critic and policy chunk sizes, which allows it to outperform our baselines by a large margin on $\text{cube-}*$ and competitive on others. **QC**: Q-chunking (Li et al., 2025b); **DQC-naive**: QC but only executing a partial action chunk open-loop; **NS**: n -step return backup; **OS**: 1-step TD-backup.

NS: n -step return TD backup. This baseline uses a single one-step critic (*i.e.*, $Q(s_t, a_t)$). Compared to DQC with $h = n$ and $h_a = 1$, this baseline tests whether using a chunked critic is important.

OS: Standard 1-step TD backup. This is the same as NS but with $n = 1$.

Beyond the ablation baselines, we also consider the following strong goal-conditioned baselines:

FBC/HFBC: Goal-conditioned and hierarchical goal-conditioned flow behavior cloning baselines considered in Park et al. (2025).

IQL/HIQL (Kostrikov et al., 2021; Park et al., 2023): These are strong goal-conditioned RL methods that train a goal-conditioned value function with implicit value backups and extract a flat (IQL) or hierarchical (HIQL) policy from the value function.

SHARSA (Park et al., 2025): The previous state-of-the-art method on the long-horizon environments that we evaluate on. The method uses a combination of n -step return and bi-level hierarchical policies.

In our ablation study, we also consider an additional baseline, **QC-NS**, that uses the idea of decoupled policy chunking and critic chunking ($h_a < h$), but without using a distilled critic. This baseline simply uses n -step return targets to directly train a critic with a chunk size of h_a without implicit maximization (Equation (28)). The performance of this baseline helps determine how important it is to learn a separate distilled critic for partial action chunks with implicit maximization. For all our main results, we run 3 seeds and report the means and the 95% confidence intervals.

Task	FBC	HFBC	IQL	HIQL	SHARSA	OS	NS	QC	DQC-naive	DQC
cube-triple-100M	53 _[48,57]	57 _[54,61]	64 _[59,68]	36 _[27,45]	82 _[78,88]	56 _[48,64]	56 _[37,71]	17 _[8,25]	36 _[24,49]	98 _[97,99]
cube-quadruple-100M	32 _[30,33]	38 _[34,41]	53 _[53,55]	24 _[18,30]	67 _[62,74]	0 _[0,0]	22 _[9,36]	29 _[22,36]	36 _[28,44]	93 _[91,95]
cube-octuple-1B	0 _[0,0]	28 _[27,28]	0 _[0,0]	18 _[14,21]	33 _[30,35]	0 _[0,0]	7 _[3,11]	0 _[0,0]	2 _[0,4]	31 _[29,33]
humanoidmaze-giant	1 _[0,3]	4 _[2,5]	4 _[2,6]	24 _[20,28]	18 _[13,25]	0 _[0,0]	97 _[95,98]	34 _[16,51]	81 _[79,83]	92 _[90,94]
puzzle-4x5	0 _[0,0]	0 _[0,0]	20 _[20,20]	0 _[0,0]	1 _[0,2]	18 _[17,19]	88 _[86,90]	22 _[20,26]	31 _[26,35]	96 _[95,97]
puzzle-4x6-1B	0 _[0,0]	5 _[3,5]	7 _[2,13]	10 _[3,17]	62 _[57,71]	19 _[19,20]	95 _[92,98]	43 _[36,50]	42 _[37,48]	81 _[77,86]

Table 1: **Comparisons with prior methods.** Our method outperforms SHARSA (Park et al., 2025) (the previous state-of-the-art method on this benchmark) on most tasks except cube-octuple where our performance is on par with SHARSA. In contrast, our n -step return baseline (NS), Q-chunking baseline (QC), and naïvely executing partial action chunks from QC (naïve DQC) all fail to outperform SHARSA on $\text{cube-}*$.

7 RESULTS

In this section, we present our experimental results to answer the following three questions:

(Q1) Does DQC improve upon n -step return, Q-chunking? Figure 1 compares DQC (ours) to both n -step and QC across six challenging long-horizon GCRL tasks, with our method performing on par or better across the board. Table 1 shows DQC also consistently outperforms the previous state-of-the-art method on this benchmark, SHARSA (Park et al., 2025), on all environments. For each environment, we tune DQC (ours), QC, NS, OS (see the tuning range in Table 8) and pick the

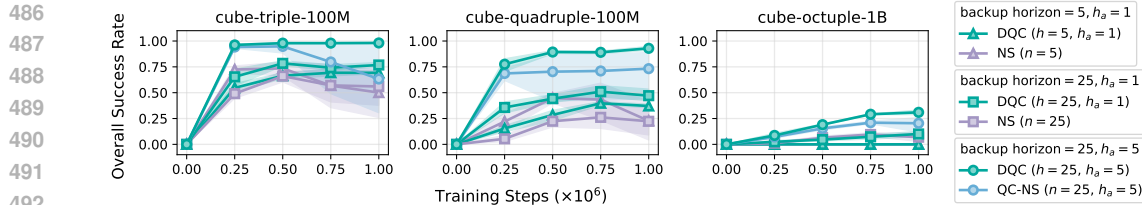


Figure 2: **Distilled critic ablations.** Each group in the legend contains DQC and its non-distilled counterpart with the same configuration (*i.e.*, same backup horizon and same policy chunk size). Our method (DQC) performs on par or better than the non-distilled counterpart across all configurations.

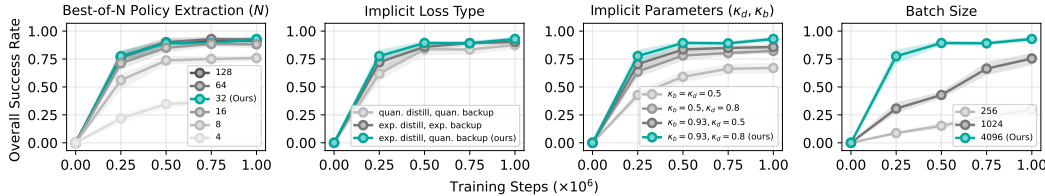


Figure 3: **Hyperparameter sensitivity analysis on cube-quadruple-100M.** *Best-of-N*: the number of action samples drawn from $\pi_\beta(\cdot | s)$ during policy evaluation; *Implicit loss type*: the implicit maximization loss function used for distillation and value backup; *Batch size*: the number of examples used in each gradient step.

best configuration (Table 7) for hyperparameters used in Figure 1 and Table 1. For all baselines from prior work (SHARSA, HIQL, IQL, HFBC, FBC), we directly use their tuned hyperparameters and run with the same batch size (*i.e.*, 4096) as used in our method and other baselines. See the complete table for all combinations of h, n, h_a in Appendix A.

(Q2) Is training a separate distilled critic Q_ψ^P necessary? In Figure 2, we compare DQC to DQC without using the distilled critic across three different (h, h_a) configurations: $(h = 25, h_a = 5)$, $(h = 25, h_a = 1)$, and $(h = 5, h_a = 1)$. For configurations with $h_a = 1$, the baseline without using the distilled critic is the same as the n -step return baseline (with $n = h$) and for the configuration with $h_a = 5$, it is the same as combining Q-chunking and n -step return. Across three configurations, DQC performs on par or better than its non-distilled counterpart. This highlights that the use of a separate distilled critic for the partial action chunk is necessary for the effectiveness of DQC.

(Q3) How sensitive is DQC to its hyperparameters? Figure 3 shows that our method is not sensitive to the implicit backup method (quantile or expectile), and somewhat sensitive to the implicit parameters κ_b, κ_d . In particular, DQC is still reasonably effective as long as some form of optimism is employed (*i.e.*, either $\kappa_b \neq 0.5$ or $\kappa_d \neq 0.5$). Using no optimism ($\kappa_b = \kappa_d = 0.5$) results in a big performance drop. The other important hyperparameters are N in best-of- N policy extraction and the batch size. Having large enough batch size (*i.e.*, 4096) and N (*e.g.*, $N = 32$) is crucial for good performance, though a larger N ($N = 128$) does not lead to better performance.

8 DISCUSSION

We provide a theoretical foundation for action chunking Q-learning and demonstrate how to effectively extract policies from chunked critics. Theoretically, we provide a formal analysis of action chunking Q-learning, identifying the TD backup bias that arises from *open-loop inconsistency* and characterizing the conditions under which action chunking Q-learning is preferred over n -step return learning. Empirically, we develop a novel technique that enables effective policy extraction from chunked critics with long action chunks, *scaling up action chunking Q-learning* to much harder environments. Together, these contributions advance the goal of tackling bootstrapping bias in TD-learning. Several challenges remain, indicating promising avenues for future research. Our method still inherits the open-loop value bias identified in Theorem 4.4, and developing techniques to actively correct for this bias could further improve performance. Moreover, our method relies on a fixed policy action chunk size h_a and critic action chunk size h across all states, even though the optimal action chunk size may vary by state. Developing practical methods that can support flexible, state-dependent chunk sizes would be a natural next step.

540 REPRODUCIBILITY STATEMENT
541

542 To facilitate future research, we include our source code as part of the supplementary materials,
543 along with example scripts for both our method and our baselines. We describe our environments
544 in Appendix D and hyperparameters in Appendix E. For our theoretical results, we fully state our
545 assumption in Assumption 4.1 and provide complete proofs in Appendix G.

547 REFERENCES
548

549 Anurag Ajay, Aviral Kumar, Pulkit Agrawal, Sergey Levine, and Ofir Nachum. OPAL: Offline
550 primitive discovery for accelerating offline reinforcement learning. In *International Conference on*
551 *Learning Representations*, 2021. URL <https://openreview.net/forum?id=V69LGwJ01IN>.

552 Pierre-Luc Bacon, Jean Harb, and Doina Precup. The option-critic architecture. In *Proceedings of*
553 *the AAAI conference on artificial intelligence*, volume 31, 2017.

555 Akhil Bagaria and George Konidaris. Option discovery using deep skill chaining. In *International*
556 *Conference on Learning Representations*, 2019.

558 Akhil Bagaria, Ben Abbatematteo, Omer Gottesman, Matt Corsaro, Sreehari Rammohan, and George
559 Konidaris. Effectively learning initiation sets in hierarchical reinforcement learning. *Advances in*
560 *Neural Information Processing Systems*, 36, 2024.

561 Philip J Ball, Laura Smith, Ilya Kostrikov, and Sergey Levine. Efficient online reinforcement learning
562 with offline data. In *International Conference on Machine Learning*, pp. 1577–1594. PMLR, 2023.

564 Boyuan Chen, Chunming Zhu, Pulkit Agrawal, Kaiqing Zhang, and Abhishek Gupta. Self-supervised
565 reinforcement learning that transfers using random features. *Advances in Neural Information*
566 *Processing Systems*, 36, 2024.

567 Xinyue Chen, Che Wang, Zijian Zhou, and Keith Ross. Randomized ensembled double q-learning:
568 Learning fast without a model. *arXiv preprint arXiv:2101.05982*, 2021.

570 Nuttapong Chentanez, Andrew Barto, and Satinder Singh. Intrinsically motivated reinforcement
571 learning. *Advances in neural information processing systems*, 17, 2004.

573 Imre Csiszár. On information-type measure of difference of probability distributions and indirect
574 observations. *Studia Sci. Math. Hungar.*, 2:299–318, 1967.

575 Christian Daniel, Gerhard Neumann, Oliver Kroemer, and Jan Peters. Hierarchical relative entropy
576 policy search. *Journal of Machine Learning Research*, 17(93):1–50, 2016.

578 Peter Dayan and Geoffrey E Hinton. Feudal reinforcement learning. *Advances in neural information*
579 *processing systems*, 5, 1992.

581 Kristopher De Asis, J Hernandez-Garcia, G Holland, and Richard Sutton. Multi-step reinforcement
582 learning: A unifying algorithm. In *Proceedings of the AAAI conference on artificial intelligence*,
583 volume 32, 2018.

584 Anita de Mello Koch, Akhil Bagaria, Bingnan Huo, Zhiyuan Zhou, Cameron Allen, and George
585 Konidaris. Learning transferable sub-goals by hypothesizing generalizing features. 2025.

587 Thomas G Dietterich. Hierarchical reinforcement learning with the maxq value function decomposi-
588 tion. *Journal of artificial intelligence research*, 13:227–303, 2000.

589 Pierluca D’Oro, Max Schwarzer, Evgenii Nikishin, Pierre-Luc Bacon, Marc G Bellemare, and Aaron
590 Courville. Sample-efficient reinforcement learning by breaking the replay ratio barrier. In *Deep*
591 *Reinforcement Learning Workshop NeurIPS 2022*, 2022.

593 Ishan P Durugkar, Clemens Rosenbaum, Stefan Dernbach, and Sridhar Mahadevan. Deep reinforce-
594 ment learning with macro-actions. *arXiv preprint arXiv:1606.04615*, 2016.

594 William Fedus, Prajit Ramachandran, Rishabh Agarwal, Yoshua Bengio, Hugo Larochelle, Mark
 595 Rowland, and Will Dabney. Revisiting fundamentals of experience replay. In *International*
 596 *conference on machine learning*, pp. 3061–3071. PMLR, 2020.

597

598 Roy Fox, Sanjay Krishnan, Ion Stoica, and Ken Goldberg. Multi-level discovery of deep options.
 599 *arXiv preprint arXiv:1703.08294*, 2017.

600 Kevin Frans, Seohong Park, Pieter Abbeel, and Sergey Levine. Unsupervised zero-shot reinforcement
 601 learning via functional reward encodings. In Ruslan Salakhutdinov, Zico Kolter, Katherine Heller,
 602 Adrian Weller, Nuria Oliver, Jonathan Scarlett, and Felix Berkenkamp (eds.), *Proceedings of the*
 603 *41st International Conference on Machine Learning*, volume 235 of *Proceedings of Machine*
 604 *Learning Research*, pp. 13927–13942. PMLR, 21–27 Jul 2024. URL <https://proceedings.mlr.press/v235/frans24a.html>.

605

606 Jonas Gehring, Gabriel Synnaeve, Andreas Krause, and Nicolas Usunier. Hierarchical skills for
 607 efficient exploration. *Advances in Neural Information Processing Systems*, 34:11553–11564, 2021.

608

609 Philippe Hansen-Estruch, Ilya Kostrikov, Michael Janner, Jakub Grudzien Kuba, and Sergey Levine.
 610 Idql: Implicit q-learning as an actor-critic method with diffusion policies. *arXiv preprint*
 611 *arXiv:2304.10573*, 2023.

612

613 Hao Hu, Yiqin Yang, Jianing Ye, Ziqing Mai, and Chongjie Zhang. Unsupervised behavior extraction
 614 via random intent priors. In *Thirty-seventh Conference on Neural Information Processing Systems*,
 615 2023. URL <https://openreview.net/forum?id=4vGVQVz5KG>.

616

617 Edward L Ionides. Truncated importance sampling. *Journal of Computational and Graphical*
 618 *Statistics*, 17(2):295–311, 2008.

619

620 Tommi Jaakkola, Michael Jordan, and Satinder Singh. Convergence of stochastic iterative dynamic
 621 programming algorithms. *Advances in neural information processing systems*, 6, 1993.

622

623 Jihwan Jeong, Xiaoyu Wang, Michael Gimelfarb, Hyunwoo Kim, Baher Abdulhai, and Scott Sanner.
 624 Conservative bayesian model-based value expansion for offline policy optimization. *arXiv preprint*
 625 *arXiv:2210.03802*, 2022.

626

627 Teun Kloek and Herman K Van Dijk. Bayesian estimates of equation system parameters: an
 628 application of integration by monte carlo. *Econometrica: Journal of the Econometric Society*, pp.
 629 1–19, 1978.

630

631 George Konidaris, Scott Niekum, and Philip S Thomas. TD $_{\gamma}$: Re-evaluating complex backups in
 632 temporal difference learning. *Advances in Neural Information Processing Systems*, 24, 2011.

633

634 George Dimitri Konidaris. *Autonomous robot skill acquisition*. University of Massachusetts Amherst,
 635 2011.

636

637 Ilya Kostrikov, Ashvin Nair, and Sergey Levine. Offline reinforcement learning with implicit Q-
 638 learning. *arXiv preprint arXiv:2110.06169*, 2021.

639

640 Tadashi Kozuno, Yunhao Tang, Mark Rowland, Rémi Munos, Steven Kapturowski, Will Dabney,
 641 Michal Valko, and David Abel. Revisiting Peng’s Q (λ) for modern reinforcement learning. In
 642 *International Conference on Machine Learning*, pp. 5794–5804. PMLR, 2021.

643

644 Tejas D Kulkarni, Karthik Narasimhan, Ardavan Saeedi, and Josh Tenenbaum. Hierarchical deep
 645 reinforcement learning: Integrating temporal abstraction and intrinsic motivation. *Advances in*
 646 *neural information processing systems*, 29, 2016.

647

648 Aviral Kumar, Aurick Zhou, George Tucker, and Sergey Levine. Conservative Q-learning for offline
 649 reinforcement learning. *Advances in Neural Information Processing Systems*, 33:1179–1191, 2020.

650

651 Seunghyun Lee, Younggyo Seo, Kimin Lee, Pieter Abbeel, and Jinwoo Shin. Offline-to-online
 652 reinforcement learning via balanced replay and pessimistic Q-ensemble. In *Conference on Robot*
 653 *Learning*, pp. 1702–1712. PMLR, 2022.

648 Ge Li, Dong Tian, Hongyi Zhou, Xinkai Jiang, Rudolf Lioutikov, and Gerhard Neumann. TOP-ERL:
 649 Transformer-based off-policy episodic reinforcement learning. In *The Thirteenth International*
 650 *Conference on Learning Representations*, 2025a. URL <https://openreview.net/forum?id=N4NhVN30ph>
 651

652 Qiyang Li, Zhiyuan Zhou, and Sergey Levine. Reinforcement learning with action chunking. *arXiv*
 653 *preprint arXiv:2507.07969*, 2025b.
 654

655 Xingchao Liu, Chengyue Gong, and Qiang Liu. Flow straight and fast: Learning to generate and
 656 transfer data with rectified flow. *arXiv preprint arXiv:2209.03003*, 2022.
 657

658 Amy McGovern and Richard S Sutton. Macro-actions in reinforcement learning: An empirical
 659 analysis. 1998.
 660

661 Ishai Menache, Shie Mannor, and Nahum Shimkin. Q-cut—dynamic discovery of sub-goals in
 662 reinforcement learning. In *Machine Learning: ECML 2002: 13th European Conference on*
 663 *Machine Learning Helsinki, Finland, August 19–23, 2002 Proceedings 13*, pp. 295–306. Springer,
 664 2002.
 665

666 Josh Merel, Leonard Hasenclever, Alexandre Galashov, Arun Ahuja, Vu Pham, Greg Wayne,
 667 Yee Whye Teh, and Nicolas Heess. Neural probabilistic motor primitives for humanoid control.
 668 *arXiv preprint arXiv:1811.11711*, 2018.
 669

670 Rémi Munos, Tom Stepleton, Anna Harutyunyan, and Marc Bellemare. Safe and efficient off-policy
 671 reinforcement learning. *Advances in neural information processing systems*, 29, 2016.
 672

673 Ofir Nachum, Shixiang Shane Gu, Honglak Lee, and Sergey Levine. Data-efficient hierarchical
 674 reinforcement learning. *Advances in neural information processing systems*, 31, 2018.
 675

676 Mitsuhiko Nakamoto, Simon Zhai, Anikait Singh, Max Sobol Mark, Yi Ma, Chelsea Finn, Aviral
 677 Kumar, and Sergey Levine. Cal-QL: Calibrated offline RL pre-training for efficient online fine-
 678 tuning. *Advances in Neural Information Processing Systems*, 36, 2024.
 679

680 Soroush Nasiriany, Tian Gao, Ajay Mandlekar, and Yuke Zhu. Learning and retrieval from prior data
 681 for skill-based imitation learning. In *Conference on Robot Learning*, 2022.
 682

683 Alexandros Paraschos, Christian Daniel, Jan R Peters, and Gerhard Neumann. Probabilistic movement
 684 primitives. *Advances in neural information processing systems*, 26, 2013.
 685

686 Kwanyoung Park and Youngwoon Lee. Model-based offline reinforcement learning with lower
 687 expectile q-learning. *arXiv preprint arXiv:2407.00699*, 2024.
 688

689 Seohong Park, Dibya Ghosh, Benjamin Eysenbach, and Sergey Levine. HIQL: Offline goal-
 690 conditioned RL with latent states as actions. In *Thirty-seventh Conference on Neural Information*
 691 *Processing Systems*, 2023. URL <https://openreview.net/forum?id=cLQCCtVDuW>.
 692

693 Seohong Park, Kevin Frans, Benjamin Eysenbach, and Sergey Levine. Ogbench: Benchmarking
 694 offline goal-conditioned rl. *ArXiv*, 2024a.
 695

696 Seohong Park, Tobias Kreiman, and Sergey Levine. Foundation policies with hilbert representations.
 697 In *Forty-first International Conference on Machine Learning*, 2024b. URL <https://openreview.net/forum?id=LhNsSaAKub>.
 698

699 Seohong Park, Kevin Frans, Deepinder Mann, Benjamin Eysenbach, Aviral Kumar, and Sergey
 700 Levine. Horizon reduction makes RL scalable. *arXiv preprint arXiv:2506.04168*, 2025.
 701

Jing Peng and Ronald J Williams. Incremental multi-step Q-learning. In *Machine Learning Proceedings 1994*, pp. 226–232. Elsevier, 1994.

Xue Bin Peng, Glen Berseth, KangKang Yin, and Michiel Van De Panne. Deeploco: Dynamic
 locomotion skills using hierarchical deep reinforcement learning. *Acm transactions on graphics*
 (tog), 36(4):1–13, 2017.

Karl Pertsch, Youngwoon Lee, and Joseph Lim. Accelerating reinforcement learning with learned
 skill priors. In *Conference on robot learning*, pp. 188–204. PMLR, 2021.

702 Doina Precup, Richard S Sutton, and Satinder Singh. Eligibility traces for off-policy policy evaluation.
 703 In *ICML*, volume 2000, pp. 759–766. Citeseer, 2000.
 704

705 Martin Riedmiller, Roland Hafner, Thomas Lampe, Michael Neunert, Jonas Degrave, Tom Wiele,
 706 Vlad Mnih, Nicolas Heess, and Jost Tobias Springenberg. Learning by playing solving sparse
 707 reward tasks from scratch. In *International conference on machine learning*, pp. 4344–4353.
 708 PMLR, 2018.

709 Mark Rowland, Will Dabney, and Rémi Munos. Adaptive trade-offs in off-policy learning. In
 710 *International Conference on Artificial Intelligence and Statistics*, pp. 34–44. PMLR, 2020.

711 Younggyo Seo and Pieter Abbeel. Reinforcement learning with action sequence for data-efficient
 712 robot learning. 2024.

713 Younggyo Seo, Jafar Uruç, and Stephen James. Continuous control with coarse-to-fine reinforcement
 714 learning. In *8th Annual Conference on Robot Learning*, 2024. URL <https://openreview.net/forum?id=WjDR48cL30>.
 715

716 Tanmay Shankar and Abhinav Gupta. Learning robot skills with temporal variational inference. In
 717 *International Conference on Machine Learning*, pp. 8624–8633. PMLR, 2020.

718 Özgür Şimşek and Andrew G. Barto. Betweenness centrality as a basis for forming skills. Working-
 719 paper, University of Massachusetts Amherst, April 2007.

720 Aravind Srinivas, Ramnandan Krishnamurthy, Peeyush Kumar, and Balaraman Ravindran. Option
 721 discovery in hierarchical reinforcement learning using spatio-temporal clustering. *arXiv preprint*
 722 *arXiv:1605.05359*, 2016.

723 Richard S Sutton, Andrew G Barto, et al. *Reinforcement learning: An introduction*, volume 1. MIT
 724 press Cambridge, 1998.

725 Richard S Sutton, Doina Precup, and Satinder Singh. Between MDPs and semi-MDPs: A framework
 726 for temporal abstraction in reinforcement learning. *Artificial intelligence*, 112(1-2):181–211, 1999.

727 Denis Tarasov, Vladislav Kurenkov, Alexander Nikulin, and Sergey Kolesnikov. Revisiting the
 728 minimalist approach to offline reinforcement learning. *Advances in Neural Information Processing*
 729 *Systems*, 36, 2024.

730 Philip S Thomas, Scott Niekum, Georgios Theocharous, and George Konidaris. Policy evaluation
 731 using the Ω -return. *Advances in Neural Information Processing Systems*, 28, 2015.

732 Dong Tian, Ge Li, Hongyi Zhou, Onur Celik, and Gerhard Neumann. Chunking the critic: A
 733 transformer-based soft actor-critic with N-step returns. *arXiv preprint arXiv:2503.03660*, 2025.

734 Ahmed Touati, Jérémie Rapin, and Yann Ollivier. Does zero-shot reinforcement learning exist? In
 735 *The Eleventh International Conference on Learning Representations*, 2022.

736 Alexander Vezhnevets, Volodymyr Mnih, Simon Osindero, Alex Graves, Oriol Vinyals, John Agapiou,
 737 et al. Strategic attentive writer for learning macro-actions. *Advances in neural information*
 738 *processing systems*, 29, 2016.

739 Alexander Sasha Vezhnevets, Simon Osindero, Tom Schaul, Nicolas Heess, Max Jaderberg, David
 740 Silver, and Koray Kavukcuoglu. Feudal networks for hierarchical reinforcement learning. In
 741 *International conference on machine learning*, pp. 3540–3549. PMLR, 2017.

742 Max Wilcoxon, Qiyang Li, Kevin Frans, and Sergey Levine. Leveraging skills from unlabeled prior
 743 data for efficient online exploration. *arXiv preprint arXiv:2410.18076*, 2024.

744 Yihong Wu. Lecture notes on information-theoretic methods for high-dimensional statistics. *Lecture*
 745 *Notes for ECE598YW (UIUC)*, 16:15, 2017.

746 Kevin Xie, Homanga Bharadhwaj, Danijar Hafner, Animesh Garg, and Florian Shkurti. Latent skill
 747 planning for exploration and transfer. In *International Conference on Learning Representations*,
 748 2021. URL <https://openreview.net/forum?id=jXe91kq3jAq>.

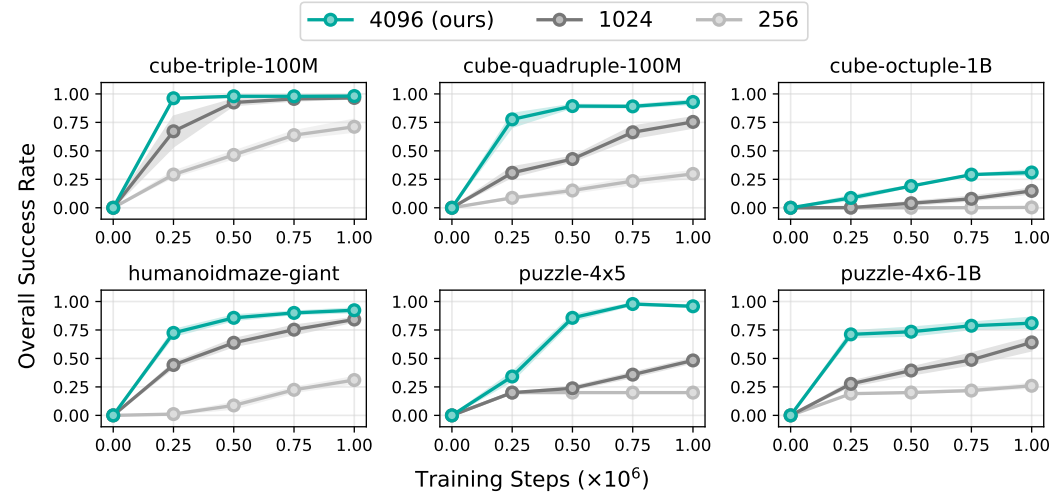
749 Tony Z Zhao, Vikash Kumar, Sergey Levine, and Chelsea Finn. Learning fine-grained bimanual
 750 manipulation with low-cost hardware. *arXiv preprint arXiv:2304.13705*, 2023.

756 A FULL RESULTS

758 Table 2 reports the performance of our method (DQC) and baselines for all hyperparameter configurations.
759 All of them use the same hyperparameters in Table 5 with the only exception that SHARSA
760 handles goal-sampling for training behavior cloning policies slightly differently as we discuss in
761 more details in Appendix E. We also include the full batch size sensitivity analysis in Figure 4.

Task	OS	$h = 5, h_a = 1$	$(h = 5, h_a = 1)$	$(h_a = 5)$	$(n = 5)$	$(h = 25, h_a = 1)$	$(h = 25, h_a = 1)$	$(h = 25, h_a = 5)$	$(h_a = 25)$				
cube-triple-100M	56 _[0.04]	69 _[0.70]	15 _[0.20]	16 _[0.21]	50 _[0.72]	77 _[0.70]	21 _[0.20]	56 _[0.71]	98 _[0.98]	36 _[0.48]	63 _[0.86]	27 _[0.82]	82 _[0.85]
cube-quadruple-100M	0 _[0.0]	37 _[0.36]	36 _[0.45]	37 _[0.44]	23 _[4.41]	47 _[0.33]	0 _[0.20]	22 _[0.36]	93 _[0.95]	18 _[2.37]	73 _[0.80]	7 _[1.15]	67 _[0.74]
cube-octuple-1B	0 _[0.0]	0 _[0.0]	0 _[0.0]	0 _[0.0]	10 _[0.15]	10 _[0.15]	0 _[0.0]	31 _[0.20]	2 _[0.41]	20 _[1.20]	0 _[0.1]	18 _[1.21]	35 _[0.35]
humanoidmaze-giant	0 _[0.0]	0 _[0.0]	31 _[0.25]	49 _[0.25]	10 _[0.15]	10 _[0.15]	0 _[0.0]	97 _[0.98]	51 _[0.98]	0 _[0.0]	0 _[0.0]	0 _[0.0]	28 _[0.28]
puzzle-4x5	18 _[17.10]	19 _[19.20]	20 _[20.20]	20 _[20.20]	66 _[0.17]	90 _[0.74]	30 _[0.20]	88 _[0.90]	96 _[0.97]	31 _[0.20]	96 _[0.97]	28 _[0.32]	20 _[0.20]
puzzle-4x6-1B	19 _[19.20]	35 _[33.27]	25 _[23.25]	26 _[24.25]	54 _[0.61]	81 _[0.47]	41 _[0.47]	95 _[0.97]	75 _[0.77]	42 _[0.40]	98 _[0.99]	45 _[11.51]	10 _[3.17]

763 Table 2: **Complete results for all configurations.** All means and 95% bootstrapped confidence intervals are
764 computed over 6 seeds. (*) indicates that we take the results from the original paper (Park et al., 2025), where
765 we take the results with larger 10M-sized datasets for `humanoidmaze-giant` (originally 4M) and `puzzle-4x5`
766 (originally 3M). For `QC` ($h = 25$), we use $\kappa_b = 0.93$ for `cube-*`, $\kappa_b = 0.9$ on `humanoidmaze-giant` and
767 `puzzle-4x5`, $\kappa_b = 0.7$ on `puzzle-4x6` (same as `QC` with $h = 5$). For `QC-NS`, we use the same implicit
768 parameters as `DQC`. For `NS` ($n = 5$), we use $\kappa_b = 0.93$ on `cube-*`, $\kappa_b = 0.7$ on `humanoidmaze-giant` and
769 `puzzle-4x5`, $\kappa_b = 0.5$ on `puzzle-4x6` (same as `NS` with $n = 25$).



773 Figure 4: **Batch size sensitivity.** Large batch size is crucial for DQC’s performance especially on hard tasks.

795 B ADDITIONAL EMPIRICAL ANALYSIS

797 To gain more insights of the role of the implicit parameters κ_b and κ_d in DQC, we plot the average
798 value of V_ξ , Q_ϕ and Q_ψ^P over the course of training for each task in Figure 5.

801 C COMPUTATION RESOURCE

803 All our experiments are run NVIDIA RTX-A5000 GPU. On average, each 1M-training-step ex-
804 periment takes about 8-10 hours (depending on the method). To reproduce our main results
805 (e.g., Table 2), we estimate it would take around $\underbrace{10}_{\text{hours per single run}} \times \underbrace{14}_{\# \text{ of methods}} \times \underbrace{6}_{\# \text{ of tasks}} \times \underbrace{6}_{\# \text{ of seeds}}$ =

807 5 040 GPU hours. Reproducing our sensitivity analysis in Figure 3 and Figure 4 would take an-
808 other extra $\underbrace{10}_{\text{hours per single run}} \times \underbrace{22}_{\# \text{ of analysis curves}} \times \underbrace{6}_{\# \text{ of seeds}} = 1 320$ GPU hours. We also report the training
809 speed and the parameter count for both our method and all our baselines in Table 3.

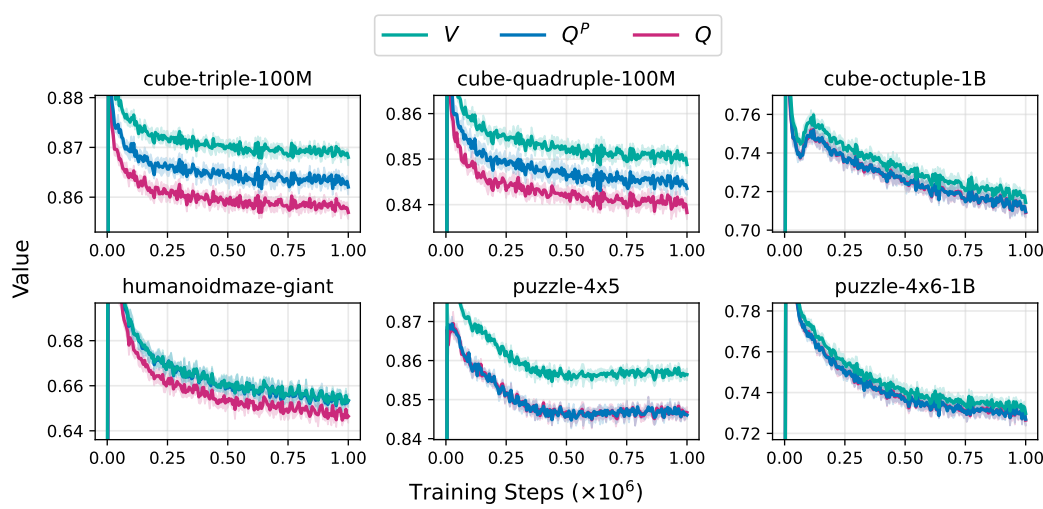


Figure 5: **Value of V_ξ, Q_ϕ, Q_ψ^P over the course of training of our method, DQC.** For cube-triple and cube-quadruple, DQC uses $\kappa_b = 0.93, \kappa_d = 0.8$. This is reflected as the value gap between V, Q^P and Q . The partial critic Q^P optimistically distills from the full critic Q and the value V optimistically backs up from Q^P . For cube-octuple and puzzle-4x5, we use $\kappa_d = 0.5$, which causes Q^P to closely track Q . For humanoidmaze-giant, DQC uses $\kappa_b = 0.5$ and $\kappa_d = 0.8$ which make V closely tracks Q^P and Q optimistically distills from Q . Finally, for puzzle-4x6, we use $\kappa_b = \kappa_d = 0.5$ which causes all value functions to output a similar value.

	DQC	QC	NS / OS	SHARSA	HIQL	IQL	HFBC	FBC
training speed (sec/step)	0.0271	0.0203	0.0200	0.0235	0.0401	0.0243	0.0101	0.0066
parameter count	26 218 528	19 507 230	19 384 330	22 677 526	22 605 853	19 390 474	6 490 129	3 237 893

Table 3: **Training speed and parameter count for each method on cube-quadruple-100M.**

D ENVIRONMENTS AND DATASETS

To evaluate our method, we consider 8 goal-conditioned environments in OGBench with varying difficulties (Figure 6). The dataset size, episode length, and the action dimension for each environment is available in Table 4. We describe each of the environments and the datasets we use as follows.

Environment cube-*: We consider three cube environments (cube-triple, cube-quadruple, cube-octuple). As the names suggest, the goal of these environments involve using a robot arm to manipulate 3/4/8 cubes from some initial configuration to some specified goal configuration. We use the same five evaluation tasks used in OGBench (Park et al., 2024a) for cube-triple and cube-quadruple and the same five evaluation tasks used in Park et al. (2025) for cube-octuple. We refer the environment detail to the corresponding references.

Environment	Dataset Size	Episode Length	Action Dim. (A)
cube-triple-100M	100M	1000	5
cube-quadruple-100M	100M	1000	5
cube-octuple-1B	1B	1500	5
humanoidmaze-giant	4M (default)	4000	21
puzzle-4x5	3M (default)	1000	5
puzzle-4x6-1B	1B	1000	5

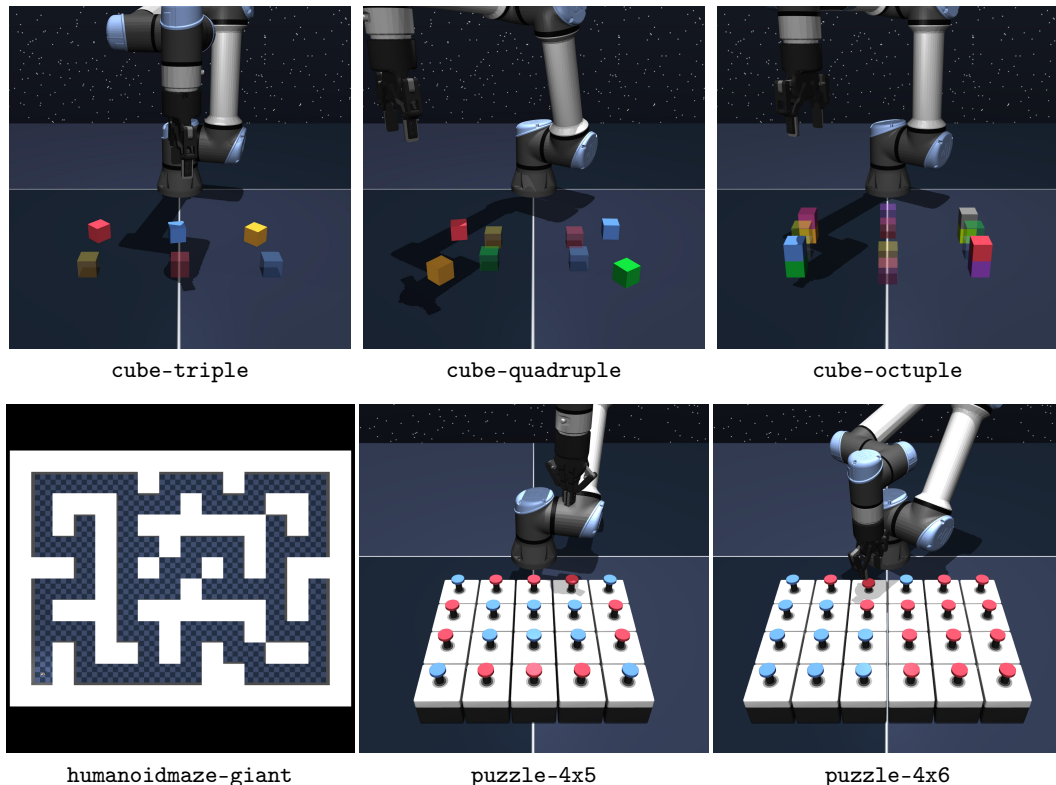
Table 4: **Environment metadata.** For both humanoidmaze-giant and puzzle-4x5, we use the default dataset that is released in the original OGBench benchmark (Park et al., 2024a). For the other environments, we use larger datasets as we find them to be essential for achieving good performances on these environments.

864 **Environment humanoidmaze-***: We also consider the hardest locomotion environment available
 865 in OGBench. The goal of the environment is to control and navigate a humanoid agent from some
 866 initial location to some specified goal location in a 16×12 maze. This environment also has the
 867 longest episode length (4000, more than twice as long as the second longest episode length as used in
 868 cube-octuple). We refer the environment detail to [Park et al. \(2024a\)](#).

869 **Environment puzzle-***: Finally, we consider two environments that involve solving a combinatorial
 870 puzzle with a robot arm. The puzzle consists of a board of 4×5 or 4×6 buttons, organized as a
 871 regular grid (4 rows and 5 or 6 columns). Each button has a binary state. Whenever the end-effector
 872 of the arm touches a button, the button and all its adjacent four buttons (three or two if the button
 873 is on the edge of the grid or in the corner) flip its binary state. The goal of the environment is to
 874 transform the board from some initial state to some specified goal state. We refer the environment
 875 detail to [Park et al. \(2025\)](#).

876 At the test-time/evaluation-time, the goal-conditioned agent is tested on five evaluation tasks for each
 877 of the six environments we consider. The overall success rate is the average over 5 tasks with 50
 878 evaluation trials each.

879 **Datasets.** We use play datasets for all cube-* and puzzle-* environments and navigate
 880 dataset for humanoidmaze-*. We use the original datasets available for humanoidmaze-giant and
 881 puzzle-4x5 because they are sufficient for solving the environments. Using larger datasets on these
 882 environments do not help differentiating among different methods/baselines. For each of the other
 883 environments, we use the largest dataset available from [Park et al. \(2025\)](#) as we find it to be necessary
 884 to solve these environments (or achieve non-trivial performance on the hardest cube-octuple
 885 environment).



915 **Figure 6: Visualization of environments.**

E HYPERPARAMETERS AND IMPLEMENTATION DETAILS

Hyperparameters. Table 5 describes the common hyperparameters used in all our experiments. Table 7 describe the environment-specific hyperparameters and Table 8 describes the range of hyperparameters we use for tuning each method.

Parameter	Value
Batch size	4096
Discount factor (γ)	0.999
Optimizer	Adam
Learning rate	3×10^{-4}
Target network update rate (λ)	5×10^{-3}
Critic ensemble size (K)	2
Critic target	$\min(Q_1, Q_2)$ for cube-*
Implicit Backup Quantile (κ_b)	$(Q_1 + Q_2)/2$ for puzzle-* and humanoid-*
Value loss type	0.9
Best-of- N sampling (N)	binary cross entropy
Number of flow steps	32
Number of training steps	10
Network width	10^6
Network depth	1024
Value goal sampling ($w_{\text{cur}}^v, w_{\text{geom}}^v, w_{\text{traj}}^v, w_{\text{rand}}^v$)	4 hidden layers
Actor goal sampling ($w_{\text{cur}}^p, w_{\text{geom}}^p, w_{\text{traj}}^p, w_{\text{rand}}^p$)	(0.2, 0, 0.5, 0.3)
	DQC/QC/NS/OS: π_β is not goal-conditioned
	SHARSA (cube): (0, 1, 0, 0)
	SHARSA (puzzle): (0, 0, 1, 0)
	SHARSA (humanoidmaze): (0, 0, 1, 0)

Table 5: **Common hyperparameters.** For the GCRL goal-sampling distribution we follow the same hyperparameters used in Park et al. (2025).

Goal-conditioned RL implementation details. While we have described in the main body of the paper how DQC works as a general RL algorithm, we have not touched on how DQC and similarly all our baselines work with the goal-conditioned RL (GCRL) setting. We consider the setting where we have access to an oracle goal representation $\Psi : \mathcal{S} \rightarrow \mathcal{G}$ where \mathcal{G} is the goal space (see Table 6 for the oracle goal representation description for each environment). The goal-conditioned reward function $r : (s, g) \mapsto \mathbb{I}_{\Psi(s)=g}$ is a binary reward function where its output is 1 if the goal g is reached by the current state s . We can treat g as part of an extended state $\tilde{s} = [s, g] \in \tilde{\mathcal{S}} = \mathcal{S} \times \mathcal{G}$ and learn value functions (e.g., $Q_\phi(\tilde{s}, a)$) normally with such extended state.

Environment	Goal Representation (Ψ)	Goal Domain (\mathcal{G})
cube-triple	(x, y, z) of three cubes (rel. to center)	\mathbb{R}^9
cube-quadruple	(x, y, z) of four cubes (rel. to center)	\mathbb{R}^{12}
cube-octuple	(x, y, z) of eight cubes (rel. to center)	\mathbb{R}^{24}
humanoidmaze-giant	(x, y) of the humanoid	\mathbb{R}^2
puzzle-4x5	the binary state for each button	$\{0, 1\}^{20}$
puzzle-4x6	the binary state for each button	$\{0, 1\}^{24}$

Table 6: Oracle goal representation description for each environment. Following Park et al. (2025), we assume access to an oracle goal representation for each environment. More detailed definition of these oracle goal representations is available in OGBench (Park et al., 2024a).

A common trick in the GCRL setting is to use goal relabeling. That is, during training for each (s, a) pair in the training batch, a goal g is sampled from some distribution (*i.e.*, $p^{\mathcal{D}}(\cdot \mid s, a)$) and the reward of the transition is relabeled with the goal-conditioned reward function. Following Park et al. (2025),

Environment	DQC	DQC-naïve	QC	NS	OS	SHARSA	HIQL	IQL	HFBC
	$(h, h_a, \kappa_b, \kappa_d)$	(h, h_a, κ_b)	$(h = h_a, \kappa_b)$	(n, κ_b)	(κ_b)	(n)	(h, κ, α)	(α)	(h)
cube-triple-100M	(25, 5, 0.93, 0.8)	(25, 5, 0.93)	(5, 0.93)	(25, 0.5)	0.5	25	(25, 0.5, 10)	3	25
cube-quadruple-100M	(25, 5, 0.93, 0.8)	(5, 1, 0.93)	(5, 0.93)	(25, 0.5)	0.7	25	(25, 0.5, 10)	3	25
cube-octuple-1B	(25, 5, 0.93, 0.5)	(25, 5, 0.93)	(25, 0.93)	(25, 0.97)	0.7	25	(50, 0.5, 10)	10	50
humanoidmaze-giant	(25, 1, 0.5, 0.8)	(5, 1, 0.9)	(5, 0.9)	(25, 0.7)	0.5	50	(50, 0.5, 3)	0.3	50
puzzle-4x5	(25, 5, 0.9, 0.5)	(25, 5, 0.9)	(5, 0.9)	(25, 0.7)	0.7	50	(25, 0.7, 3)	1	25
puzzle-4x6-1B	(25, 1, 0.7, 0.5)	(25, 5, 0.7)	(5, 0.7)	(25, 0.5)	0.7	50	(25, 0.7, 3)	1	25

Table 7: **Environment-specific hyperparameters for DQC, QC, NS, OS, and SHARSA**. For SHARSA, we follow the hyperparameters in the original paper (Park et al., 2025).

Table 8: **Hyperparameter tuning range for all methods**. For NS, we only tune κ_b and n because the policy chunk size is always 1 and there is no distilled critic. Similarly, for QC, we only tune κ_b and $h = h_a$ because the policy chunk size is the same as the critic chunk size and there is no distilled critic. For OS, we only tune κ_b .

the goal distribution $P^g(\cdot | s, a) : \mathcal{S} \times \mathcal{A} \rightarrow \Delta_{\mathcal{G}}$ is a mixture of four distributions, conditioned on the training state-action example:

$$P^g = w_{\text{cur}} P_{\text{cur}}^g + w_{\text{geom}} P_{\text{geom}}^g + w_{\text{traj}} P_{\text{traj}}^g + w_{\text{rand}} P_{\text{rand}}^g, \quad (32)$$

where

1. $P_{\text{cur}}^g(\cdot | s, a) = \delta_{\Psi(s)}$: the goal is the same as the current state;
2. $P_{\text{geom}}^g(\cdot | s, a)$: geometric distribution over the future states in the same trajectory that (s, a) is from;
3. $P_{\text{traj}}^g(\cdot | s, a)$: uniform distribution over the future states in the same trajectory that (s, a) is from; and finally
4. $P_{\text{rand}}^g(\cdot | s, a) = \Psi(\mathcal{U}_{\mathcal{D}(s)})$: uniform distribution over the dataset $(\mathcal{D}(s))$ is the distribution of states in the dataset.

and $w_{\text{cur}}, w_{\text{geom}}, w_{\text{traj}}, w_{\text{rand}} > 0$ are the corresponding weights for each of the distribution components with $w_{\text{cur}} + w_{\text{geom}} + w_{\text{traj}} + w_{\text{rand}} = 1$.

In practice, it has been found to be beneficial to use a separate set of goal sampling weights for TD backup (Park et al., 2024a) (*i.e.*, $(w_{\text{cur}}^v, w_{\text{geom}}^v, w_{\text{traj}}^v, w_{\text{rand}}^v)$) and for policy learning (*i.e.*, $(w_{\text{cur}}^p, w_{\text{geom}}^p, w_{\text{traj}}^p, w_{\text{rand}}^p)$). However, in our implementation of DQC/QC/NS/OS, we do not train a goal-conditioned policy, as our policy extraction is done entirely at test-time by best-of-N sampling from an *unconditional* (*i.e.*, not goal-conditioned) behavior policy π_{β} . In particular, we use an unconditioned flow policy $\pi_{\beta}(\cdot | s)$ that is parameterized by a velocity field $v_{\beta} : \mathcal{S} \times \mathbb{R}^A \times [0, 1] \rightarrow \mathbb{R}^A$ that is trained with the standard flow-matching objective:

$$L_{\text{FM}}(\beta) = \mathbb{E}_{u \sim \mathcal{U}[0,1], z \sim \mathcal{N}, (s, a) \sim \mathcal{D}} [\|v_{\beta}(s, (1-u)z + ua, u) - a + z\|_2^2] \quad (33)$$

For SHARSA, we use the official implementation where both flow policies (high-level and low-level) are goal-conditioned (and thus are trained with the goal distribution mixture specified by $w_{\text{cur}}^p, w_{\text{geom}}^p, w_{\text{traj}}^p, w_{\text{rand}}^p$). The goal sampling distribution for training the value networks (for all methods) and the goal sampling distribution for the policy networks (for SHARSA only) are provided in Table 5.

1026 **F LOWER-BOUND ANALYSES**1028 **F.1 AC VALUE BIAS (PROOF IN APPENDIX G.3)**

1029 **Theorem F.1** (Worst-case AC Value Bias). *For any $\gamma \in [0, 1], \varepsilon_h \in [0, 1/2]$, there exists an MDP*
 1030 *\mathcal{M} and a weakly ε_h -open-loop consistent \mathcal{D} such that for some $s \in \text{supp}(P_{\mathcal{D}}(s_t))$,*

$$1033 V_{\text{ac}}(s) - \hat{V}_{\text{ac}}(s) = \pm \frac{\gamma \varepsilon_h}{(1 - \gamma)(1 - (1 - \varepsilon_h)\gamma^h)}. \quad (34)$$

1035 **F.2 OPTIMALITY GAP FOR ACTION CHUNKING POLICY (PROOF IN APPENDIX G.5)**

1036 **Corollary F.2** (Worse-case Optimality Gap for Action Chunking Policy). *For any $\gamma \in [0, 1], \varepsilon_h \in [0, 1/2]$, there exists an MDP \mathcal{M} whose optimal policy π^* induces a data distribution \mathcal{D}^* that is*
 1037 *weakly ε_h -open-loop consistent, such that for some $s \in \text{supp}(P_{\mathcal{D}^*}(s_t))$,*

$$1041 V^*(s) - V_{\text{ac}}^*(s) = \frac{\gamma \varepsilon_h}{(1 - \gamma)(1 - (1 - \varepsilon_h)\gamma^h)}. \quad (35)$$

1044 **F.3 Q-LEARNING WITH ACTION CHUNKING POLICY (PROOF IN APPENDIX G.7)**

1045 **Theorem F.3** (Worst-case Analysis of Q-Learning with Action Chunking Policy on Off-policy Data).
 1046 *For any $\varepsilon_h \in (0, 1/5)$, $\gamma \in (0, 1)$, $c_1 \in (0, \varepsilon_h/2)$, and $c_2 \in (0, 2\varepsilon_h\gamma)$, there exists an MDP \mathcal{M}*
 1047 *and strongly ε_h -open-loop consistent data distribution \mathcal{D} and \mathcal{D}^* with $\text{supp}(P_{\mathcal{D}}(s_t, a_{t:t+h})) \supseteq$*
 1048 *$\text{supp}(P_{\mathcal{D}^*}(s_t, a_{t:t+h}))$, such that for some $s \in \text{supp}(P_{\mathcal{D}^*}(s_t))$,*

$$1050 V^*(s) - V_{\text{ac}}^*(s) = \frac{2\varepsilon_h\gamma - c_2}{(1 - \gamma)(1 - (1 - 2\varepsilon_h)\gamma^h)} + \frac{\varepsilon_h\gamma}{(1 - \gamma)(1 - (1 - \varepsilon_h - c_1)\gamma^h)}, \quad (36)$$

1053 where V^* is the value of an optimal policy and V_{ac}^* is the true value of π_{ac}^* . As $c_1, c_2 \rightarrow 0$,

$$1055 V^*(s) - V_{\text{ac}}^*(s) \rightarrow \frac{\varepsilon_h\gamma}{1 - \gamma} \left[\frac{2}{1 - (1 - 2\varepsilon_h)\gamma^h} + \frac{1}{1 - (1 - \varepsilon_h)\gamma^h} \right]. \quad (37)$$

1058 **F.4 CLOSED-LOOP AC POLICY UNDER BOV (PROOF IN APPENDIX G.11)**

1059 **Theorem F.4** (Worst-case Closed-loop AC Policy under BOV). *For any $\gamma \in (0, 1), \vartheta_h^G, \vartheta_h^L \in$*
 1060 *$(0, \frac{\gamma - \gamma^h}{4(1 - \gamma)})$, $c \in [0, \frac{\gamma - \gamma^h}{4(1 - \gamma^h)})$, $\sigma \in (0, \frac{\min(\vartheta_h^G, \vartheta_h^L)}{1 - \gamma})$, there exists \mathcal{M} and \mathcal{D} satisfying the mixture*
 1061 *assumption in Theorem 4.11 such that there exists $s_t \in \text{supp}(P_{\mathcal{D}^*}(s_t))$, where*

$$1064 V^*(s_t) - V^*(s_t) = \frac{\vartheta_h^L}{1 - \gamma} + \frac{\vartheta_h^G + \gamma^h \min(\vartheta_h^L, \vartheta_h^G)}{(1 - \gamma)(1 - \gamma^h)} - \sigma, \quad V^*(s_t) - V_{\text{ac}}^*(s_t) \geq \frac{c}{1 - \gamma} \quad (38)$$

1067 **F.5 ε -DETERMINISTIC DYNAMICS IS WEAKLY OPEN-LOOP CONSISTENT**

1069 To provide some intuitions on what this open-loop consistency implies, we discuss a concrete
 1070 family of MDPs where any data distribution from these MDPs are (weakly) ε_h -open-loop consistent
 1071 (Proposition F.6, with proof available in Appendix G.12).

1072 **Definition F.5** (Near-deterministic Dynamics). *A transition dynamics T is ε -deterministic if there*
 1073 *exists a deterministic transition dynamics represented by function $f : \mathcal{S} \times \mathcal{A} \rightarrow \mathcal{S}$ and another*
 1074 *arbitrary transition dynamics $\tilde{T} : \mathcal{S} \times \mathcal{A} \rightarrow \Delta_{\mathcal{S}}$, and T is a combination of f and \tilde{T} :*

$$1076 T(s' | s, a) = (1 - \varepsilon)\delta_{f(s,a)}(s') + \varepsilon\tilde{T}(s' | s, a), \forall s, s' \in \mathcal{S}, a \in \mathcal{A}. \quad (39)$$

1078 **Proposition F.6** (Deterministic Dynamics are Weakly Open-loop Consistent). *If a transition dynamics*
 1079 *\mathcal{M} is ε -deterministic, then any data \mathcal{D} collected from \mathcal{M} is weakly ε_h -open-loop consistent with*
respect to \mathcal{M} for any $h \in \mathbb{N}^+$ as long as $\varepsilon_h \geq 3(1 - (1 - \varepsilon)^{h-1})$.

1080 An ε -deterministic dynamics acts like a deterministic one most of the time (with $1 - \varepsilon$ probability)
1081 and a non-deterministic one occasionally (with ε probability). This bounded stochasticity allows the
1082 results of taking an action sequence (of length h) open-loop to be deterministically determined in the
1083 event that the deterministic dynamics is ‘triggered’ (with a joint $(1 - \varepsilon)^{h-1}$ probability across h time
1084 steps). It is clear that under such event, there is no gap between the ‘replayed’ open-loop data $P_{\mathcal{D}}^{\circ}$ and
1085 the original data distribution $P_{\mathcal{D}}$, and as result there is also no value estimation bias under this event,
1086 and thus intuitively we can bound the value estimation error by a function of the probability that the
1087 stochastic dynamics is ‘triggered’ (*i.e.*, with $1 - (1 - \varepsilon)^{h-1}$ probability).

1088

1089

1090

1091

1092

1093

1094

1095

1096

1097

1098

1099

1100

1101

1102

1103

1104

1105

1106

1107

1108

1109

1110

1111

1112

1113

1114

1115

1116

1117

1118

1119

1120

1121

1122

1123

1124

1125

1126

1127

1128

1129

1130

1131

1132

1133

1134 **G PROOFS OF MAIN RESULTS**

1135 **G.1 UTILITY LEMMATA**

1136 **Lemma G.1** (Mean value theorem for conditional probabilities). *Let $P_1, P_2 \in \Delta_{\mathcal{X} \times \mathcal{Y}}$ and $P(x, y) := \hat{\alpha}(y)P_1(x, y) + (1 - \hat{\alpha}(y))P_2(x, y)$ and there exists $\alpha > 0$ such that $\hat{\alpha}(y) \leq \alpha, \forall y \in \mathcal{Y}$. Then, there exists $y \in \mathcal{Y}$ and $\tilde{\alpha} \leq \alpha$ such that*

1142
$$P(\cdot | y) = \tilde{\alpha}P_1(\cdot | y) + (1 - \tilde{\alpha})P_2(\cdot | y) \quad (40)$$

1145 *Proof.*

1147
$$\begin{aligned} \frac{P(x, y)}{P(y)} &= \frac{\hat{\alpha}(y)P_1(y)P_1(x | y) + (1 - \hat{\alpha}(y))P_2(x | y)}{\hat{\alpha}(y)P_1(y) + (1 - \hat{\alpha}(y))P_2(y)} \\ 1149 &= \beta(y)P_1(x | y) + (1 - \beta(y))P_2(x | y) \end{aligned} \quad (41)$$

1151 where $\beta(y) := \frac{\hat{\alpha}(y)P_1(y)}{\hat{\alpha}(y)P_1(y) + (1 - \hat{\alpha}(y))P_2(y)}$. We now prove $\exists y \in \mathcal{Y}, \tilde{\alpha} \leq \alpha$ for Equation (40) to hold by
1152 contradiction.

1153 We first assume $\tilde{\alpha} = \beta(y) > \alpha, \forall y \in \mathcal{Y}$. Now, substitute $\beta(y)$ in and integrate both side by y to obtain

1156
$$\hat{\alpha}(y)P_1(y) > \alpha\hat{\alpha}(y)P_1(y) + \alpha(1 - \hat{\alpha}(y))P_2(y) \quad (42)$$

1157
$$\hat{\alpha}(y) > \alpha\hat{\alpha}(y) + \alpha - \alpha\hat{\alpha}(y) = \alpha, \quad (43)$$

1158 which is a contradiction to the condition $\hat{\alpha}(y) \leq \alpha$.

1159 Therefore, there must exist $y \in \mathcal{Y}$ with $\tilde{\alpha} \leq \alpha$ such that Equation (40) holds. \square

1163 **Lemma G.2** (Expectation difference for bounded function and TV). *For two distributions $P, Q \in \Delta_{\mathcal{X}}$
1164 and two bounded functions $f, g : \mathcal{X} \rightarrow [0, 1]$, if the TV distance between P and Q is no larger than ε
1165 and $\|f - g\|_{\infty} \leq \delta$ under $\text{supp}(P) \cap \text{supp}(Q)$, then*

1167
$$|\mathbb{E}_{x \sim P}[f(x)] - \mathbb{E}_{x \sim Q}[g(x)]| \leq (1 - \varepsilon)\delta + \varepsilon. \quad (44)$$

1169 *Proof.* Let's decompose the probability mass of P and Q in terms of $d_P, d_{PQ}, d_Q : \mathcal{X} \rightarrow \mathbb{R}$ as the
1170 following:

1173
$$P(x) = d_P(x) + d_{PQ}(x), \quad (45)$$

1174
$$Q(x) = d_{PQ}(x) + d_Q(x). \quad (46)$$

1176 The $\int d_P(x)dx$ maximizing solution is

1178
$$d_P(x) = \max(P(x), Q(x)) - Q(x) \quad (47)$$

1179
$$d_Q(x) = \max(P(x), Q(x)) - P(x) \quad (48)$$

1180
$$d_{PQ}(x) = P(x) + Q(x) - \max(P(x), Q(x)). \quad (49)$$

1182 It is clear that under this decomposition,

1184
$$\int d_P(x)dx = \int d_Q(x)dx = \hat{\varepsilon} \leq \varepsilon, \quad (50)$$

1185
$$\int d_{PQ}(x)dx = 1 - \hat{\varepsilon} \geq 1 - \varepsilon. \quad (51)$$

1188 Now we are ready to bound the expectation difference:
1189
1190 $|\mathbb{E}_{x \sim P}[f(x)] - \mathbb{E}_{x \sim Q}[g(x)]|$
1191 $= \left| \left(\int d_P(x)f(x)dx - \int d_Q(x)g(x)dx \right) + \left(\int d_{PQ}(x)(f(x) - g(x))dx \right) \right|$
1192 $\leq \left| \int d_P(x)f(x)dx - \int d_Q(x)g(x)dx \right| + \left| \int d_{PQ}(x)(f(x) - g(x))dx \right|$
1193 $\leq \max \left(\sup_x f(x) \int d_P(x)dx - \inf_x g(x) \int d_Q(x)dx, \sup_x g(x) \int d_Q(x)dx - \inf_x f(x) \int d_P(x)dx \right)$
1194
1195 $+ \left| \left(\sup_{x: d_{PQ}(x) > 0} |f(x) - g(x)| \right) \int d_{PQ}(x)dx \right|$
1196
1197 $\leq \hat{\varepsilon} + \left(\sup_{x \in \text{supp}(P) \cap \text{supp}(Q)} |f(x) - g(x)| \right) (1 - \hat{\varepsilon})$
1198
1199 $= \hat{\varepsilon} + \|f - g\|_\infty (1 - \hat{\varepsilon})$
1200
1201 $\leq \hat{\varepsilon}(1 - \delta) + \delta$
1202
1203 $= (1 - \varepsilon)\delta + \varepsilon$
1204
1205 as desired. (52) \square
1206
1207
1208

1209 **Lemma G.3** (Total variation under event conditioning). *For two random variables $X \in \Delta_{\mathcal{X}}$ and
1210 $Y \in \Delta_{\mathcal{Y}}$ and any $y \in \mathcal{Y}$,*

1211 $D_{\text{TV}}(P(X | Y = y) \| P(X)) \leq 1 - P(Y = y)$ (53)
1212

1213 *Proof.* Let $p = P(Y = y)$

1214 $D_{\text{TV}}(P(X | Y = y) \| P(X))$
1215
1216 $= \frac{1}{2} \int |P(x) - P(x | y)|dx$
1217
1218 $= \frac{1}{2} \int |P(x | Y = y)(P(Y = y) - 1) + P(x | Y \neq y)P(Y \neq y)|dx$ (54)
1219
1220 $= \frac{1-p}{2} \int |(P(x | Y \neq y) - P(x | Y = y))|dx$
1221
1222 $= (1-p)D_{\text{TV}}(P(X | Y = y) \| P(X | Y \neq y))$
1223
1224 $\leq 1 - p$ □
1225

1226 **Lemma G.4** (Data Processing Inequality for f -divergence (Csiszár, 1967)). *For two random variables
1227 $A, B \in \Delta_{\mathcal{X}}$ and a deterministic function $f : \mathcal{X} \rightarrow \mathcal{Y}$, and $C := g(A), D := g(B)$*

1228 $D_f(P_A \| P_B) \geq D_f(P_C \| P_D).$ (55)

1229 Since TV-distance is a f -divergence with $f = |x - 1|$, we have

1230 $D_{\text{TV}}(P_A \| P_B) \geq D_{\text{TV}}(P_C \| P_D).$ (56)
1231

1232 *Proof from Wu (2017).*

1233 $D_f(P_A \| P_B) = \mathbb{E}_{x \sim P_B} [f(P_A(x)/P_B(x))]$
1234
1235 $= \mathbb{E}_{P_{BD}} [f(P_{AC}/P_{BD})]$
1236
1237 $= \mathbb{E}_{(x,y) \sim P_D} [\mathbb{E}_{P_{B|D}} [f(P_{AC}(x,y)/P_{BD}(x,y))]]$ (57)
1238
1239 $\geq \mathbb{E}_{y \sim P_D} [f(\mathbb{E}_{x \sim P_{B|D=y}} [P_{AC}(x,y)/P_{BD}(x,y)])]$
1240
1241 $= \mathbb{E}_{y \sim P_D} [f(\mathbb{E}_{x \sim P_{B|D=y}} [P_C(y)/P_D(y)])]$
1242
1243 $= D_f(P_C \| P_D).$ □

1242 **G.2 PROOF OF THEOREM 4.4**
12431244 **Theorem 4.4** (Bias of Action Chunking Critic). *Let $\hat{V}_{\text{ac}} : \mathcal{S} \rightarrow [0, 1/(1-\gamma)]$ be a solution of*

1245
$$\hat{V}_{\text{ac}}(s_t) = \mathbb{E}_{s_{t+1:t+h+1}, a_{t:t+h} \sim P_{\mathcal{D}}(\cdot|s_t)} \left[R_{t:t+h} + \gamma^h \hat{V}_{\text{ac}}(s_{t+h}) \right], \quad (12)$$

1246 *with $R_{t:t+h} = \sum_{t'=t}^{t+h} \gamma^{t'-t} r(s_{t'}, a_{t'})$ and V_{ac} is the true value of $\pi_{\mathcal{D}}^{\circ} : s_t \mapsto P_{\mathcal{D}}(a_{t:t+h} | s_t)$. If \mathcal{D} is ε_h -open-loop consistent, then under $\text{supp}(\mathcal{D})$,*

1247
$$\|V_{\text{ac}} - \hat{V}_{\text{ac}}\|_{\infty} \leq \frac{\varepsilon_h \gamma}{(1 - (1 - \varepsilon_h) \gamma^h)(1 - \gamma)} \leq \frac{\varepsilon_h}{(1 - \gamma^h)(1 - \gamma)}. \quad (13)$$

1248 *Proof.* Since \mathcal{D} is $\varepsilon_{h'}$ -open-loop consistent in state-action for $h' < h$, the state-action distribution
1249 leading up to step h admits the following bound:

1250
$$D_{\text{TV}}(P_{\mathcal{D}}(s_{t+h}, a_{t+h} | s_t) \| P_{\mathcal{D}}^{\circ}(s_{t+h}, a_{t+h} | s_t)) \leq \varepsilon_h \quad (58)$$

1251 Let $R_{t:t+h} = \sum_{k=0}^{h-1} \gamma^k r(s_{t+k}, a_{t+k})$ be the h -step reward distribution. Then the difference in h -step
1252 reward is bounded by

1253
$$\begin{aligned} & \left| \mathbb{E}_{P_{\mathcal{D}}(\cdot|s_t)} [R_{t:t+h}] - \mathbb{E}_{P_{\mathcal{D}}^{\circ}(\cdot|s_t)} [R_{t:t+h}] \right| \\ & \leq \sum_{h'=1}^{h-1} \left[\gamma^{h'} \mathbb{E}_{P_{\mathcal{D}}(s_{t+h'}, a_{t+h'} | s_t)} [r(s_{t+h'}, a_{t+h'})] - \mathbb{E}_{P_{\mathcal{D}}^{\circ}(s_{t+h'}, a_{t+h'} | s_t)} [r(s_{t+h'}, a_{t+h'})] \right] \\ & \leq \sum_{h'=1}^{h-1} \gamma^{h'} \varepsilon_h. \end{aligned} \quad (59)$$

1254 where the first inequality uses Lemma G.2 and the fact that TV distance is bounded (Equation (58)).

1255 Since \mathcal{D} is ε_h -open-loop consistent for h in state, we have

1256
$$D_{\text{TV}}(P_{\mathcal{D}}(s_{t+h} | s_t) \| P_{\mathcal{D}}^{\circ}(s_{t+h} | s_t)) \leq \varepsilon_h, \quad (60)$$

1257 which can then be used to bound the estimation error using Lemma G.2:

1258
$$\begin{aligned} & \left| \mathbb{E}_{s_{t+h} \sim P_{\mathcal{D}}(s_{t+h} | s_t)} \left[\hat{V}_{\text{ac}}(s_{t+h}) \right] - \mathbb{E}_{s_{t+h} \sim P_{\mathcal{D}}^{\circ}(s_{t+h} | s_t)} [V_{\text{ac}}(s_{t+h})] \right| \\ & \leq \frac{\varepsilon_h}{1 - \gamma} + (1 - \varepsilon_h) \sup_{s_{t+h} \in \text{supp}(P_{\mathcal{D}}(s_{t+h} | s_t))} \left[|\hat{V}_{\text{ac}}(s_{t+h}) - V_{\text{ac}}(s_{t+h})| \right] \end{aligned} \quad (61)$$

1259 For all $s_t \in \text{supp}(P_{\mathcal{D}}(s_t))$,

1260
$$\begin{aligned} & \left| \hat{V}_{\text{ac}}(s_t) - V_{\text{ac}}(s_t) \right| \\ & \leq \left| \mathbb{E}_{P_{\mathcal{D}}(\cdot|s_t)} [R_{t:t+h}] - \mathbb{E}_{P_{\mathcal{D}}^{\circ}(\cdot|s_t)} [R_{t:t+h}] \right| \\ & \quad + \gamma^h \left| \mathbb{E}_{s_{t+h} \sim P_{\mathcal{D}}(s_{t+h} | s_t)} \left[\hat{V}_{\text{ac}}(s_{t+h}) \right] - \mathbb{E}_{s_{t+h} \sim P_{\mathcal{D}}^{\circ}(s_{t+h} | s_t)} [V_{\text{ac}}(s_{t+h})] \right| \\ & \leq \sum_{h'=0}^{h-1} \left[\gamma^{h'} \varepsilon_h \right] + \frac{\gamma^h \varepsilon_h}{1 - \gamma} + \gamma^h (1 - \varepsilon_h) \sup_{s_{t+h} \in \text{supp}(P_{\mathcal{D}}(s_{t+h} | s_t))} \left[|\hat{V}_{\text{ac}}(s_{t+h}) - V_{\text{ac}}(s_{t+h})| \right]. \end{aligned} \quad (62)$$

1261 Since the support of $s_{t+h} | s_t$ is a subset of the support for s_t by Assumption 4.1, we can recursively
1262 apply the inequality to obtain,

1263
$$\begin{aligned} & \left| \hat{V}_{\text{ac}}(s_t) - V_{\text{ac}}(s_t) \right| \leq \frac{1}{1 - (1 - \varepsilon_h) \gamma^h} \left(\sum_{h'=1}^{h-1} \left[\gamma^{h'} \varepsilon_h \right] + \frac{\gamma^h \varepsilon_h}{1 - \gamma} \right) \\ & = \frac{\gamma \varepsilon_h}{(1 - \gamma)(1 - (1 - \varepsilon_h) \gamma^h)}, \end{aligned} \quad (63)$$

1264 as desired. \square

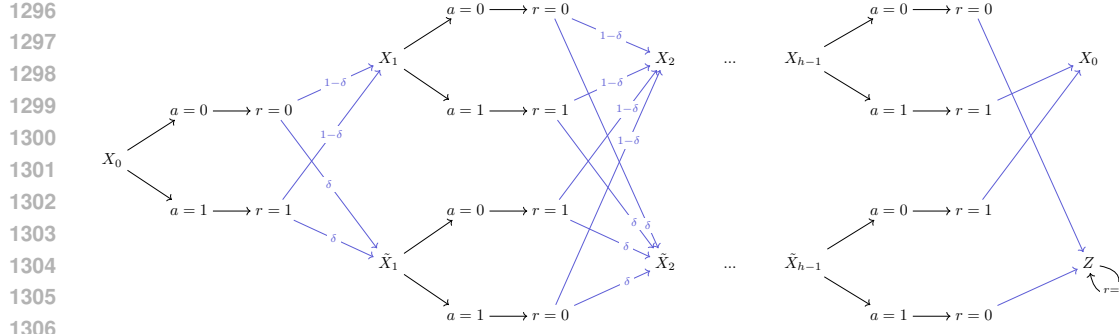


Figure 7: **A $2h$ -state MDP that is constructed to meet the upper-bound in Theorem 4.4.** The data distribution \mathcal{D} that achieves such upper-bound is collected by the optimal policy: $\pi(X_i) = 1, \pi(\tilde{X}_i) = 0$.

G.3 PROOF OF THEOREM F.1

Theorem F.1 (Worst-case AC Value Bias). *For any $\gamma \in [0, 1], \varepsilon_h \in [0, 1/2]$, there exists an MDP \mathcal{M} and a weakly ε_h -open-loop consistent \mathcal{D} such that for some $s \in \text{supp}(P_{\mathcal{D}}(s_t))$,*

$$V_{\text{ac}}(s) - \hat{V}_{\text{ac}}(s) = \pm \frac{\gamma \varepsilon_h}{(1 - \gamma)(1 - (1 - \varepsilon_h)\gamma^h)}. \quad (34)$$

Proof. Let $\delta \in [0, 1]$ be any value that satisfies $\varepsilon_h = 2\delta(1 - \delta)$. δ must exist because $\varepsilon_h \in [0, 1/2]$. Let us define a MDP that has $S = 2h$ states, $\mathcal{S} = \{X_0, X_1, \tilde{X}_1, \dots, X_{h-1}, \tilde{X}_{h-1}, Z\}$, and $A = 2$ actions, $\mathcal{A} = \{0, 1\}$, and the following transition function T and reward function r (see a diagram in Figure 7):

$$\begin{aligned} T(\tilde{X}_{i+1} | X_i, a) &= T(\tilde{X}_{i+1} | \tilde{X}_i, a) = \delta, & \forall a \in \{0, 1\}, i \in \{1, \dots, h-2\} \\ T(X_{i+1} | X_i, a) &= T(X_{i+1} | \tilde{X}_i, a) = 1 - \delta, & \forall a \in \{0, 1\}, i \in \{0, \dots, h-2\} \\ T(Z | \tilde{X}_{h-1}, a=1) &= T(Z | X_{h-1}, a=0) = 1 \\ T(X_0 | \tilde{X}_{h-1}, a=0) &= T(X_0 | X_{h-1}, a=1) = 1 \\ r(\tilde{X}_i, a=0) &= r(X_i, a=1) = 1, & \forall i \in \{0, \dots, h-1\} \\ r(\tilde{X}_i, a=1) &= r(X_i, a=0) = 0, & \forall i \in \{0, \dots, h-1\} \\ r(Z, a=1) &= r(Z, a=0) = 0 \\ T(Z | Z, a=0) &= T(Z | Z, a=1) = 1 \end{aligned} \quad (64)$$

Now, we assume that the data \mathcal{D} is collected by the optimal closed-loop policy where

$$\pi(X_i) = 1, \pi(\tilde{X}_i) = 0. \quad (65)$$

First, we check \mathcal{D} is ε_h -open-loop consistent.

We can show that by computing the distribution for $P_{\mathcal{D}}(s_{t+i}, a_{t+i} | s_t = X_0)$ and $P_{\mathcal{D}}^{\circ}(s_{t+i}, a_{t+i} | s_t = X_0)$ as follows:

$$\begin{aligned} \begin{bmatrix} P_{\mathcal{D}}(s_{t+i} = \tilde{X}_i, a_{t+i} = 0 | X_0) & P_{\mathcal{D}}(s_{t+i} = \tilde{X}_i, a_{t+i} = 1 | X_0) \\ P_{\mathcal{D}}(s_{t+i} = X_i, a_{t+i} = 0 | X_0) & P_{\mathcal{D}}(s_{t+i} = X_i, a_{t+i} = 1 | X_0) \end{bmatrix} &= \begin{bmatrix} \delta & 0 \\ 0 & 1 - \delta \end{bmatrix} \\ \begin{bmatrix} P_{\mathcal{D}}^{\circ}(s_{t+i} = \tilde{X}_i, a_{t+i} = 0 | X_0) & P_{\mathcal{D}}^{\circ}(s_{t+i} = \tilde{X}_i, a_{t+i} = 1 | X_0) \\ P_{\mathcal{D}}^{\circ}(s_{t+i} = X_i, a_{t+i} = 0 | X_0) & P_{\mathcal{D}}^{\circ}(s_{t+i} = X_i, a_{t+i} = 1 | X_0) \end{bmatrix} &= \begin{bmatrix} \delta^2 & (1 - \delta)\delta \\ \delta(1 - \delta) & (1 - \delta)^2 \end{bmatrix} \end{aligned} \quad (66)$$

From the calculation above, it is clear that

$$D_{\text{TV}}(P_{\mathcal{D}}^{\circ}(s_{t+i}, a_{t+i} | s_t) \| P_{\mathcal{D}}(s_{t+i}, a_{t+i} | s_t)) = \varepsilon_h, \quad \forall i \in \{1, 2, \dots, h-1\}. \quad (67)$$

From the computed values of $P_{\mathcal{D}}^{\circ}(s_{t+h-1}, a_{t+h-1} | s_t)$ and $P_{\mathcal{D}}(s_{t+h-1}, a_{t+h-1} | s_t)$, we can derive

$$\begin{aligned} P_{\mathcal{D}}(s_{t+h} = Z | s_t = X_0) &= 0, \\ P_{\mathcal{D}}^{\circ}(s_{t+h} = Z | s_t = X_0) &= 2(1 - \delta)\delta = \varepsilon_h. \end{aligned} \quad (68)$$

1350 From the calculation above, it is clear that
 1351

$$1352 D_{\text{TV}}(P_{\mathcal{D}}^{\circ}(s_{t+h} | s_t) \| P_{\mathcal{D}}(s_{t+h} | s_t)) = \varepsilon_h. \quad (69)$$

1353

1354 Up to now, we have checked that \mathcal{D} is ε_h -open-loop consistent. Now, we are left with analyzing \hat{V}_{ac}
 1355 and V_{ac} . With some calculations, we can obtain the following:

$$1356 \mathbb{E}_{P_{\mathcal{D}}^{\circ}}[R_{t:t+h}] = 1 + \frac{(1 - \varepsilon_h)(\gamma - \gamma^h)}{1 - \gamma}, \\ 1357 \hat{V}_{\text{ac}}(X_0) = \frac{1}{1 - \gamma}, \\ 1358 \quad V_{\text{ac}}(Z) = 0. \quad (70)$$

1362

1363 Now, we are ready to compute $V_{\text{ac}}(X_0)$:

$$1364 V_{\text{ac}}(X_0) = \frac{(1 - \gamma^h) - \varepsilon_h(\gamma - \gamma^h)}{(1 - \gamma)} + \gamma^h [(1 - \varepsilon_h)V_{\text{ac}}(X_0) + \varepsilon_h V_{\text{ac}}(Z)] \\ 1365 = \frac{1 - \gamma^h - \varepsilon_h(\gamma - \gamma^h)}{(1 - \gamma)(1 - \gamma^h(1 - \varepsilon_h))} \quad (71)$$

1369

1370 Finally, with $X_0 \in \text{supp}(\mathcal{D})$, we obtain the desired value difference

$$1371 \hat{V}_{\text{ac}}(X_0) - V_{\text{ac}}(X_0) = \frac{\varepsilon_h \gamma}{(1 - \gamma)(1 - \gamma^h(1 - \varepsilon_h))}. \quad (72)$$

1373

1374 By symmetry, we can flip the reward value (*i.e.*, 0 \rightarrow 1 and 1 \rightarrow 0) to construct the example such that

$$1375 V_{\text{ac}}(X_0) - \hat{V}_{\text{ac}}(X_0) = \frac{\varepsilon_h \gamma}{(1 - \gamma)(1 - \gamma^h(1 - \varepsilon_h))}. \quad (73)$$

1378

□

1379

1380

1381

1382

1383

1384

1385

1386

1387

1388

1389

1390

1391

1392

1393

1394

1395

1396

1397

1398

1399

1400

1401

1402

1403

1404 G.4 PROOF OF COROLLARY 4.5
14051406 **Corollary 4.5** (Optimal Action Chunking Policy). *Let $\pi^* : \mathcal{S} \rightarrow \Delta_{\mathcal{A}}$ be an optimal policy in \mathcal{M} and*
1407 *\mathcal{D}^* be the data collected by π^* . If \mathcal{D}^* is ε_h -open-loop consistent, then under $\text{supp}(\mathcal{D}^*)$,*

1408
$$\|V_{\text{ac}}^* - V^*\|_\infty \leq \|\tilde{V}_{\text{ac}} - V^*\|_\infty \leq \frac{\varepsilon_h \gamma}{(1 - (1 - \varepsilon_h)\gamma^h)(1 - \gamma)} \leq \frac{\varepsilon_h}{(1 - \gamma^h)(1 - \gamma)}, \quad (14)$$

1410

1411 where V^* is the value of the optimal policy π^* , V_{ac}^* is the true value of the optimal action chunking
1412 policy, and \tilde{V}_{ac} is the true value of the action chunking policy from cloning the data \mathcal{D}^* :

1413
$$\tilde{\pi}_{\text{ac}}(a_{t:t+h} \mid s_t) : s_t \mapsto P_{\mathcal{D}^*}(\cdot \mid s_t). \quad (15)$$

1414

1415 *Proof.* Let \hat{V}_{ac} be the fixed point of the following equation:
1416

1417
$$\hat{V}_{\text{ac}}(s_t) = \mathbb{E}_{s_{t+1:t+h+1}, a_{t:t+h} \sim P_{\mathcal{D}^*}(\cdot \mid s_t)} [R_{t:t+h} + \gamma^h \hat{V}_{\text{ac}}(s_{t+h})] \quad (74)$$

1418

1419 where again $R_{t:t+h} = \sum_{t'=t}^{t+h} \gamma^{t'-t} r(s_{t'}, a_{t'})$. The value of the optimal policy is the fixed point of
1420 the following equation:
1421

1422
$$\begin{aligned} V^*(s_t) &= \mathbb{E}_{s_{t+1}, a_t \sim P_{\mathcal{D}^*}(\cdot \mid s_t)} [r(s_t, a_t) + \gamma V^*(s_{t+1})] \\ &= \mathbb{E}_{s_{t:t+2}, a_{t:t+1} \sim P_{\mathcal{D}^*}(\cdot \mid s_t)} [r(s_t, a_t) + \gamma r(s_{t+1}, a_{t+1}) + \gamma V^*(s_{t+2})] \\ &\dots \\ &= \mathbb{E}_{s_{t+1:t+h+1}, a_{t:t+h} \sim P_{\mathcal{D}^*}(\cdot \mid s_t)} [R_{t:t+h} + \gamma^h V^*(s_{t+h})] \end{aligned} \quad (75)$$

1425

1426 which is equivalent to fixed-point equation for \hat{V}_{ac} . Therefore $\hat{V}_{\text{ac}} = V^*$. By Theorem 4.4, we
1427 know that the true value V_{ac} of the action chunking policy $\tilde{\pi}_{\text{ac}}$ that clones \mathcal{D}^* is close to \hat{V}_{ac} . More
1428 specifically, for all $s_t \in \text{supp}(\mathcal{D}^*)$,
1429

1430
$$|\hat{V}_{\text{ac}}(s_t) - \tilde{V}_{\text{ac}}(s_t)| \leq \frac{\gamma \varepsilon_h}{(1 - \gamma)(1 - (1 - \varepsilon_h)\gamma^h)}, \quad (76)$$

1431

1432 which means that
1433

1434
$$V^*(s_t) - \tilde{V}_{\text{ac}}(s_t) \leq \frac{\gamma \varepsilon_h}{(1 - \gamma)(1 - (1 - \varepsilon_h)\gamma^h)}, \quad (77)$$

1435

1436 where we can remove the absolute value operator because $V^*(s_t)$ is by definition always at least
1437 as large as $\tilde{V}_{\text{ac}}(s_t)$. Since the optimal action chunking policy, by definition, attains equally good
1438 or better values (over \mathcal{S}) represented by V_{ac} , and the optimal policy π^* also attains equally good
1439 or better value (i.e., V^*) compared to that of the optimal action chunking policy π_{ac}^* (i.e., V_{ac}^*), the
1440 following inequality holds for all $s_t \in \text{supp}(\mathcal{D}^*)$:
1441

1442
$$V^*(s_t) \geq V_{\text{ac}}^*(s_t) \geq \tilde{V}_{\text{ac}}(s_t). \quad (78)$$

1443

1444 Therefore,
1445

1446
$$V_{\text{ac}}^*(s_t) - V^*(s_t) \leq \tilde{V}_{\text{ac}}(s_t) - V^*(s_t) \leq \frac{\gamma \varepsilon_h}{(1 - \gamma)(1 - (1 - \varepsilon_h)\gamma^h)}, \quad (79)$$

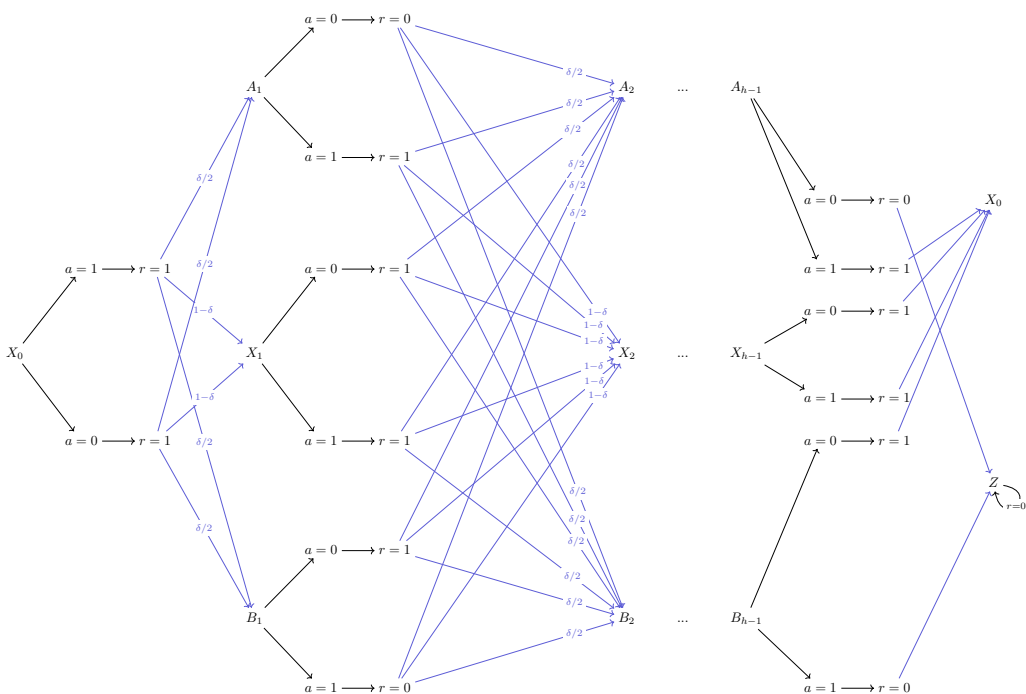
1447

1448 as desired. \square
14491450
1451
1452
1453
1454
1455
1456
1457

1458 G.5 PROOF OF COROLLARY F.2
14591460 **Corollary F.2** (Worse-case Optimality Gap for Action Chunking Policy). *For any $\gamma \in [0, 1], \varepsilon_h \in$
1461 $[0, 1/2]$, there exists an MDP \mathcal{M} whose optimal policy π^* induces a data distribution \mathcal{D}^* that is
1462 weakly ε_h -open-loop consistent, such that for some $s \in \text{supp}(P_{\mathcal{D}^*}(s_t))$,*

1463
1464
$$V^*(s) - V_{\text{ac}}^*(s) = \frac{\gamma \varepsilon_h}{(1 - \gamma)(1 - (1 - \varepsilon_h)\gamma^h)}. \quad (35)$$

1465

1466
1467 *Proof.* To show this, we need a slightly more complicated MDP (compared to the $2h$ -state MDP we
1468 use in the proof Appendix G.3). The MDP we construct for this proof is a $(3h - 1)$ -state MDP as
1469 illustrated in Figure 8.
14701493 Figure 8: A $(3h - 1)$ -state MDP that is constructed to meet the upper-bound in Corollary 4.5.
14941495
1496 The optimal policy we pick is described as the following:
1497

1498
$$\begin{aligned} \pi^*(a = 0 | X_i) &= 1/2 \\ 1499 \pi^*(a = 1 | X_i) &= 1/2 \\ 1500 \pi^*(a = 1 | A_i) &= 1 \\ 1501 \pi^*(a = 0 | B_i) &= 1/2 \end{aligned} \quad (80)$$

1502

1503 This induces the following state distribution,
1504

1505
$$\begin{aligned} P_{\mathcal{D}^*}(s_{t+i} = A_i | s_t = X_0) &= P_{\mathcal{D}^*}(s_{t+i} = B_i | s_t = X_0) \\ 1506 P_{\mathcal{D}^*}^o(s_{t+i} = A_i | s_t = X_0) &= P_{\mathcal{D}^*}^o(s_{t+i} = B_i | s_t = X_0) = \delta/2, \\ 1507 P_{\mathcal{D}^*}(s_{t+i} = X_i | s_t = X_0) &= P_{\mathcal{D}^*}(s_{t+i} = X_i | s_t = X_0) = 1 - \delta, \end{aligned} \quad (81)$$

1508

1509 and a fully factorized distribution for the action chunk,
1510

1511
$$P_{\mathcal{D}^*}^o(a_{t+i} = 0 | s_t) = P_{\mathcal{D}^*}^o(a_{t+i} = 0 | s_t, a_{t:t+i}) = \frac{1}{2}(\delta_{a=0} + \delta_{a=1}). \quad (82)$$

1512 Now, we derive the condition on δ when the optimal data \mathcal{D}^* is ε_h -open-loop consistent. We start by
 1513 calculating the TV distance discrepancy for the future state-action distribution:

$$\begin{aligned} 1515 \quad & D_{\text{TV}}(P_{\mathcal{D}^*}^{\text{open}}(s_{t+i}, a_{t+i} | s_t) \| P_{\mathcal{D}^*}(s_{t+i}, a_{t+i} | s_t)) \\ 1516 \quad &= \frac{1}{2} \left\| \begin{bmatrix} 0 & \delta/2 \\ (1-\delta)/2 & (1-\delta)/2 \\ \delta/2 & 0 \end{bmatrix} - \begin{bmatrix} \delta/4 & \delta/4 \\ (1-\delta)/2 & (1-\delta)/2 \\ \delta/4 & \delta/4 \end{bmatrix} \right\|_{1,1} \\ 1518 \quad &= \delta/2. \\ 1519 \end{aligned} \quad (83)$$

1520 In the second line of the equations above, each row in the matrix corresponds to a distinct action
 1521 $a_{t+i} \in \{0, 1\}$ and each row in the matrix corresponds to a distinct state $s_{t+i} \in \{A_i, X_i, B_i\}$.

1522 Next, we calculate the TV distance discrepancy for s_{t+h} :

$$\begin{aligned} 1524 \quad & D_{\text{TV}}(P_{\mathcal{D}^*}^{\text{open}}(s_{t+h} | s_t) \| P_{\mathcal{D}^*}(s_{t+h} | s_t)) \\ 1525 \quad &= \frac{1}{2} \|[1 \ 0] - [1 - \delta/2 \ \delta/2]\|_1 \\ 1526 \quad &= \delta/2. \\ 1527 \end{aligned} \quad (84)$$

1528 In the second line of the equations above, each element in the vector corresponds to a distinct state
 1529 $s_{t+h} \in \{X_0, Z\}$. Up to now, we have concluded that \mathcal{D}^* is $(\delta/2)$ -open-loop consistent.

1530 Due to the symmetric structure of this MDP, it is clear that any action chunking policy $\pi_{\text{ac}}(X_0) =$
 1531 $a_{t:t+h} \in \{0, 1\}$ is optimal and achieve the following value:

$$\begin{aligned} 1534 \quad & V_{\text{ac}}^*(X_0) = 1 + (1 - \delta/2) \left[\frac{\gamma - \gamma^h}{1 - \gamma} + \gamma^h V_{\text{ac}}^*(X_0) \right] \\ 1535 \quad &= \frac{(1 - \gamma) + (1 - \delta/2)(\gamma - \gamma^h)}{(1 - \gamma)(1 - (1 - \delta/2)\gamma^h)}. \\ 1536 \end{aligned} \quad (85)$$

1537 The optimal closed-loop policy can achieve the maximum possible return

$$1538 \quad V^*(X_0) = \frac{1}{1 - \gamma}. \quad (86)$$

1539 Therefore, with $\varepsilon_h = \delta/2$, the optimality gap achieved by this $(3h - 1)$ -state MDP is

$$1540 \quad V^*(X_0) - V_{\text{ac}}^*(X_0) = \frac{\varepsilon_h \gamma}{(1 - \gamma)(1 - (1 - \varepsilon_h)\gamma^h)}, \quad (87)$$

1541 as desired. □

1542
 1543
 1544
 1545
 1546
 1547
 1548
 1549
 1550
 1551
 1552
 1553
 1554
 1555
 1556
 1557
 1558
 1559
 1560
 1561
 1562
 1563
 1564
 1565

1566 G.6 PROOF OF THEOREM 4.6
1567

1568 **Theorem 4.6** (Q-Learning with Action Chunking Policy on Off-policy Data). *If \mathcal{D} is strongly ε_h -
1569 open-loop consistent and $\text{supp}(\mathcal{D}) \supseteq \text{supp}(\mathcal{D}^*)$, with \mathcal{D}^* being the data distribution of an arbitrary
1570 optimal policy π^* under \mathcal{M}), then the following bound holds under $\text{supp}(\mathcal{D}^*)$:*

$$1572 \|V_{\text{ac}}^+ - V^*\|_\infty \leq \frac{\varepsilon_h \gamma}{1 - \gamma} \left[\frac{2}{1 - (1 - 2\varepsilon_h)\gamma^h} + \frac{1}{1 - (1 - \varepsilon_h)\gamma^h} \right] \leq \frac{3\varepsilon_h}{(1 - \gamma)(1 - \gamma^h)}. \quad (18)$$

1574 where V^* is the value of an optimal policy under \mathcal{M} .

1576

1577 *Proof of Theorem 4.6.* We start by constructing a bound between \hat{Q}_{ac}^+ and Q_{ac}^* , the solution of the
1578 following bellman equation:

$$1580 Q_{\text{ac}}^*(s_t, a_{t:t+h}) = \mathbb{E}_{s_{t+1:t+h+1} \sim P_{\mathcal{D}}^\circ(\cdot|s_t, a_{t:t+h})} \left[R_{t:t+h} + \gamma^h \max_{a_{t+h:t+2h}} Q_{\text{ac}}^*(s_{t+h}, a_{t+h:t+2h}) \right]. \quad (88)$$

1582 Intuitively, Q_{ac}^* is the Q-function of the optimal action chunking policy π_{ac}^* that can be learned from
1583 \mathcal{D} . Because $\text{supp}(\mathcal{D}) \supseteq \text{supp}(\mathcal{D}^*)$, π_{ac}^* is at least as good as $\tilde{\pi}_{\text{ac}}$, the action chunking policy obtained
1584 by behavior cloning \mathcal{D}^* . Bounding the difference between \hat{Q}_{ac}^+ and Q_{ac}^* allows us to leverage the
1585 bound in Corollary 4.5 to form a bound between \hat{V}_{ac}^+ and V^* .

1586 Since \mathcal{D} is strongly ε_h -open-loop consistent,

$$1589 D_{\text{TV}}(T(s_{t+h'} | s_t, a_{t:t+h'}) \| P_{\mathcal{D}}(s_{t+h'} | s_t, a_{t:t+h})) \leq \varepsilon_h, \forall h' \in \{1, \dots, h-1\}. \quad (89)$$

1590

1591 Since \mathcal{D}^* is also strongly ε_h -open-loop consistent,

$$1593 D_{\text{TV}}(T(s_{t+h'} | s_t, a_{t:t+h'}) \| P_{\mathcal{D}^*}(s_{t+h'} | s_t, a_{t:t+h})) \leq \varepsilon_h, \forall h' \in \{1, \dots, h-1\}. \quad (90)$$

1594 Using the transitive property of TV distance, we have

$$1596 D_{\text{TV}}(P_{\mathcal{D}}(s_{t+h'} | s_t, a_{t:t+h}) \| P_{\mathcal{D}^*}(s_{t+h'} | s_t, a_{t:t+h})) \leq 2\varepsilon_h, \forall h' \in \{1, \dots, h-1\}. \quad (91)$$

1597

1598 Now, for the h -step reward, we have

$$1600 \left| \mathbb{E}_{P_{\mathcal{D}}(\cdot|s_t, a_{t:t+h})} [R_{t:t+h}] - \mathbb{E}_{P_{\mathcal{D}^*}(\cdot|s_t, a_{t:t+h})} [R_{t:t+h}] \right| \\ 1601 \leq \sum_{h'=1}^{h-1} \left[\gamma^{h'} D_{\text{TV}}(P_{\mathcal{D}}(s_{t+h'} | s_t, a_{t:t+h}) \| P_{\mathcal{D}^*}(s_{t+h'} | s_t, a_{t:t+h})) \right] \\ 1602 \leq \frac{2(\gamma - \gamma^h)\varepsilon_h}{1 - \gamma}. \quad (92)$$

1607 Similarly, for the value h -step into the future, we can use Lemma G.2 to obtain the following bound:
1608

$$1609 \left| \mathbb{E}_{s_{t+h} \sim P_{\mathcal{D}}(s_{t+h} | s_t)} [V^*(s_{t+h})] - \mathbb{E}_{s_{t+h} \sim P_{\mathcal{D}^*}(s_{t+h} | s_t)} [\hat{V}_{\text{ac}}^+(s_{t+h})] \right| \\ 1610 \leq 2\varepsilon_h + (1 - 2\varepsilon_h) \sup_{s_{t+h} \in \mathcal{D}^*} |V^*(s_{t+h}) - \hat{V}_{\text{ac}}^+(s_{t+h})|. \quad (93)$$

1613

1614 We define $Q^*(s_t, a_{t:t+h})$ to be

$$1616 Q^*(s_t, a_{t:t+h}) := \mathbb{E}_{P_{\mathcal{D}^*}(\cdot|s_t, a_{t:t+h})} [R_{t:t+h} + \gamma^h V^*(s_{t+h})]. \quad (94)$$

1617 It is clear that

$$1619 V^*(s_t) = \mathbb{E}_{a_{t:t+h} \sim P_{\mathcal{D}^*}} [Q^*(s_t, a_{t:t+h})]. \quad (95)$$

Combining the bound for the h -step reward and the bound on the value for s_{t+h} , for all $s_t, a_{t:t+h} \in \text{supp}(P_{\mathcal{D}^*}(s_t, a_{t:t+h}))$,

$$\begin{aligned}
 \Delta(s_t, a_{t:t+h}) &= Q^*(s_t, a_{t:t+h}) - \hat{Q}_{\text{ac}}^+(s_t, a_{t:t+h}) \\
 &\leq 2\varepsilon_h \gamma^h + \frac{2(\gamma - \gamma^h)\varepsilon_h}{1 - \gamma} + (1 - 2\varepsilon_h)\gamma^h \left(V^*(s_{t+h}) - \hat{V}_{\text{ac}}^+(s_{t+h}) \right) \\
 &\leq \frac{2\varepsilon_h \gamma}{1 - \gamma} + (1 - 2\varepsilon_h)\gamma^h \left(\mathbb{E}_{P_{\mathcal{D}^*}}[Q^*(s_{t+h}, a_{t+h:t+2h})] - \sup_{a_{t+h:t+2h}} \hat{Q}_{\text{ac}}^+(s_{t+h}, a_{t+h:t+2h}) \right) \\
 &\leq \frac{2\varepsilon_h \gamma}{1 - \gamma} + (1 - 2\varepsilon_h)\gamma^h \left(\mathbb{E}_{P_{\mathcal{D}^*}}[\hat{Q}_{\text{ac}}^+(s_{t+h}, a_{t+h:t+2h}) + \Delta(s_{t+h}, a_{t+h:t+2h})] - \sup_{a_{t+h:t+2h}} \hat{Q}_{\text{ac}}^+(s_{t+h}, a_{t+h:t+2h}) \right) \\
 &\leq \frac{2\varepsilon_h \gamma}{1 - \gamma} + (1 - 2\varepsilon_h)\gamma^h \sup_{s_{t+h}, a_{t+h:t+2h}} [\Delta(s_{t+h}, a_{t+h:t+2h})],
 \end{aligned} \tag{96}$$

which can be recursively expanded to obtain

$$V^*(s_t) - \hat{V}_{\text{ac}}^+(s_t) \leq \frac{2\varepsilon_h \gamma}{(1-\gamma)(1-(1-2\varepsilon_h)\gamma^h)}. \quad (97)$$

By Theorem 4.4, for all $s_t \in \text{supp}(\mathcal{D})$,

$$\left| \hat{V}_{\text{ac}}^+(s_t) - V_{\text{ac}}^+(s_t) \right| \leq \frac{\varepsilon_h \gamma}{(1 - \gamma)(1 - (1 - \varepsilon_h)\gamma^h)}. \quad (98)$$

Combining the two inequalities above, for all $\epsilon \in \text{supp}(\mathcal{D}^*)$

$$V^*(s_t) - V_{\text{ac}}^+(s_t) \leq \frac{\varepsilon_h \gamma}{1 - \gamma} \left[\frac{2}{1 - (1 - 2\gamma) \gamma^h} + \frac{1}{1 - (1 - \gamma) \gamma^h} \right]. \quad (99)$$

1

1674 **G.7 PROOF OF THEOREM F.3**
1675

1676 **Theorem F.3** (Worst-case Analysis of Q-Learning with Action Chunking Policy on Off-policy Data).
 1677 *For any $\varepsilon_h \in (0, 1/5)$, $\gamma \in (0, 1)$, $c_1 \in (0, \varepsilon_h/2)$, and $c_2 \in (0, 2\varepsilon_h\gamma)$, there exists an MDP \mathcal{M}
 1678 and strongly ε_h -open-loop consistent data distribution \mathcal{D} and \mathcal{D}^* with $\text{supp}(P_{\mathcal{D}}(s_t, a_{t:t+h})) \supseteq$
 1679 $\text{supp}(P_{\mathcal{D}^*}(s_t, a_{t:t+h}))$, such that for some $s \in \text{supp}(P_{\mathcal{D}^*}(s_t))$,*

$$1680 \quad V^*(s) - V_{\text{ac}}^+(s) = \frac{2\varepsilon_h\gamma - c_2}{(1-\gamma)(1 - (1-2\varepsilon_h)\gamma^h)} + \frac{\varepsilon_h\gamma}{(1-\gamma)(1 - (1-\varepsilon_h - c_1)\gamma^h)}, \quad (36)$$

1683 where V^* is the value of an optimal policy and V_{ac}^+ is the true value of π_{ac}^+ . As $c_1, c_2 \rightarrow 0$,

$$1685 \quad V^*(s) - V_{\text{ac}}^+(s) \rightarrow \frac{\varepsilon_h\gamma}{1-\gamma} \left[\frac{2}{1 - (1-2\varepsilon_h)\gamma^h} + \frac{1}{1 - (1-\varepsilon_h)\gamma^h} \right]. \quad (37)$$

1687 The examples in the following proof of Theorem F.3 (available in Appendix G.7) provide insights
 1688 on the factor of 3 in $V^* - V_{\text{ac}}^+ \leq 3\varepsilon_h H \bar{H}$ (with $H = 1/(1-\gamma)$, $\bar{H} = 1/(1-\gamma^h)$) is necessary. In
 1689 particular, the worse case can be roughly seen as a combination of the two main results that we have
 1690 presented so far:

- 1692 1. $V^* - V_{\text{ac}}^* \approx \varepsilon_h H \bar{H}$ (Corollary 4.5, Corollary F.2): the optimal action chunking policy is
 1693 $(\varepsilon_h H^2)$ -suboptimal due to its inability to react to environment stochasticity, quantified by
 1694 the strongly- ε_h open-loop consistency of \mathcal{D}^* .
- 1695 2. $V_{\text{ac}}^* - \hat{V}_{\text{ac}}^+ \approx \varepsilon_h H \bar{H}$ (a transformation of Theorem 4.4 and Theorem F.1 on the optimal
 1696 action chunking policy π_{ac}^*): the value *under-estimation* bias can incur another factor of
 1697 $\varepsilon_h H \bar{H}$ bringing up the sub-optimality of \hat{V}_{ac}^+ to at most $2\varepsilon_h H \bar{H}$, and finally,
- 1699 3. $\hat{V}_{\text{ac}}^+ - V_{\text{ac}}^+ \approx \varepsilon_h H \bar{H}$ (Theorem 4.4, Theorem F.1): the action chunking value function may
 1700 prefer an *overestimated* action chunking policy π_{ac}^+ where its actual value is again $\varepsilon_h H \bar{H}$
 1701 from its estimated value, resulting in a total sub-optimality of $3\varepsilon_h H \bar{H}$.

1702 Our construction (in the proof of Theorem F.3) directly builds on the above insights by using a 2-part
 1703 MDP where the first part corresponds to an $(\varepsilon_h H \bar{H})$ -underestimated action chunking policy that has
 1704 a $(\varepsilon_h H \bar{H})$ -optimality gap from the optimal closed-loop policy and the second part corresponds to an
 1705 $(\varepsilon_h H \bar{H})$ -overestimated action chunking policy that has a $(3\varepsilon_h H \bar{H})$ -optimality gap that is preferred
 1706 by the value function.

1707 Before we start our main proof, we first introduce a Lemma that helps simplifies the inequalities.

1709 **Lemma G.5** (Optimality gap comparator). *For any $\tilde{\gamma} \in [0, 1)$ and $0 < \varepsilon_1 < \varepsilon_2 < 1$,*

$$1710 \quad \frac{\varepsilon_1}{1 - (1 - \varepsilon_1)\tilde{\gamma}} < \frac{\varepsilon_2}{1 - (1 - \varepsilon_2)\tilde{\gamma}}. \quad (100)$$

1713 *Proof.*

$$\begin{aligned} 1715 \quad 0 &< (1 - \gamma)(\varepsilon_2 - \varepsilon_1) \\ 1716 \quad &= \varepsilon_2 - \varepsilon_2\tilde{\gamma} - \varepsilon_1 + \varepsilon_1\tilde{\gamma} \\ 1717 \quad &= \varepsilon_2 - \varepsilon_2\tilde{\gamma} + \varepsilon_1\varepsilon_2\tilde{\gamma} - \varepsilon_1 + \varepsilon_1\tilde{\gamma} - \varepsilon_1\varepsilon_2\tilde{\gamma} \\ 1718 \quad &= \varepsilon_2(1 - (1 - \varepsilon_1)\tilde{\gamma}) - \varepsilon_1(1 - (1 - \varepsilon_2)\tilde{\gamma}) \end{aligned} \quad (101)$$

1719 Since $1 - (1 - \varepsilon_1)\tilde{\gamma} > 0$ and $1 - (1 - \varepsilon_2)\tilde{\gamma} > 0$, we can divide both sides by $(1 - (1 - \varepsilon_1)\tilde{\gamma})(1 -$
 1720 $(1 - \varepsilon_2)\tilde{\gamma})$ to get

$$1722 \quad 0 < \frac{\varepsilon_2}{1 - (1 - \varepsilon_2)\tilde{\gamma}} - \frac{\varepsilon_1}{1 - (1 - \varepsilon_1)\tilde{\gamma}}, \quad (102)$$

1724 as desired. □

1725 Now, we begin the main proof as follows.

1728
1729 *Proof of Theorem F.3.* We prove by constructing the following $(2h + 4)$ -state MDP where the agent
1730 can take any of the three actions $\{0, 1, 2\}$ at each state (see a diagram in Figure 9).

1731 **Notations:** we start by introducing some abbreviations for all action chunks that appear in this proof:

$$\begin{aligned} a_{t:t+h}^* &= (0, 0, 0, \dots, 0) \\ a_{t:t+h}^\diamond &= (0, 1, 0, \dots, 0) \\ a_{t:t+h}^\bullet &= (0, 2, 0, \dots, 0) \\ a_{t:t+h}^\triangle &= (1, 1, 1, \dots, 1) \\ a_{t:t+h}^\circ &= (1, 0, 1, \dots, 1) \\ a_{t:t+h}^\times &= (1, 2, 1, \dots, 1) \end{aligned} \tag{103}$$

1740 The first three action chunks $a_{t:t+h}^*, a_{t:t+h}^\diamond, a_{t:t+h}^\bullet$ are only possible in the top branch and the last
1741 three action chunks $a_{t:t+h}^\triangle, a_{t:t+h}^\circ, a_{t:t+h}^\times$ are only possible in the bottom branch because the first
1742 action in the action chunk deterministically divides it into the two branches.

1743 Among these action chunks, it is clear by inspection that $\pi_{ac}(X_0) = (0, 0, \dots, 0)$ is the optimal
1744 action chunking policy, and thus we directly use ‘ $*$ ’ to denote $a_{t:t+h}^* = (0, 0, \dots, 0)$. $a_{t:t+h}^\triangle$ is also of
1745 great importance: as we will show later, $\pi_{ac}^+(X_0) = a_{t:t+h}^\triangle$. The *actual* values and *nominal/estimated*
1746 values for these action chunks are $(V_{ac}^*, V_{ac}^\diamond, V_{ac}^\bullet, V_{ac}^\triangle, V_{ac}^\circ, V_{ac}^\times)$ and $(\hat{V}_{ac}^*, \hat{V}_{ac}^\diamond, \hat{V}_{ac}^\bullet, \hat{V}_{ac}^\triangle, \hat{V}_{ac}^\circ, \hat{V}_{ac}^\times)$
1747 respectively. Much of the focus of this proof is to calculate the optimality gap, which is the difference
1748 between the optimal closed-loop value and the action chunking policy value (either estimated or
1749 actual):

$$\text{actual optimality gap: } V^*(X_0) - V_{ac}^{[\cdot]}(X_0) \tag{104}$$

$$\text{nominal optimality gap: } V^*(X_0) - \hat{V}_{ac}^{[\cdot]}(X_0) \tag{105}$$

1755 **High-level proof sketch:** The MDP contains two branches: a top branch where (as we will show)
1756 both the optimal policy π^* and the optimal action chunking policy π_{ac}^* take, and a bottom branch
1757 where (as we will also show) the learned action chunking policy π_{ac}^+ takes. The key idea of the
1758 construction is that for the top branch, we have

$$V^*(X_0) - \hat{V}_{ac}^*(X_0) \approx \frac{2\varepsilon_h\gamma}{(1-\gamma)(1-(1-2\varepsilon_h)\gamma^h)}, \tag{106}$$

1762 and for the bottom branch, we have

$$\hat{V}_{ac}^*(X_0) < \hat{V}_{ac}^+(X_0) \approx V_{ac}^+(X_0) + \frac{\varepsilon_h\gamma}{(1-\gamma)(1-(1-\varepsilon_h)\gamma^h)}. \tag{107}$$

1766 Combining these two together gives

$$V^*(X_0) - V_{ac}^+(X_0) \approx \frac{\varepsilon_h\gamma}{1-\gamma} \left[\frac{2}{1-(1-2\varepsilon_h)\gamma^h} + \frac{1}{1-(1-\varepsilon_h)\gamma^h} \right]. \tag{108}$$

1770 We use ‘ \approx ’ because the equalities are not strictly achievable but (as we will show) can be made
1771 arbitrarily close.

1772 The proof can be roughly divided into the following steps (we use ‘ \approx ’ to help illustrate the high-level
1773 idea below and use more precise argument in the actual proof):

1. **MDP description:** we formally describe the transition dynamics T and the reward function
1776 r for each state-action pair for both the top and the bottom branches.
2. **Strong ε_h -open-loop consistency of \mathcal{D}^* :** we then check the strong open-loop con-
1779 sistency assumption for \mathcal{D}^* .
3. **Data distribution \mathcal{D}_{top} for the top branch:** we use a mixture data distribution
1781 from two policies to construct \mathcal{D}_{top} .

1782 4. Strong ε_h -open-loop consistency of \mathcal{D}_{top} : we then check that the constructed
 1783 data distribution of the top branch satisfies the strongly open-loop consistency assumption.
 1784 Note that we can do so separately for the top and the bottom because these two distributions
 1785 have non-overlapping support in $a_{t:t+h}$.
 1786

1787 5. The optimality gap and value estimation error for the top branch: we prove that $V^*(X_0) - V_{\text{ac}}^*(X_0) = \frac{\varepsilon_h \gamma}{(1-\gamma)(1-(1-2\varepsilon_h)\gamma^h)}$ and $V^*(X_0) - \hat{V}_{\text{ac}}^*(X_0) = \frac{2\varepsilon_h \gamma}{(1-\gamma)(1-(1-2\varepsilon_h)\gamma^h)}$ and the other two possible action chunks $a_{t:t+h}^\diamond = (0, 1, 0, \dots)$ and
 1788 $a_{t:t+h}^\bullet = (0, 2, 0, \dots)$ both admit lower estimated values compared to $a_{t:t+h}^*$: $\hat{V}_{\text{ac}}^\diamond(X_0) < \hat{V}_{\text{ac}}^*(X_0)$ and $\hat{V}_{\text{ac}}^\bullet(X_0) < \hat{V}_{\text{ac}}^*(X_0)$.
 1789

1790 6. Data distribution $\mathcal{D}_{\text{bottom}}$ for the bottom branch: we again use a mixture data
 1791 distribution from two different policies to construct $\mathcal{D}_{\text{bottom}}$.
 1792

1793 7. Strong ε_h -open-loop consistency of $\mathcal{D}_{\text{bottom}}$: we then check that the constructed
 1794 data distribution of the bottom branch satisfies the strongly open-loop consistency assumption.
 1795

1796 8. The optimality gap and value estimation error for the bottom branch: we prove that $V^*(X_0) - \hat{V}_{\text{ac}}^\Delta(X_0) \approx \frac{2\varepsilon_h \gamma}{(1-\gamma)(1-(1-2\varepsilon_h)\gamma^h)}$ and $\hat{V}_{\text{ac}}^\Delta(X_0) - V_{\text{ac}}^\Delta(X_0) = \frac{\varepsilon_h \gamma}{(1-\gamma)(1-(1-\varepsilon_h)\gamma^h)}$, and the other two possible action chunks $a_{t:t+h}^\diamond = (1, 0, 0, \dots)$ and
 1797 $a_{t:t+h}^\times = (1, 2, 0, \dots)$ both admit lower estimated values compared to $a_{t:t+h}^\Delta$:
 1798 $\hat{V}_{\text{ac}}^\diamond(X_0) < \hat{V}_{\text{ac}}^\Delta(X_0)$ and $\hat{V}_{\text{ac}}^\times(X_0) < \hat{V}_{\text{ac}}^\Delta(X_0)$. Moreover $a_{t:t+h}^*$ also admits a lower estimated value compared to $a_{t:t+h}^\Delta$: $\hat{V}_{\text{ac}}^*(X_0) < \hat{V}_{\text{ac}}^\Delta(X_0)$ which proves $\pi_{\text{ac}}^+(X_0) = a_{t:t+h}^\Delta$ and thus concluding our proof: $V^*(X_0) - V_{\text{ac}}^+(X_0) \approx \frac{2\varepsilon_h \gamma}{(1-\gamma)(1-(1-2\varepsilon_h)\gamma^h)} + \frac{\varepsilon_h \gamma}{(1-\gamma)(1-(1-\varepsilon_h)\gamma^h)}$.
 1799

1800 Now we begin our proof as follows.
 1801

1802 Step 1. MDP description (Figure 9).
 1803

1804 The transition function T of the MDP is defined as follows (from left to right):
 1805

$$\begin{aligned}
 T(Z \mid Z, a) &= T(G \mid G, a) = 1, \quad \forall a, \\
 T(Z \mid s, a = 2) &= 1, \quad \forall a, \forall s : s \neq G \\
 T(X_1 \mid X_0, a = 0) &= 1 - 2\varepsilon_h \\
 T(\tilde{X}_1 \mid X_0, a = 0) &= \varepsilon_h \\
 T(C \mid X_0, a = 0) &= \varepsilon_h \\
 T(Y_1 \mid X_0, a = 1) &= 1 - \varepsilon_h - c_1 \\
 T(\tilde{Y}_1 \mid X_0, a = 1) &= \varepsilon_h \\
 T(G \mid X_0, a = 1) &= c_1 \\
 T(X_2 \mid X_1, a = 0) &= 1 \\
 T(X_2 \mid \tilde{X}_1, a = 1) &= 1 \\
 T(X_2 \mid C, a = 1) &= 1 \tag{109} \\
 T(Z \mid X_1, a = 1) &= 1 \\
 T(Z \mid C, a = 0) &= 1 \\
 T(G \mid \tilde{X}_1, a = 0) &= 1 \\
 T(Y_2 \mid Y_1, a = 1) &= 1 \\
 T(Y_2 \mid \tilde{Y}_1, a = 0) &= 1 \\
 T(Z \mid Y_1, a = 0) &= 1 \\
 T(Z \mid \tilde{Y}_1, a = 1) &= 1 \\
 T(X_{i+1} \mid X_i, a \in \{0, 1\}) &= T(Y_{i+1} \mid Y_i, a \in \{0, 1\}) = 1, \quad \forall i \in \{2, \dots, h-2\} \\
 T(X_0 \mid X_{h-1}, a \in \{0, 1\}) &= T(Y_0 \mid Y_{h-1}, a \in \{0, 1\}) = 1
 \end{aligned}$$

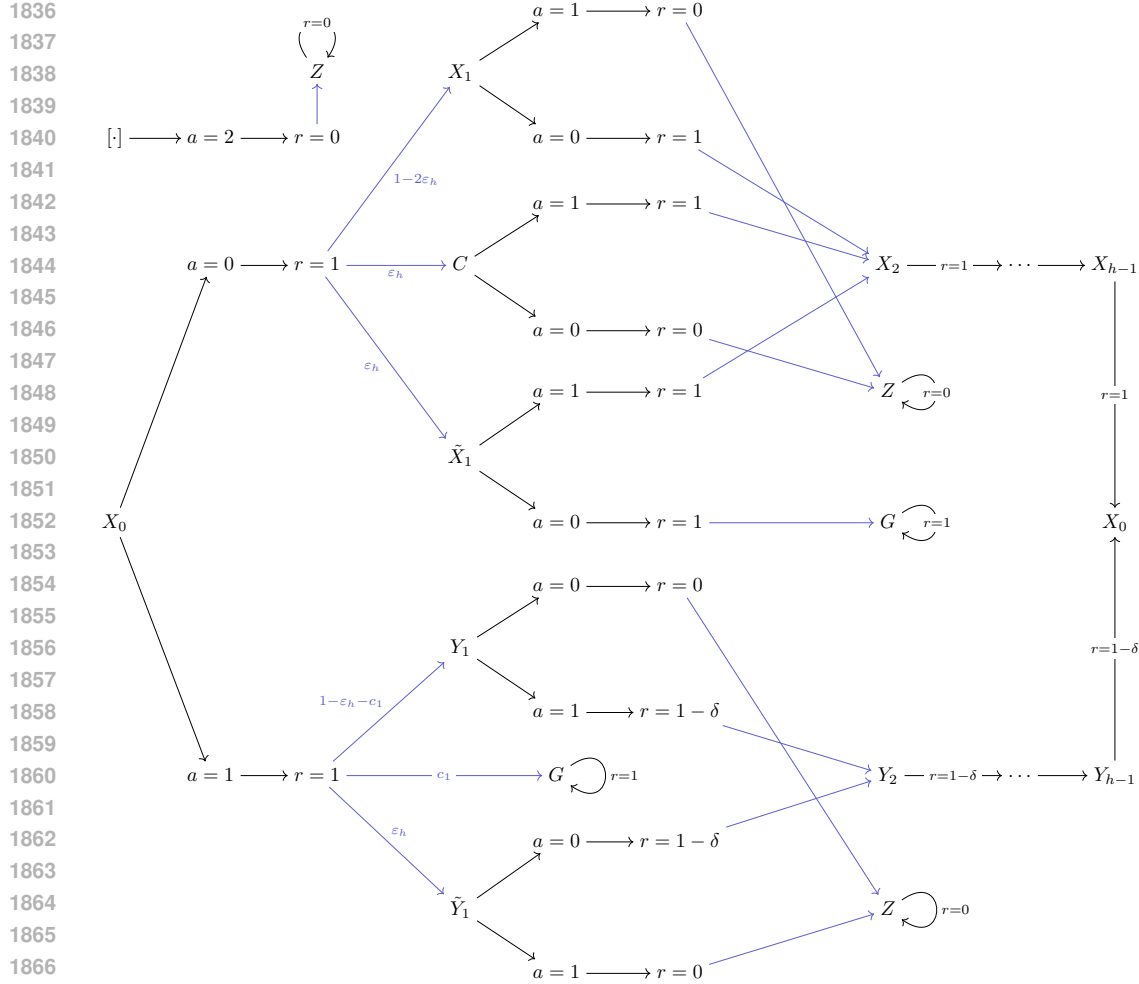


Figure 9: A $(2h + 4)$ -state MDP that is constructed to illustrate the MDP constructed to meet the exact upper-bound optimality gap in Theorem 4.6. We redraw the same states Z, G, X_0 in multiple locations in the diagram above for better clarity.

The reward function is defined as

$$\begin{aligned}
 r(Z, a) &= 0, \quad \forall a \\
 r(G, a) &= 1, \quad \forall a \\
 r(s, a=2) &= 0, \quad \forall s : s \neq G \\
 r(X_0, a=0) &= r(X_0, a=1) = 1, \\
 r(C, a=1) &= r(X_1, a=0) = r(\tilde{X}_1, a \in \{0, 1\}) = 1, \\
 r(C, a=0) &= r(X_1, a=1) = 0, \\
 r(Y_1, a=1) &= r(\tilde{Y}_1, a=0) = 1 - \delta, \\
 r(Y_1, a=0) &= r(\tilde{Y}_1, a=1) = 0, \\
 r(X_i, a \in \{0, 1\}) &= 1, \quad \forall i \in \{2, \dots, h-1\} \\
 r(Y_i, a \in \{0, 1\}) &= 1 - \delta, \quad \forall i \in \{2, \dots, h-1\}
 \end{aligned} \tag{110}$$

Notably, there are some special states:

- State Z : a self-looping “black hole” state that always gets 0 reward at each time step and thus has a constant value of 0.

- 1890 • State G : a self-looping ‘‘black hole’’ state that always gets 1 reward at each time step and
1891 thus has a constant value of $1/(1-\gamma)$.
- 1892
- 1893 • State X_0 : the special state that branches out based on the action taken. The agent periodically
1894 visit this state every h steps unless it has been trapped in either Z or G . As we proceed in
1895 the proof, we will encounter factors in the form of $\frac{1}{1-b\gamma^h}$ in the calculation of the optimality
1896 gap. These factors come from the agent looping around and revisiting X_0 with b -probability
1897 each cycle.

1898 These two absorbing states are important because their values sit at the boundary of the value range of
1899 our value function $V(s) \in [0, 1/(1-\gamma)]$. Shifting the reaching probability from Z to G or the other
1900 way around results in the biggest possible difference in the policy value. Our construction hinges on
1901 the constructing \mathcal{D} such that

- 1903 1. $P_{\mathcal{D}}(\cdot | s_t, \pi^*(s_t))$ and $T(\cdot | s_t, \pi^*(s_t))$ differs by only ε_h (in TV distance as required by the
1904 strongly open-loop consistency assumption) where precisely ε_h probability mass is moved
1905 from reaching state Z to reaching state G . This causes the \hat{V}_{ac}^* to precisely underestimate
1906 the value of V_{ac}^* by $\frac{\varepsilon_h \gamma^h}{(1-\gamma)(1-(1-2\varepsilon_h)\gamma^h)}$. It is worth noting that we cannot make the $2\varepsilon_h$ in
1907 the denominator ε_h because \hat{V}_{ac}^* needs to simultaneously maintain a value gap with V^* . If
1908 we were to construct an example where $\hat{V}_{ac}^*(X_0) - V_{ac}^*(X_0) = V_{ac}^*$ be $\frac{\varepsilon_h \gamma^h}{(1-\gamma)(1-(1-\varepsilon_h)\gamma^h)}$,
1909 it would enforce $V_{ac}^*(X_0) = V^*(X_0)$ because there would be no probability mass left to
1910 create the gap between V^* and V_{ac}^* . With an extra ε_h in the denominator, we can also make
1911 the optimality gap of V_{ac}^* precisely $\frac{\varepsilon_h \gamma^h}{(1-\gamma)(1-(1-2\varepsilon_h)\gamma^h)}$, bringing the combined value gap
1912 (between V^* and \hat{V}_{ac}^*) up to $\frac{2\varepsilon_h \gamma^h}{(1-\gamma)(1-(1-2\varepsilon_h)\gamma^h)}$.
- 1913 2. $P_{\mathcal{D}}(\cdot | s_t, \pi^+(s_t))$ and $T(\cdot | s_t, \pi^+(s_t))$ differs by only ε_h (again in TV distance as required
1914 by the strongly open-loop consistency assumption) where precisely ε_h probability mass
1915 is moved from reaching state G to reaching state Z . This causes the \hat{V}_{ac}^+ to precisely
1916 overestimate the value of V_{ac}^+ by $\frac{\varepsilon_h \gamma^h}{(1-\gamma)(1-(1-\varepsilon_h)\gamma^h)}$.

1917 We use a special action $a = 2$ where upon taking the action the agent immediately transitions to Z
1918 and receives a reward of 0 (except in G). As we will see soon, this action is useful for constructing a
1919 data distribution with an easily ‘controllable’ probability of reaching Z for the top branch and an
1920 easily ‘controllable’ probability of reaching G for the bottom branch. Before we start constructing \mathcal{D} ,
1921 we first check the condition that \mathcal{D}^* is strongly ε_h -open-loop consistent.

1922 Step 2. Strong ε_h -open-loop consistency of \mathcal{D}^* : It is clear that one possible π^* that
1923 achieves $1/(1-\gamma)$ value is

$$\begin{aligned} \pi^*(X_i) &= 0 \\ \pi^*(C) &= 1 \\ \pi^*(\tilde{X}) &= 0 \end{aligned} \tag{111}$$

1924 We can easily check that \mathcal{D}^* collected by π^* is strongly ε_h -open-loop consistent by observing that
1925 the only path that π^* outputs $(0, 1, 0, 0, \dots)$ has ε_h probability, which causes the state distribution of
1926 s_{t+1} to differ by at most ε_h under the TV distance (subject to $a = (0, 1, 0, 0, \dots)$ or $a = (0, 0, 0, \dots)$
1927 conditioning). This concludes that \mathcal{D}^* generated by π^* above is strongly ε_h -open-loop consistent.

1928 Now, depending on the first action a_t , the MDP can be decomposed into two parts: *the top* ($a = 0$)
1929 and *the bottom* ($a = 1$). We construct the data distribution for each branch and analyze the *actual*
1930 and *nominal* optimality gap for each branch in the following steps.

1931 Step 3. Data distribution \mathcal{D}_{top} for the top branch: we use a mixture of the following
1932 two policies to construct a strongly ε_h -open-loop consistent \mathcal{D}_{top} .

1933 *Policy π_{top}^1 :*

$$\begin{aligned} \pi_{top}^1(X_0) &= \pi_{top}^1(C) = \pi_{top}^1(Z) = 0, \\ \pi_{top}^1(X_1) &= \pi_{top}^1(\tilde{X}_1) = 2. \end{aligned} \tag{112}$$

1944 π_{top}^1 always take $a = 2$ unless it is in state X_0, C or Z where it always takes $a = 0$. It is clear that
 1945 this policy only produces two possible action chunks: $a_{t:t+h} = (0, 0, \dots, 0)$ or $a_{t:t+h} = a_{t:t+h}^{\bullet} :=$
 1946 $(0, 2, 0, \dots)$. We note that the $a_{t:t+h}$ policy always leads to state Z :

1947 $P_{\mathcal{D}_{\pi_{\text{top}}^1}}(s_{t+h} = Z \mid s_t, a_{t:t+h} = 0) = 1.$ (113)

1949 *Policy π_{top}^2 :*

1951 $\pi_{\text{top}}^2(X_0) = 0,$
 1952 $\pi_{\text{top}}^2(\tilde{X}_1) = \pi_{\text{top}}^2(\tilde{C}) = 1,$
 1953 $\pi_{\text{top}}^2(a = 0 \mid X_1) = 1 - \delta_G,$
 1954 $\pi_{\text{top}}^2(a = 1 \mid X_1) = \delta_G,$ (114)

1956 with some $\delta_G \in (0, 1)$. π_{top}^2 can also only produce two possible action chunks: $a_{t:t+h} = (0, 0, \dots, 0)$
 1957 or $a_{t:t+h} = a_{t:t+h}^{\diamond} := (0, 1, 0, \dots, 0)$.

1959 The distribution of s_{t+h} conditioned on $a_{t:t+h} = 0$ is

1960 $P_{\mathcal{D}_{\pi_{\text{top}}^2}}(s_{t+h} = Z \mid s_t, a_{t:t+h} = 0) = 0,$
 1961 $P_{\mathcal{D}_{\pi_{\text{top}}^2}}(s_{t+h} = G \mid s_t, a_{t:t+h} = 0) = 0,$
 1962 $P_{\mathcal{D}_{\pi_{\text{top}}^2}}(s_{t+h} = X_0 \mid s_t, a_{t:t+h} = 0) = 1.$ (115)

1965 *Mixing π_{top}^1 and π_{top}^2 :* Let \mathcal{D}_{top} be a mixture of $\mathcal{D}_{\pi_{\text{top}}^1}$ and $\mathcal{D}_{\pi_{\text{top}}^2}$:

1967 $P_{\mathcal{D}_{\text{top}}} = (1 - \varsigma)P_{\mathcal{D}_{\pi_{\text{top}}^1}} + \varsigma P_{\mathcal{D}_{\pi_{\text{top}}^2}},$ (116)

1968 where

1969 $\varsigma = \frac{1}{2(1 - \delta_G) + 1}.$ (117)

1972 It is clear that $0 < \varsigma < 1$ (because $\delta_G \in (0, 1)$), making it valid mixing ratio.

1973 We now compute the marginal state distribution of the mixture by first analyzing the action probability:

1975 $P_{\mathcal{D}_{\text{top}}^1}(a_{t:t+h}^* \mid s_t) = \varepsilon_h,$
 1976 $P_{\mathcal{D}_{\text{top}}^2}(a_{t:t+h}^* \mid s_t) = (1 - 2\varepsilon_h)(1 - \delta_G).$ (118)

1977 The state marginals are then

1979 $P_{\mathcal{D}_{\text{top}}}(s_{t+h} = Z \mid s_t, a_{t:t+h}^*) = \frac{P_{\mathcal{D}_{\text{top}}}(s_{t+h} = Z, a_{t:t+h}^* \mid s_t)}{P_{\mathcal{D}_{\text{top}}}(a_{t:t+h}^* \mid s_t)}$
 1980 $= \frac{(1 - \varsigma)P_{\mathcal{D}_{\pi_{\text{top}}^1}}(a_{t:t+h}^* \mid s_t)}{(1 - \varsigma)P_{\mathcal{D}_{\pi_{\text{top}}^1}}(a_{t:t+h}^* \mid s_t) + \varsigma P_{\mathcal{D}_{\pi_{\text{top}}^2}}(a_{t:t+h}^* \mid s_t)}$ (119)
 1981 $= \frac{\varepsilon_h(1 - \varsigma)}{\varepsilon_h(1 - \varsigma) + (1 - 2\varepsilon_h)(1 - \delta_G)\varsigma}$
 1982 $= 2\varepsilon_h.$

1988 Therefore,

1989 $P_{\mathcal{D}_{\text{top}}}(s_{t+h} = Z \mid s_t, a_{t:t+h}^*) = 2\varepsilon_h,$
 1990 $P_{\mathcal{D}_{\text{top}}}(s_{t+h} = X_0 \mid s_t, a_{t:t+h}^*) = 1 - 2\varepsilon_h,$
 1991 $P_{\mathcal{D}_{\text{top}}}(s_{t+h} = G \mid s_t, a_{t:t+h}^*) = 0.$ (120)

1993 Step 4. Strong ε_h -open-loop consistency of \mathcal{D}_{top} : Now, we check for strong open-
 1994 loop consistency for the three possible action chunks on the top branch:

1995 $a_{t:t+h}^* = (0, 0, 0, \dots)$
 1996 $a_{t:t+h}^{\diamond} = (0, 1, 0, \dots)$
 1997 $a_{t:t+h}^{\bullet} = (0, 2, 0, \dots)$ (121)

1998 For $a_{t:t+h}^* = 0$, we can compute open-loop marginal state distribution as follows:
 1999

$$\begin{aligned} T(s_{t+h} = Z \mid s_t, a_{t:t+h}^*) &= \varepsilon_h, \\ T(s_{t+h} = X_0 \mid s_t, a_{t:t+h}^*) &= 1 - 2\varepsilon_h, \\ T(s_{t+h} = G \mid s_t, a_{t:t+h}^*) &= \varepsilon_h. \end{aligned} \quad (122)$$

2000 Combining this with the data distribution calculated in Equation (120), it is clear that
 2001

$$D_{\text{TV}}(T(s_{t+h} \mid s_t, a_{t:t+h} = 0) \parallel P_{\mathcal{D}_{\text{top}}}(s_{t+h} \mid s_t, a_{t:t+h} = 0)) = \varepsilon_h. \quad (123)$$

2002 We can repeat the same procedure to show that
 2003

$$D_{\text{TV}}(T(s_{t+h'} \mid s_t, a_{t:t+h'} = 0) \parallel P_{\mathcal{D}_{\text{top}}}(s_{t+h'} \mid s_t, a_{t:t+h} = 0)) = \varepsilon_h, \quad \forall h' \in \{1, \dots, h-1\} \quad (124)$$

2010 because the only difference in these distributions is that they occupy $s_{t+h'} = X_{h'}$ with $2\varepsilon_h$ probability
 2011 instead of $s_{t+h} = X_0$ with $2\varepsilon_h$ probability.
 2012

2013 For $a_{t:t+h}^\bullet = (0, 2, 0, \dots)$, it is clear that
 2014

$$D_{\text{TV}}(T(s_{t+h'} \mid s_t, a_{t:t+h} = a_{t:t+h}^\bullet) \parallel P_{\mathcal{D}_{\text{top}}}(s_{t+h'} \mid s_t, a_{t:t+h} = a_{t:t+h}^\bullet)) = \varepsilon_h \quad (125)$$

2015 holds for any $h' \in \{1, 2, \dots, h\}$ since the only difference between these two distributions is the ε_h -
 2016 probability path (i.e., $X_0 \rightarrow C \rightarrow Z$ where the probability is under $T(\cdot \mid s_t, a_{t:t+h}^\bullet)$).
 2017

2018 For $a_{t:t+h}^\diamond = (0, 1, 0, \dots)$, we first compute the marginal state distributions:
 2019

$$\begin{aligned} P_{\mathcal{D}_{\text{top}}}(s_{t+h} = Z \mid s_t, a_{t:t+h}^\diamond) &= \frac{(1 - 2\varepsilon_h)\delta_G}{2\varepsilon_h + (1 - 2\varepsilon_h)\delta_G}, \\ P_{\mathcal{D}_{\text{top}}}(s_{t+h} = X_0 \mid s_t, a_{t:t+h}^\diamond) &= \frac{2\varepsilon_h}{2\varepsilon_h + (1 - 2\varepsilon_h)\delta_G}, \\ P_{\mathcal{D}_{\text{top}}}(s_{t+h} = G \mid s_t, a_{t:t+h}^\diamond) &= 0. \\ P_{\mathcal{D}_{\text{top}}}(s_{t+1} = X_1 \mid s_t, a_{t:t+h}^\diamond) &= \frac{(1 - 2\varepsilon_h)\delta_G}{2\varepsilon_h + (1 - 2\varepsilon_h)\delta_G}. \\ P_{\mathcal{D}_{\text{top}}}(s_{t+1} = \tilde{X}_1 \mid s_t, a_{t:t+h}^\diamond) &= \frac{\varepsilon_h}{2\varepsilon_h + (1 - 2\varepsilon_h)\delta_G}. \\ P_{\mathcal{D}_{\text{top}}}(s_{t+1} = C \mid s_t, a_{t:t+h}^\diamond) &= \frac{\varepsilon_h}{2\varepsilon_h + (1 - 2\varepsilon_h)\delta_G}. \end{aligned} \quad (126)$$

2020 We can also compute the open-loop marginal state distribution as follows:
 2021

$$\begin{aligned} T(s_{t+h} = Z \mid s_t, a_{t:t+h}^\diamond) &= 1 - 2\varepsilon_h \\ T(s_{t+h} = X_0 \mid s_t, a_{t:t+h}^\diamond) &= 2\varepsilon_h \\ T(s_{t+h} = G \mid s_t, a_{t:t+h}^\diamond) &= 0. \\ T(s_{t+1} = X_1 \mid s_t, a_{t:t+h}^\diamond) &= 1 - 2\varepsilon_h. \\ T(s_{t+1} = \tilde{X}_1 \mid s_t, a_{t:t+h}^\diamond) &= \varepsilon_h. \\ T(s_{t+1} = C \mid s_t, a_{t:t+h}^\diamond) &= \varepsilon_h. \end{aligned} \quad (127)$$

2041 Let c_3 be any value that satisfies $c_3 \in (0, \varepsilon_h/2)$, we can set
 2042

$$\delta_G = \frac{\varepsilon_h(1 - 2\varepsilon_h - 2c_3)}{(\varepsilon_h + c_3)(1 - 2\varepsilon_h)}, \quad (128)$$

2043 such that
 2044

$$\begin{aligned} P_{\mathcal{D}_{\text{top}}}(s_{t+h} = Z \mid s_t, a_{t:t+h}^\diamond) &= 1 - 2\varepsilon_h - 2c_3, \\ P_{\mathcal{D}_{\text{top}}}(s_{t+h} = X_0 \mid s_t, a_{t:t+h}^\diamond) &= 2\varepsilon_h + 2c_3, \\ P_{\mathcal{D}_{\text{top}}}(s_{t+h} = G \mid s_t, a_{t:t+h}^\diamond) &= 0, \\ P_{\mathcal{D}_{\text{top}}}(s_{t+1} = X_1 \mid s_t, a_{t:t+h}^\diamond) &= 1 - 2\varepsilon_h - 2c_3, \\ P_{\mathcal{D}_{\text{top}}}(s_{t+1} = \tilde{X}_1 \mid s_t, a_{t:t+h}^\diamond) &= \varepsilon_h + c_3, \\ P_{\mathcal{D}_{\text{top}}}(s_{t+1} = C \mid s_t, a_{t:t+h}^\diamond) &= \varepsilon_h + c_3. \end{aligned} \quad (129)$$

2052 It is easy to check that $0 < \delta_G < 1$ (a valid probability) because in Equation (128), each term in the
 2053 numerator has a larger term in the denominator (*i.e.*, $\varepsilon_h < \varepsilon_h + c_3$ and $1 - 2\varepsilon_h - 2c_3 < 1 - 2\varepsilon_h$).
 2054

2055 Now, for all $h' \in \{1, 2, \dots, h\}$, using the values calculated in Equation (127) and Equation (129),
 2056 we have

$$2057 D_{\text{TV}}(T(s_{t+h'} | s_t, a_{t:t+h'} = a_{t:t+h'}^\diamond) \| P_{\mathcal{D}_{\text{top}}}(s_{t+h'} | s_t, a_{t:t+h} = a_{t:t+h}^\diamond)) = 2c_3. \quad (130)$$

2058 Since $c_3 < \varepsilon_h/2$, the strong open-loop consistency assumption holds for $a_{t:t+h}^\diamond$ as well.
 2059

2060 Step 5. The optimality gap and value estimation error for the top branch:
 2061 Now we can compute the optimality gap for the estimated value for $a_{t:t+h}^\diamond$:

$$2062 V^*(X_0) - \hat{V}_{\text{ac}}^\diamond(X_0) = \frac{(1 - 2\varepsilon_h - 2c_3)\gamma}{(1 - \gamma)(1 - 2(\varepsilon_h + c_3)\gamma^h)}, \quad (131)$$

2064 where the h -step reward suboptimality gap is a sole result of the reaching Z with $(1 - 2\varepsilon_h - 2c_3)$
 2065 probability (and hence the $(1 - 2\varepsilon_h - 2c_3)\gamma$ term in the numerator), and the h -step distribution gap
 2066 is reflected in the $(1 - 2(\varepsilon_h + c_3)\gamma^h)$ term at bottom because the probability of reaching X_0 after h
 2067 steps is $2(\varepsilon_h + c_3)$.

2068 Similarly, we can compute the optimality gap for V_{ac}^* and \hat{V}_{ac}^* :

$$2070 V^*(X_0) - V_{\text{ac}}^*(X_0) = \varepsilon_h \frac{\gamma - \gamma^h}{1 - \gamma} + \frac{\varepsilon_h \gamma^h}{1 - \gamma} + \gamma^h (1 - 2\varepsilon_h) (V^* - \hat{V}_{\text{ac}}) \\ 2071 = \frac{\varepsilon_h \gamma}{(1 - \gamma)(1 - (1 - 2\varepsilon_h)\gamma^h)}, \quad (132)$$

$$2074 V^*(X_0) - \hat{V}_{\text{ac}}^*(X_0) = \frac{2\varepsilon_h(\gamma - \gamma^h)}{1 - \gamma} + \frac{2\varepsilon_h \gamma^h}{1 - \gamma} \gamma^h (1 - 2\varepsilon_h) (V^* - \hat{V}_{\text{ac}}) \\ 2075 = \frac{2\varepsilon_h \gamma}{(1 - \gamma)(1 - (1 - 2\varepsilon_h)\gamma^h)}. \quad (133)$$

2079 Now, we observe that

$$2080 1 - 2\varepsilon_h - 2c_3 > 1 - 3\varepsilon_h > 2\varepsilon_h, \quad (134)$$

2081 where the first inequality is due to $c_3 \in (0, \varepsilon_h/2)$ and the second inequality is due to $\varepsilon_h \in (0, 1/5)$
 2082 in our assumption.
 2083

2084 This allows us to lower-bound the estimated optimality gap for $a_{t:t+h}^\diamond$ as follows:

$$2085 V^*(X_0) - \hat{V}_{\text{ac}}^\diamond(X_0) = \frac{(1 - 2\varepsilon_h - 2c_3)\gamma}{(1 - \gamma)(1 - 2(\varepsilon_h + c_3)\gamma^h)} \\ 2086 > \frac{2\varepsilon_h \gamma}{(1 - \gamma)(1 - (1 - 2\varepsilon_h)\gamma^h)} \\ 2087 = V^*(X_0) - \hat{V}_{\text{ac}}^*(X_0), \quad (135)$$

2091 where the inequality is obtained by triggering Lemma G.5 (*e.g.*, by setting $\varepsilon_1 = 2\varepsilon_h$, $\varepsilon_2 = (1 - 2\varepsilon_h - 2c_3)$, $\tilde{\gamma} = \gamma^h$). The bound above rules out the possibility of $a_{t:t+h}^\diamond$ being picked by $\hat{\pi}_{\text{ac}}^+$ because it
 2092 has a lower estimated value compared to $a_{t:t+h}^*$.
 2093

2094 Finally, for $a_{t:t+h}^\bullet$, since it is correlated with $s_{t+h} = Z$ and receives no reward except the first step in
 2095 \mathcal{D}_{top} , the estimated value is just 1, being trivially smaller than $\hat{V}_{\text{ac}}^*(X_0)$ and would never get picked
 2096 by $\hat{\pi}_{\text{ac}}^+$.
 2097

2098 Up to now, we have finished our data distribution construction and analysis for the top branch. We
 2099 summarize the key intermediate results as the remark below:

2100 **Remark G.6** (Intermediate results from Step 1-4). *The optimal action chunk is $a_{t:t+h}^*$ and the
 2101 estimated values for the two other possible action chunks $a_{t:t+h}^\bullet$, $a_{t:t+h}^\diamond$ are smaller than that of
 2102 $a_{t:t+h}^*$:*

$$2103 \hat{V}_{\text{ac}}^\bullet(X_0) < \hat{V}_{\text{ac}}^\diamond(X_0) < \hat{V}_{\text{ac}}^*(X_0) = V^*(X_0) - \frac{2\varepsilon_h \gamma}{(1 - \gamma)(1 - (1 - 2\varepsilon_h)\gamma^h)}. \quad (136)$$

2104 In addition, both \mathcal{D}_{top} and \mathcal{D}^* are strongly ε_h -open-loop consistent.
 2105

2106 Next, we move on to the bottom branch.
 2107

2108 Step 6. Data distribution $\mathcal{D}_{\text{bottom}}$ for the bottom branch: For the bottom, we again
 2109 use two policies.
 2110

2111 *Policy π_{bottom}^1 :*

$$\begin{aligned} 2112 \pi_{\text{bottom}}^1(X_0) &= \pi_{\text{bottom}}^1(G) = \pi_{\text{bottom}}^1(Z) = 1, \\ 2113 \pi_{\text{bottom}}^1(Y_1) &= \pi_{\text{bottom}}^1(\tilde{Y}_1) = 2. \end{aligned} \quad (137)$$

2116 π_{bottom}^1 takes $a = 1$ at X_0 and G and Z , and takes $a = 2$ otherwise (at Y_1, \tilde{Y}_1). It is clear that this
 2117 policy only produces two possible action chunks: $a_{t:t+h}^{\triangle} = (1, 1, 1, \dots)$ or $a_{t:t+h}^{\times} = (1, 2, 1, \dots)$.
 2118

2119 *Policy π_{bottom}^2 :*

$$\begin{aligned} 2122 \pi_{\text{bottom}}^2(X_0) &= 1, \\ 2123 \pi_{\text{bottom}}^2(a = 0 \mid Y_1) &= \delta_Z, \\ 2124 \pi_{\text{bottom}}^2(a = 1 \mid Y_1) &= 1 - \delta_Z, \\ 2125 \pi_{\text{bottom}}^2(\tilde{Y}_1) &= 0, \\ 2126 \pi_{\text{bottom}}^2(Y_i) &= 1, \quad \forall i \in \{2, \dots, h-1\}, \end{aligned} \quad (138)$$

2129 where $\delta_Z \in (0, 1)$ and we shall specify the exact value of δ_Z shortly.
 2130

2131 π_{bottom}^2 takes $a = 1$ when it is at Y_i and takes either $a = 0$ (with δ_Z probability) or $a = 1$ (with
 2132 $1 - \delta_Z$ probability) when it is at \tilde{Y}_1 . It is clear that this policy only produces two possible action
 2133 chunks: $a_{t:t+h}^{\triangle} = (1, 1, 1, \dots)$ or $a_{t:t+h}^{\circ} = (1, 0, 1, \dots)$.
 2134

2135 Now, we observe that the marginal state distributions for both policies conditioned on $a_{t:t+h}^{\triangle}$ are
 2136 independent of c_1 and δ_Z because the action chunk only appears when π_{bottom}^1 reaches G and when
 2137 π_{bottom}^2 reaches X_0 . More specifically,

$$2138 P_{\mathcal{D}_{\text{bottom}}^1}(s_{t+1} = G \mid s_t, a_{t:t+h}^{\triangle}) = P_{\mathcal{D}_{\text{bottom}}^1}(s_{t+h} = G \mid s_t, a_{t:t+h}^{\triangle}) = 1, \quad (139)$$

$$2140 P_{\mathcal{D}_{\text{bottom}}^2}(s_{t+i} = X_i \mid s_t, a_{t:t+h}^{\triangle}) = P_{\mathcal{D}_{\text{bottom}}^2}(s_{t+h} = X_0 \mid s_t, a_{t:t+h}^{\triangle}) = 1, \forall i \in \{1, \dots, h-1\}. \quad (140)$$

2142 We can now mix $\mathcal{D}_{\text{bottom}}^1$ and $\mathcal{D}_{\text{bottom}}^2$ with an appropriate ratio to control the state marginals for
 2143 $s_{t:t+h} = G$ and $s_{t:t+h} = X_0$ arbitrarily ($s_{t:t+h} = Z$ stays at 0 because none of the policies take/have
 2144 taken $a_{t:t+h}^{\triangle}$ when they reach Z).
 2145

2146 *Mixing π_{bottom}^1 and π_{bottom}^2 :* Let $\mathcal{D}_{\text{bottom}}$ be a mixture of $\mathcal{D}_{\text{bottom}}^1$ and $\mathcal{D}_{\text{bottom}}^2$:

$$2148 P_{\mathcal{D}_{\text{bottom}}} = (1 - \vartheta)P_{\mathcal{D}_{\text{bottom}}^1} + \vartheta P_{\mathcal{D}_{\text{bottom}}^2}, \quad (141)$$

2150 where we set the mixing ratio to be
 2151

$$2152 \vartheta = \frac{c_1}{c_1 + (1 - \delta_Z)(\varepsilon_h + c_1)}. \quad (142)$$

2154 This mixing ratio helps the calculations to be simpler later on.
 2155

2156 We can now compute the marginal state distribution of the mixture. We start by analyzing the action
 2157 probability:

$$\begin{aligned} 2158 P_{\mathcal{D}_{\text{bottom}}^1}(a_{t:t+h}^{\triangle} \mid s_t) &= c_1, \\ 2159 P_{\mathcal{D}_{\text{bottom}}^2}(a_{t:t+h}^{\triangle} \mid s_t) &= (1 - \varepsilon_h - c_1)(1 - \delta_Z). \end{aligned} \quad (143)$$

2160 The state marginal is then
 2161
 2162
$$P_{\mathcal{D}_{\text{bottom}}}(s_{t+h} = X_0 | s_t, a_{t:t+h}^{\Delta}) = \frac{P_{\mathcal{D}_{\text{bottom}}}(s_{t+h} = X_0, a_{t:t+h}^{\Delta} | s_t)}{P_{\mathcal{D}_{\text{bottom}}}(a_{t:t+h}^{\Delta} | s_t)}$$

 2163
 2164
$$= \frac{\vartheta P_{\mathcal{D}_{\text{bottom}}^2}(a_{t:t+h}^{\Delta} | s_t)}{(1 - \vartheta)P_{\mathcal{D}_{\text{bottom}}^1}(a_{t:t+h}^{\Delta} | s_t) + \vartheta P_{\mathcal{D}_{\text{bottom}}^2}(a_{t:t+h}^{\Delta} | s_t)}$$

 2165
 2166
$$= \frac{(1 - \varepsilon_h - c_1)(1 - \delta_Z)\vartheta}{c_1(1 - \vartheta) + (1 - \varepsilon_h - c_1)(1 - \delta_Z)\vartheta}$$

 2167
 2168
$$= 1 - \varepsilon_h - c_1.$$

 2169
 2170
 2171 (144)

2172 We can use it to deduce the rest of the marginals as follows:

2173
$$P_{\mathcal{D}_{\text{bottom}}}(s_{t+h} = G | s_t, a_{t:t+h}^{\Delta}) = \varepsilon_h + c_1, \quad \forall h' \in \{1, \dots, h-1\},$$

 2174
 2175
$$P_{\mathcal{D}_{\text{bottom}}}(s_{t+h} = X_0 | s_t, a_{t:t+h}^{\Delta}) = 1 - \varepsilon_h - c_1,$$

 2176
 2177
$$P_{\mathcal{D}_{\text{bottom}}}(s_{t+h} = Z | s_t, a_{t:t+h}^{\Delta}) = 0,$$

 2178
 2179
$$P_{\mathcal{D}_{\text{bottom}}}(s_{t+h'} = Y_{h'} | s_t, a_{t:t+h}^{\Delta}) = 1 - \varepsilon_h - c_1, \quad \forall h' \in \{1, \dots, h-2\},$$

 2180
 2181
$$P_{\mathcal{D}_{\text{bottom}}}(s_{t+1} = \tilde{Y}_1 | s_t, a_{t:t+h}^{\Delta}) = 0.$$

 2182
 2183

2184 Up to now, we have established $\mathcal{D}_{\text{bottom}}$ and we are ready to check the strong open-loop consistency.

2185 Step 7. Strong ε_h -open-loop consistency of $\mathcal{D}_{\text{bottom}}$:

2186 For $a_{t:t+h}^{\Delta} = (1, 1, \dots)$, we can compute the open-loop marginals as follows:

2187
$$T(s_{t+h'} = G | s_t, a_{t:t+h}^{\Delta}) = c_1, \quad \forall h' \in \{1, \dots, h-1\},$$

 2188
 2189
$$T(s_{t+h} = X_0 | s_t, a_{t:t+h}^{\Delta}) = 1 - \varepsilon_h - c_1,$$

 2190
 2191
$$T(s_{t+h} = Z | s_t, a_{t:t+h}^{\Delta}) = \varepsilon_h.$$

 2192
 2193
$$T(s_{t+h'} = Y_{h'} | s_t, a_{t:t+h}^{\Delta}) = 1 - \varepsilon_h - c_1, \quad \forall h' \in \{1, \dots, h-2\}$$

 2194
 2195
$$T(s_{t+1} = \tilde{Y}_1 | s_t, a_{t:t+h}^{\Delta}) = \varepsilon_h.$$

 2196
 2197

2198 Combining it with the marginals calculated in Equation (145), it is clear that for all $h' \in \{1, \dots, h-1\}$,

2199
$$D_{\text{TV}}(T(s_{t+h'} | s_t, a_{t:t+h'} = a_{t:t+h'}^+) \parallel P_{\mathcal{D}_{\text{bottom}}}(s_{t+h'} | s_t, a_{t:t+h} = a_{t:t+h}^+)) = \varepsilon_h, \quad (147)$$

 2200 satisfying the open-loop consistency.

2201 For $a_{t:t+h}^{\times} = (1, 2, 1, \dots)$, the data and open-loop state marginals are

2202
$$P_{\mathcal{D}_{\text{bottom}}}(s_{t+h} = Z | s_t, a_{t:t+h}^{\times}) = 1,$$

 2203
 2204
$$P_{\mathcal{D}_{\text{bottom}}}(s_{t+1} = Y_1 | s_t, a_{t:t+h}^{\times}) = \frac{1 - \varepsilon_h - c_1}{1 - c_1},$$

 2205
 2206
$$P_{\mathcal{D}_{\text{bottom}}}(s_{t+1} = \tilde{Y}_1 | s_t, a_{t:t+h}^{\times}) = \frac{\varepsilon_h}{1 - c_1},$$

 2207
 2208
$$T(s_{t+h} = Z | s_t, a_{t:t+h}^{\times}) = 1 - c_1,$$

 2209
 2210
$$T(s_{t+h} = G | s_t, a_{t:t+h}^{\times}) = c_1,$$

 2211
 2212
$$T(s_{t+1} = Y_1 | s_t, a_{t:t+h}^{\times}) = 1 - \varepsilon_h - c_1,$$

 2213
 2214
$$T(s_{t+1} = \tilde{Y}_1 | s_t, a_{t:t+h}^{\times}) = \varepsilon_h,$$

 2215
 2216
$$T(s_{t+1} = G | s_t, a_{t:t+h}^{\times}) = c_1.$$

 2217
 2218

2219 This allows us to bound the TV distance for all $h' \in \{1, \dots, h-1\}$ as

2220
$$D_{\text{TV}}(T(s_{t+h'} | s_t, a_{t:t+h'} = a_{t:t+h'}^{\times}) \parallel P_{\mathcal{D}_{\text{bottom}}}(s_{t+h'} | s_t, a_{t:t+h} = a_{t:t+h}^{\times})) \leq \frac{c_1}{1 - c_1}. \quad (149)$$

 2221
 2222

2214 Since $c_1 < \varepsilon_h/2 < 1/10$,

$$\frac{c_1}{1 - c_1} < \frac{10}{9} c_1 < 5\varepsilon_h/9 < \varepsilon_h, \quad (150)$$

2218 satisfying the strong open-loop consistency assumption.

2219 For $a_{t:t+h}^\circ = (1, 0, 1, \dots)$, we first compute the state marginals in $\mathcal{D}_{\text{bottom}}$ as follows:

$$\begin{aligned} P_{\mathcal{D}_{\text{bottom}}}(s_{t+h} = Z \mid s_t, a_{t:t+h}^\circ) &= \frac{(1 - \varepsilon_h - c_1)\delta_Z}{\varepsilon_h + (1 - \varepsilon_h - c_1)\delta_Z}, \\ P_{\mathcal{D}_{\text{bottom}}}(s_{t+h} = X_0 \mid s_t, a_{t:t+h}^\circ) &= \frac{\varepsilon_h}{\varepsilon_h + (1 - \varepsilon_h - c_1)\delta_Z}, \\ P_{\mathcal{D}_{\text{bottom}}}(s_{t+1} = Y_1 \mid s_t, a_{t:t+h}^\circ) &= \frac{(1 - \varepsilon_h - c_1)\delta_Z}{\varepsilon_h + (1 - \varepsilon_h - c_1)\delta_Z}. \\ P_{\mathcal{D}_{\text{bottom}}}(s_{t+1} = \tilde{Y}_1 \mid s_t, a_{t:t+h}^\circ) &= \frac{\varepsilon_h}{\varepsilon_h + (1 - \varepsilon_h - c_1)\delta_Z}. \end{aligned} \quad (151)$$

2230 We can also compute the open-loop marginal state distribution as follows:

$$\begin{aligned} T(s_{t+h} = Z \mid s_t, a_{t:t+h}^\circ) &= 1 - \varepsilon_h - c_1, \\ T(s_{t+h} = X_0 \mid s_t, a_{t:t+h}^\circ) &= \varepsilon_h, \\ T(s_{t+h} = G \mid s_t, a_{t:t+h}^\circ) &= c_1, \\ T(s_{t+1} = Y_1 \mid s_t, a_{t:t+h}^\circ) &= 1 - \varepsilon_h - c_1, \\ T(s_{t+1} = \tilde{Y}_1 \mid s_t, a_{t:t+h}^\circ) &= \varepsilon_h, \\ T(s_{t+1} = G \mid s_t, a_{t:t+h}^\circ) &= c_1. \end{aligned} \quad (152)$$

2240 Let $c_4 \in (c_1, \varepsilon_h)$, and we set

$$\delta_Z = \frac{\varepsilon_h(1 - \varepsilon_h - c_4)}{(\varepsilon_h + c_4)(1 - \varepsilon_h - c_1)}. \quad (153)$$

2244 Then, we have

$$\begin{aligned} P_{\mathcal{D}_{\text{bottom}}}(s_{t+h} = Z \mid s_t, a_{t:t+h}^\circ) &= 1 - \varepsilon_h - c_4, \\ P_{\mathcal{D}_{\text{bottom}}}(s_{t+h} = X_0 \mid s_t, a_{t:t+h}^\circ) &= \varepsilon_h + c_4, \\ P_{\mathcal{D}_{\text{bottom}}}(s_{t+h} = G \mid s_t, a_{t:t+h}^\circ) &= 0, \\ P_{\mathcal{D}_{\text{bottom}}}(s_{t+1} = Y_1 \mid s_t, a_{t:t+h}^\circ) &= 1 - \varepsilon_h - c_4, \\ P_{\mathcal{D}_{\text{bottom}}}(s_{t+1} = \tilde{Y}_1 \mid s_t, a_{t:t+h}^\circ) &= \varepsilon_h + c_4. \end{aligned} \quad (154)$$

2251 The TV distance is then

$$D_{\text{TV}}(T(s_{t+h} \mid s_t, a_{t:t+h}^\circ) \parallel P_{\mathcal{D}_{\text{bottom}}}(s_{t+h} \mid s_t, a_{t:t+h}^\circ)) = c_4. \quad (155)$$

2254 Since $c_4 < \varepsilon_h$, the strong open-loop consistency is also satisfied for $a_{t:t+h}^\circ$.

2255 Up to now, we have checked that all three possible action chunks in the bottom branch satisfy the
2256 strong open-loop consistency assumption. Since \mathcal{D}_{top} and $\mathcal{D}_{\text{bottom}}$ have non-overlapping supports
2257 for $a_{t:t+h}$, and they are both strongly ε_h -open-loop consistent on their own, we can construct \mathcal{D} as

$$P_{\mathcal{D}}(\cdot \mid s_t) = (1 - \varrho)P_{\mathcal{D}_{\text{top}}}(\cdot \mid s_t) + \varrho P_{\mathcal{D}_{\text{bottom}}}(\cdot \mid s_t), \quad (156)$$

2261 for any $\varrho \in (0, 1)$, and conclude that

2262 **Remark G.7** (Intermediate result from Step 5-7). \mathcal{D} is strongly ε_h -open-loop consistent.

2264 Up to now, we have constructed and checked both \mathcal{D} and \mathcal{D}^* are strongly ε_h -open-loop consistent.

2265 As the final step, we calculate the optimality gap and value estimation error for these action chunks.

2266 Step 8. The optimality gap and value estimation error for the bottom
2267 branch:

We first note that similar to $a_{t:t+h}^\bullet$, $a_{t:t+h}^\times$ is correlated with $s_{t+h} = Z$ and always receives 0 reward except the first step in \mathcal{D} . Thus, the estimated value \hat{V}^\times is just 1, being trivially smaller than $\hat{V}_{\text{ac}}^\star$ and would never get picked by $\hat{\pi}_{\text{ac}}^\triangle$. The only top contenders are $a_{t:t+h}^+$, $a_{t:t+h}^\circ$ and $a_{t:t+h}^\star$ (which we already analyzed in Step 5 above).

We start with $a_{t:t+h}^\circ$ where we can compute optimality gap as follows:

$$V^*(X_0) - \hat{V}_{\text{ac}}^\circ(X_0) = \frac{(1 - \varepsilon_h - c_4)\gamma + \delta(1 - \gamma) + (\varepsilon_h + c_4)\delta(\gamma - \gamma^h)}{(1 - \gamma)(1 - (\varepsilon_h + c_4)\gamma^h)}. \quad (157)$$

Now, observe that

$$\varepsilon_h + c_4 < 2\varepsilon_h < 1 - 2\varepsilon_h, \quad (158)$$

where again the last inequality comes from the fact that $\varepsilon_h < 1/4$.

We can now lower-bound the optimality gap as follows:

$$\begin{aligned} V^*(X_0) - \hat{V}_{\text{ac}}^\circ(X_0) &> \frac{2\varepsilon_h\gamma + \delta(1 - \gamma) + (\varepsilon_h + c_4)\delta(\gamma - \gamma^h)}{(1 - \gamma)(1 - (1 - 2\varepsilon_h)\gamma^h)} \\ &> \frac{2\varepsilon_h\gamma}{(1 - \gamma)(1 - (1 - 2\varepsilon_h)\gamma^h)} \\ &= V^*(X_0) - \hat{V}_{\text{ac}}^\star(X_0). \end{aligned} \quad (159)$$

where the first inequality is obtained by triggering Lemma G.5 (e.g., by setting $\varepsilon_1 = 2\varepsilon_h$, $\varepsilon_2 = (1 - \varepsilon_h - c_4)$, $\tilde{\gamma} = \gamma^h$).

With this lower-bound, we can conclude that $a_{t:t+h}^\circ$ would not be picked by π_{ac}^+ as well because $\hat{V}_{\text{ac}}^\circ(X_0) < \hat{V}_{\text{ac}}^\star(X_0)$.

Up to now, we have eliminated both $a_{t:t+h}^\circ$ and $a_{t:t+h}^\times$ (for the possibility of being picked by π_{ac}^+) and the only remaining contender left is $a_{t:t+h}^\triangle$.

We can also compute the estimated and the actual values for $a_{t:t+h} = a_{t:t+h}^\triangle = 1$ in terms of their optimality gaps:

$$V^*(X_0) - \hat{V}_{\text{ac}}^\triangle(X_0) = \frac{\delta(1 - \varepsilon_h - c_1)\gamma}{(1 - \gamma)(1 - (1 - \varepsilon_h - c_1)\gamma^h)}, \quad (160)$$

$$V^*(X_0) - V_{\text{ac}}^\triangle(X_0) = \frac{[\delta(1 - \varepsilon_h - c_1) + \varepsilon_h]\gamma}{(1 - \gamma)(1 - (1 - \varepsilon_h - c_1)\gamma^h)}. \quad (161)$$

Let

$$\delta = \frac{2\varepsilon_h\gamma - c_2}{(1 - \varepsilon_h - c_1)\gamma} \frac{1 - (1 - \varepsilon_h - c_1)\gamma^h}{1 - (1 - 2\varepsilon_h)\gamma^h}. \quad (162)$$

We first check $1 - \delta$ is a valid reward value (within $[0, 1]$):

$$\begin{aligned} \delta &< \frac{2\varepsilon_h}{1 - \varepsilon_h - c_1} \frac{1 - (1 - \varepsilon_h - c_1)\gamma^h}{1 - (1 - 2\varepsilon_h)\gamma^h} \\ &< \frac{2\varepsilon_h}{1 - 2\varepsilon_h} \frac{1 - (1 - 2\varepsilon_h)\gamma^h}{1 - (1 - 2\varepsilon_h)\gamma^h} \\ &= \frac{2\varepsilon_h}{1 - 2\varepsilon_h} \\ &\leq 1, \end{aligned} \quad (163)$$

where the first inequality is because $c_2 > 0$, the second inequality is due to $c_1 < \varepsilon_h$, and the final inequality is due to $\varepsilon_h < 1/4$.

It is also clear that $\delta > 0$ because all terms are positive in the fraction (Equation (162)).

2322 Next, we substitute δ in to obtain
 2323

$$2324 V^*(X_0) - \hat{V}_{\text{ac}}^\Delta(X_0) = \frac{2\varepsilon_h\gamma - c_2}{(1-\gamma)(1-(1-2\varepsilon_h)\gamma^h)}, \quad (164)$$

$$2326 V^*(X_0) - V_{\text{ac}}^\Delta(X_0) = \frac{2\varepsilon_h\gamma - c_2}{(1-\gamma)(1-(1-2\varepsilon_h)\gamma^h)} + \frac{\varepsilon_h\gamma}{(1-\gamma)(1-(1-\varepsilon_h-c_1)\gamma^h)}, \quad (165)$$

2328 where intuitively the second term in $V^*(X_0) - V_{\text{ac}}^\Delta(X_0)$ is due to the fact that from $P_{\mathcal{D}}(\cdot | s_t, a_{t:t+h}^\Delta)$
 2329 to $T(\cdot | s_t, a_{t:t+h}^\Delta)$, there is a shift in ε_h probability mass from $s_{t:t+h} = (X_0, G, \dots)$ to $s_{t:t+h} =$
 2330 $(X_0, \tilde{Y}_1, Z, \dots)$ incurring an additional $\frac{\varepsilon_h\gamma}{1-\gamma}$ suboptimality in terms of the h -step reward, and then
 2331 amplified by the value recursion by an additional factor of $\frac{1}{1-(1-\varepsilon_h-c_1)\gamma^h}$ (where $1-\varepsilon_h-c_1$ is the
 2332 probability that $a_{t:t+h}^\Delta$ reaches X_0 for the value recursion to occur).
 2334

2335 Since $c_2 > 0$, we can now show that $a_{t:t+h}^\Delta$ achieves the highest estimated value among six possible
 2336 action chunks:

$$2338 V^* - \hat{V}_{\text{ac}}^\Delta < V^* - \hat{V}_{\text{ac}}^* = \frac{2\varepsilon_h\gamma}{(1-\gamma)(1-(1-2\varepsilon_h)\gamma^h)}, \quad (166)$$

2340 which means that $\pi_{\text{ac}}^+(X_0) = a_{t:t+h}^\Delta = (1, 1, \dots)$, or equivalently $\hat{V}_{\text{ac}}^\Delta = \hat{V}_{\text{ac}}^+$!
 2341

2342 Finally, putting everything together, we have

$$2343 V^*(X_0) - V_{\text{ac}}^+(X_0) = \frac{2\varepsilon_h\gamma - c_2}{(1-\gamma)(1-(1-2\varepsilon_h)\gamma^h)} + \frac{\varepsilon_h\gamma}{(1-\gamma)(1-(1-\varepsilon_h-c_1)\gamma^h)}, \quad (167)$$

2345 as desired. \square

2347 G.8 PROOF OF PROPOSITION 4.9

2349 **Proposition 4.9** (Optimality of Closed-loop Execution of Action Chunking Policy). *Let V^* be the
 2350 value of the one-step policy, π^* , defined as the closed-loop execution of the action chunking policy
 2351 π_{ac}^+ learned from \mathcal{D} . That is, for each $s_t \in \text{supp}(P_{\mathcal{D}}(s_t))$,*

$$2353 \pi^*(s_t) = a_t^+, \quad \text{where } a_{t:t+h}^+ = \pi_{\text{ac}}^+(s_t). \quad (21)$$

2354 *If we assume \mathcal{D} and \mathcal{D}^* are both strongly ε_h -open-loop consistent and $\text{supp}(P_{\mathcal{D}}(s_t, a_{t:t+h})) \supseteq$
 2355 $\text{supp}(P_{\mathcal{D}^*}(s_t, a_{t:t+h}))$, then under $\text{supp}(\mathcal{D}^*)$,*

$$2357 \|V^* - V^*\|_\infty \leq \frac{\varepsilon_h\gamma}{(1-\gamma)^2} \left[\frac{2}{1-(1-2\varepsilon_h)\gamma^h} + \frac{1}{1-(1-\varepsilon_h)\gamma^h} \right] \leq \frac{3\varepsilon_h}{(1-\gamma)^2(1-\gamma^h)}. \quad (22)$$

2359 *Proof.* We observe that

$$2361 V_{\text{ac}}^+(s_t) = Q_{\text{ac}}^+(s_t, a_{t:t+h}^+) \leq Q^*(s_t, a_t^+). \quad (168)$$

2363 Combining this with Theorem 4.6, we get

$$2365 Q^*(s_t, a_t^+) \geq V^*(s_t) - \Delta, \quad (169)$$

2366 where $\Delta = \frac{\varepsilon_h\gamma}{1-\gamma} \left[\frac{2}{1-(1-2\varepsilon_h)\gamma^h} + \frac{1}{1-(1-\varepsilon_h)\gamma^h} \right]$.

2368 Now, we can bound V^* as follows:

$$2370 V^*(s_t) - V^*(s_t) \leq Q^*(s_t, a_t^+) - Q^*(s_t, a_t^+) + \Delta \leq \gamma \mathbb{E}_{T(\cdot | s_t, a_t^+)} [V^*(s_{t+1}) - V^*(s_{t+1})] + \Delta \leq \frac{\varepsilon_h\gamma}{(1-\gamma)^2} \left[\frac{2}{1-(1-2\varepsilon_h)\gamma^h} + \frac{1}{1-(1-\varepsilon_h)\gamma^h} \right]. \quad (170)$$

2375 \square

2376 G.9 PROOF OF THEOREM 4.8
23772378 **Theorem 4.8.** Let \mathcal{D} be strongly ε_h -open-consistent, δ_n -suboptimal, and $\text{supp}(\mathcal{D}) \supseteq \text{supp}(\mathcal{D}^*)$. Let
2379 π_n^* be the optimal n -step return policy learned from \mathcal{D} , as the solution of

2380
$$Q_n^*(s_t, a_t) = \mathbb{E}_{P_{\mathcal{D}}} [R_{t:t+n} + \gamma^n Q_n^*(s_{t+n}, \pi_n^*(s_{t+n}))], \quad \pi_n^* : s_t \mapsto \arg \max_{a_t} Q_n^*(s_t, a_t). \quad (20)$$

2381

2382 As long as $\delta_n > \frac{3\varepsilon_h(1-\gamma^n)}{(1-\gamma)(1-\gamma^h)}$, then from all $s \in \text{supp}(\mathcal{D}^*)$, the action chunking policy, π_{ac}^+ (Equa-
2383 tion (17)), is better than the n -step return policy, π_n (Equation (20)) (i.e., $V_{\text{ac}}^+(s) > V_n^*(s)$).
23842385 To prove Theorem 4.8, we first prove the following helper Lemma G.8 to quantify sub-optimality for
2386 n -step return policy.2387 **Lemma G.8.** Let Q_n^* be the solution of the uncorrected n -step return backup equation:

2388
$$Q_n^*(s_t, a_t) = \mathbb{E}_{P_{\mathcal{D}}(\cdot|s_t, a_t)} \left[R_{t:t+n} + \gamma^n \max_{a_{t+n}} Q_n^*(s_{t+n}, a_{t+n}) \right] \quad (171)$$

2389

2390 The following inequality holds as long as \mathcal{D} is δ_n -suboptimal:

2391
$$Q^*(s_t, a_t) \geq Q_n^*(s_t, a_t) + \frac{\delta_n}{1-\gamma^n}, \forall s_t \in \mathcal{S}, a_t \in \mathcal{A} \quad (172)$$

2392

2393 where Q^* is the Q -function of the optimal policy in \mathcal{M} . For the n -step return policy

2394
$$\pi_n^* : s_t \mapsto \arg \max_{a_t} Q_n^*(s_t, a_t), \quad (173)$$

2395

2396 its corresponding value admits a similar bound:

2397
$$V^*(s_t) \geq V_n^*(s_t) + \frac{\delta_n}{1-\gamma^n}, \forall s_t \quad (174)$$

2398

2400 *Proof.* Using the definition of suboptimal data (Definition 4.7), we have

2401
$$\begin{aligned} Q_n^*(s_t, a_t) &= \mathbb{E}_{P_{\mathcal{D}}(\cdot|s_t, a_t)} \left[R_{t:t+n} + \gamma^n \max_{a_{t+n}} Q_n^*(s_{t+n}, a_{t+n}) \right] \\ 2402 &\leq Q^*(s_t, a_t) - \delta_n + \gamma^h \mathbb{E}_{P_{\mathcal{D}}(\cdot|s_t, a_t)} \left[\max_{a_{t+n}} Q_n^*(s_{t+n}, a_{t+n}) - V^*(s_{t+h}) \right] \end{aligned} \quad (175)$$

2403

2404 Rearranging the inequality above yields

2405
$$Q_n^*(s_t, a_t) - Q^*(s_t, a_t) \leq -\delta_n + \gamma^n \mathbb{E}_{P_{\mathcal{D}}(\cdot|s_t)} [V_n^*(s_{t+n}) - V^*(s_{t+n})], \forall s_t \in \mathcal{S}, a_t \in \mathcal{A} \quad (176)$$

2406

2407 By recursively applying the inequality above, we have

2408
$$Q^*(s_t, a_t) \geq Q_n^*(s_t, a_t) + \frac{\delta_n}{1-\gamma^n}, \forall s_t \in \mathcal{S}, a_t \in \mathcal{A} \quad (177)$$

2409

2410 By choosing $a_t^* = \pi_n^*(s_t)$, we see that

2411
$$\begin{aligned} V^*(s_t) &\geq Q^*(s_t, a_t) \\ 2412 &\geq Q_n^*(s_t, a_t^*) + \frac{\delta_n}{1-\gamma^n} \\ 2413 &= V_n^*(s_t) + \frac{\delta_n}{1-\gamma^n} \end{aligned} \quad (178)$$

2414

2415 \square

2416 Now we are ready to prove the main Theorem 4.8.

2417 *Proof of Theorem 4.8.* From Lemma G.8 and Theorem 4.6, we have

2418
$$V_n^*(s) + \frac{\delta_n}{1-\gamma^n} \leq V^*(s) \leq V_{\text{ac}}^+(s) + \frac{\varepsilon_h \gamma}{1-\gamma} \left[\frac{2}{1-(1-2\varepsilon_h)\gamma^h} + \frac{1}{1-(1-\varepsilon_h)\gamma^h} \right]. \quad (179)$$

2419

2420 Rearranging the terms give

2421
$$V_{\text{ac}}^+(s) - V_n^*(s) \geq \frac{\delta_n}{1-\gamma^n} - \frac{\varepsilon_h \gamma}{1-\gamma} \left[\frac{2}{1-(1-2\varepsilon_h)\gamma^h} + \frac{1}{1-(1-\varepsilon_h)\gamma^h} \right]. \quad (180)$$

2422

2423 \square

2430 G.10 PROOF THEOREM 4.11
2431

2432 **Theorem 4.11** (Closed-loop AC Policy under Bounded OV). *Let \mathcal{D}^* be the data distribution col-
2433 lected by an optimal policy. Assume \mathcal{D} can be decomposed into a mixture of data distributions
2434 $\{\mathcal{D}^*, \mathcal{D}_1, \mathcal{D}_2, \dots, \mathcal{D}_N\}$ such that each data distribution component satisfies Assumption 4.1 and for
2435 some $\vartheta_h^L, \vartheta_h^G \geq 0$, they satisfy the following two conditions:*

2436 **1. Locally bounded optimality variability condition:** every \mathcal{D}_i (including \mathcal{D}^*) exhibits ϑ_h^L -bounded
2437 variability in optimality conditioned on s_t, a_t for all $(s_t, a_t) \in \text{supp}(P_{\mathcal{D}_i}(s_t, a_t))$, and
2438

2439 **2. Globally bounded optimality variability condition:** \mathcal{D} as a whole exhibits ϑ_h^G -variability in
2440 optimality conditioned on $s_t, a_{t:t+h}$ for all $(s_t, a_{t:t+h}) \in \text{supp}(P_{\mathcal{D}}(s_t, a_{t:t+h}))$.

2441 Then for all $s_t \in \text{supp}(P_{\mathcal{D}^*}(s_t))$,

$$2442 V^*(s_t) - V^*(s_t) \leq \frac{\vartheta_h^L}{1-\gamma} + \frac{\vartheta_h^G + \gamma^h \min(\vartheta_h^L, \vartheta_h^G)}{(1-\gamma)(1-\gamma^h)} \leq \vartheta_h^L H + 2\vartheta_h^G H \bar{H} \quad (24)$$

2443 The proof of Theorem 4.11 below is made possible by observing that $V^*(s_t) - \hat{V}_{\text{ac}}^+(s_t)$ and $\hat{V}_{\text{ac}}^+(s_t) - Q^*(s_t, a_t^+)$ are bounded by $\vartheta_h^G/(1-\gamma^h)$ and $\vartheta_h^L/(1-\gamma^h)$ respectively. Combining this two bounds
2444 naively already allows us to derive a relatively loose bound $V^*(s_t) - Q^*(s_t, a_t^+) \leq (\vartheta_h^L + \vartheta_h^G)/(1-\gamma^h)$ which leads to $V^*(s_t) - V^*(s_t) \leq (\vartheta_h^L + \vartheta_h^G)/(1-\gamma^h)/(1-\gamma)$. To obtain the tight bound in
2445 Theorem 4.11, we leverage a key insight that the amount of overestimation in V_{ac}^+ can *never exceed*
2446 $\vartheta_h^L + \frac{\vartheta_h^G}{1-\gamma^h}$ as otherwise the nominal value of the action chunking policy h -step into the future,
2447 $\hat{V}_{\text{ac}}^+(s_{t+h})$, would have an optimality gap higher than $\vartheta_h^G/(1-\gamma^h)$, which is impossible under the
2448 global optimality variability condition. Forming this tight bound is important because it effectively
2449 shaves off a factor of $\bar{H} = 1/(1-\gamma^h)$ from the ϑ_h^L term (the stronger local condition) and only
2450 bumps up a factor of ≈ 2 to the ϑ_h^G term (the weaker global condition).

2451 *Proof of Theorem 4.11.* Consider any $s_t \in \text{supp}(P_{\mathcal{D}^*}(s_t))$. Let $a_{t:t+h}^+ = \pi_{\text{ac}}^+(s_t)$ and
2452 $a_{t:t+h}^\circ := \arg \max_{a_{t:t+h} \in \text{supp}(P_{\mathcal{D}^*}(a_{t:t+h} | s_t))} [\mathbb{E}_{P_{\mathcal{D}^*}(\cdot | s_t, a_{t:t+h})} [R_{t:t+h} + \gamma^h V^*(s_{t+h})]]$. (181)

2453 We first observe that

$$2454 \mathbb{E}_{P_{\mathcal{D}^*}(\cdot | s_t, a_{t:t+h}^\circ)} [R_{t:t+h} + \gamma^h V^*(s_{t+h})] \geq V^*(s_t), \quad (182)$$

2455 because

$$2456 V^*(s_t) = \mathbb{E}_{a_{t:t+h} \sim P_{\mathcal{D}^*}(\cdot | s_t)} [\mathbb{E}_{P_{\mathcal{D}^*}(\cdot | s_t, a_{t:t+h})} [R_{t:t+h} + \gamma^h V^*(s_{t+h})]], \quad (183)$$

2457 and the maximum value of a random variable is no less than its expectation.

2458 Let

$$2459 \tilde{Q}_{\min}(s_t, a_{t:t+h}^\circ) := \min_{\text{supp}(P_{\mathcal{D}^*}(\cdot | s_t, a_{t:t+h}^\circ))} [R_{t:t+h} + V^*(s_{t+h})], \quad (184)$$

$$2460 \tilde{Q}_{\max}(s_t, a_{t:t+h}^\circ) := \max_{\text{supp}(P_{\mathcal{D}^*}(\cdot | s_t, a_{t:t+h}^\circ))} [R_{t:t+h} + V^*(s_{t+h})]. \quad (185)$$

2461 Since \mathcal{D} exhibits ϑ_h^G -variability in optimality, we have

$$2462 \tilde{Q}_{\min}(s_t, a_{t:t+h}^\circ) \geq \tilde{Q}_{\max}(s_t, a_{t:t+h}^\circ) - \vartheta_h^G. \quad (186)$$

2463

$$\begin{aligned} 2464 V^*(s_t) - Q^*(s_t, a_t^+) \\ 2465 &= V^*(s_t) - \hat{V}_{\text{ac}}^+(s_t) + \hat{V}_{\text{ac}}^+(s_t) - Q^*(s_t, a_t^+) \\ 2466 &= V^*(s_t) - \hat{Q}_{\text{ac}}^+(s_t, a_{t:t+h}^+) + \hat{Q}_{\text{ac}}^+(s_t, a_{t:t+h}^+) - Q^*(s_t, a_t^+) \\ 2467 &\leq V^*(s_t) - \hat{Q}_{\text{ac}}^+(s_t, a_{t:t+h}^\circ) + \vartheta_h^L + \gamma^h \mathbb{E}_{P_{\mathcal{D}^*}(\cdot | s_t, a_{t:t+h}^\circ)} [\hat{V}_{\text{ac}}^+(s_{t+h}) - V^*(s_{t+h})] \\ 2468 &= V^*(s_t) - \hat{Q}_{\text{ac}}^+(s_t, a_{t:t+h}^\circ) + \vartheta_h^L + \gamma^h \mathbb{E}_{P_{\mathcal{D}^*}(\cdot | s_t, a_{t:t+h}^\circ)} [\hat{V}_{\text{ac}}^+(s_{t+h}) - Q^*(s_{t+h}, a_{t+h}^+)] - \\ 2469 &\quad \gamma^h \mathbb{E}_{P_{\mathcal{D}^*}(\cdot | s_t, a_{t:t+h}^\circ)} [V^*(s_{t+h}) - Q^*(s_{t+h}, a_{t+h}^+)]. \end{aligned} \quad (187)$$

We can use it to lower-bound $\hat{V}_{\text{ac}}^+(s_t)$ as follows:

$$\begin{aligned}
\hat{V}_{\text{ac}}^+(s_t) &= \hat{Q}_{\text{ac}}^+(s_t, a_{t:t+h}^+) \\
&\geq \hat{Q}_{\text{ac}}^+(s_t, a_{t:t+h}^\circ) \\
&= \mathbb{E}_{P_{\mathcal{D}}(\cdot|s_t, a_{t:t+h}^\circ)} \left[R_{t:t+h} + \gamma^h \hat{V}_{\text{ac}}^+(s_{t+h}) \right] \\
&= \mathbb{E}_{P_{\mathcal{D}}(\cdot|s_t, a_{t:t+h}^\circ)} \left[R_{t:t+h} + \gamma^h V^*(s_{t+h}) \right] + \mathbb{E}_{P_{\mathcal{D}}(\cdot|s_t, a_{t:t+h}^\circ)} \left[\gamma^h (\hat{V}_{\text{ac}}^+(s_{t+h}) - V^*(s_{t+h})) \right] \\
&\geq \tilde{Q}_{\min}(s_t, a_{t:t+h}^\circ) + \mathbb{E}_{P_{\mathcal{D}}(\cdot|s_t, a_{t:t+h}^\circ)} \left[\gamma^h (\hat{V}_{\text{ac}}^+(s_{t+h}) - V^*(s_{t+h})) \right] \\
&\geq \tilde{Q}_{\max}(s_t, a_{t:t+h}^\circ) - \vartheta_h^G + \mathbb{E}_{P_{\mathcal{D}}(\cdot|s_t, a_{t:t+h}^\circ)} \left[\gamma^h (\hat{V}_{\text{ac}}^+(s_{t+h}) - V^*(s_{t+h})) \right] \\
&\geq \mathbb{E}_{P_{\mathcal{D}^*}(\cdot|s_t, a_{t:t+h}^\circ)} \left[R_{t:t+h} + \gamma^h V^*(s_{t+h}) \right] - \vartheta_h^G + \gamma^h \mathbb{E}_{P_{\mathcal{D}}(\cdot|s_t, a_{t:t+h}^\circ)} \left[(\hat{V}_{\text{ac}}^+(s_{t+h}) - V^*(s_{t+h})) \right] \\
&\geq V^*(s_t) - \vartheta_h^G + \gamma^h \mathbb{E}_{P_{\mathcal{D}}(\cdot|s_t, a_{t:t+h}^\circ)} \left[(\hat{V}_{\text{ac}}^+(s_{t+h}) - V^*(s_{t+h})) \right] \\
&\geq V^*(s_t) - \frac{\vartheta_h^G}{1 - \gamma^h}.
\end{aligned} \tag{188}$$

Let $\mathbb{M}^+ = \{\tilde{\mathcal{D}}_1, \dots, \tilde{\mathcal{D}}_{M^+}\}$ be all data distributions from $\{\mathcal{D}^*, \mathcal{D}_1, \mathcal{D}_2, \dots, \mathcal{D}_N\}$ where $(s_t, a_{t:t+h}^+)$ is in the support. Let $\tilde{\mathcal{D}}^+$ be any mixture of \mathbb{M} where each mixture component has non-zero weight:

$$P_{\tilde{\mathcal{D}}^+} = \sum_{i=1}^M w_i P_{\tilde{\mathcal{D}}_i}, \quad (189)$$

where $w_i > 0, \sum_i w_i = 1$.

Let

$$\tilde{Q}_{\min}^*(s_t, a_t) := \min_{\text{supp}(P_{\mathcal{D}^*}(\cdot | s_t, a_t))} [R_{t:t+h} + V^*(s_{t+h})], \quad (190)$$

$$\tilde{Q}_{\max}^*(s_t, a_t) := \max_{\text{supp}(P_{\mathcal{D}^*}(\cdot | s_t, a_t))} [R_{t:t+h} + V^*(s_{t+h})], \quad (191)$$

$$\tilde{Q}_{\min}^i(s_t, a_t) := \min_{\text{supp}(P_{\mathcal{D}^i}(\cdot | s_t, a_t))} [R_{t:t+h} + V^*(s_{t+h})], \quad (192)$$

$$\tilde{Q}_{\max}^i(s_t, a_t) := \max_{\text{supp}(P_{\mathcal{D}^i}(\cdot|s_t, a_t))} [R_{t:t+h} + V^\star(s_{t+h})], \quad (193)$$

$$\tilde{Q}_{\max}^+(s_t, a_t^+) := \max_{\text{supp}(P_{\mathcal{D}^+}(\cdot | s_t, a_t^+))} [R_{t:t+h} + V^*(s_{t+h})], \quad (194)$$

$$\tilde{Q}_{\max}^+(s_t, a_{t:t+h}^+) := \max_{\text{supp}(P_{\mathcal{D}^+}(\cdot | s_t, a_{t:t+h}^+))} [R_{t:t+h} + V^\star(s_{t+h})]. \quad (195)$$

The minimum and the maximum is over the remaining trajectory conditioned on s_t, a_t or $s_t, a_{t:h}$ that is still in the support of the corresponding data distribution.

From the ϑ_h^L -bounded variability in optimality and the Assumption 4.1 of each data mixture, we observe that

$$Q^\star(s_t, a_t) \geq \tilde{Q}_{-i-}^i(s_t, a_t) \geq \tilde{Q}_{-i-}^i(s_t, a_t) - \vartheta_L^L, \quad \forall i \in \{1, 2, \dots, N\} \quad (196)$$

$$Q^*(s_t, a_t) \geq \tilde{Q}_{\text{...}}^*(s_t, a_t) \geq \tilde{Q}_{\text{...}}^*(s_t, a_t) = \vartheta_{\text{...}}^L. \quad (197)$$

We can then derive that

$$\begin{aligned}\tilde{Q}_{\max}^+(s_t, a_t^+) &= \max(\tilde{Q}_{\max}^*(s_t, a_t^+), \tilde{Q}_{\max}^1(s_t, a_t^+), \dots, \tilde{Q}_{\max}^N(s_t, a_t^+)) \\ &\leq Q^*(s_t, a_t) + \beta_t^L.\end{aligned}\tag{198}$$

2538 With this, we can now upper-bound $\hat{V}_{\text{ac}}^+(s_t)$ as follows:
 2539

$$\begin{aligned}
 2540 \quad \hat{V}_{\text{ac}}^+(s_t) &= \hat{Q}_{\text{ac}}^+(s_t, a_{t:t+h}^+) \\
 2541 &= \mathbb{E}_{P_{\mathcal{D}}(\cdot|s_t, a_{t:t+h}^+)} \left[R_{t:t+h} + \gamma^h \hat{V}_{\text{ac}}^+(s_{t+h}) \right] \\
 2542 &= \mathbb{E}_{P_{\hat{\mathcal{D}}^+}(\cdot|s_t, a_{t:t+h}^+)} \left[R_{t:t+h} + \gamma^h \hat{V}_{\text{ac}}^+(s_{t+h}) \right] \\
 2543 &= \mathbb{E}_{P_{\hat{\mathcal{D}}^+}(\cdot|s_t, a_{t:t+h}^+)} \left[R_{t:t+h} + \gamma^h V^*(s_{t+h}) \right] + \gamma^h \mathbb{E}_{P_{\hat{\mathcal{D}}^+}(\cdot|s_t, a_{t:t+h}^+)} \left[\hat{V}_{\text{ac}}^+(s_{t+h}) - V^*(s_{t+h}) \right] \\
 2544 &\leq \tilde{Q}_{\text{max}}^+(s_t, a_{t:t+h}^+) + \gamma^h \mathbb{E}_{P_{\mathcal{D}}(\cdot|s_t, a_{t:t+h}^+)} \left[\hat{V}_{\text{ac}}^+(s_{t+h}) - V^*(s_{t+h}) \right] \\
 2545 &\leq \tilde{Q}_{\text{max}}^+(s_t, a_t^+) + \gamma^h \mathbb{E}_{P_{\mathcal{D}}(\cdot|s_t, a_{t:t+h}^+)} \left[\hat{V}_{\text{ac}}^+(s_{t+h}) - V^*(s_{t+h}) \right] \\
 2546 &\leq Q^*(s_t, a_t^+) + \vartheta_h^L + \gamma^h \mathbb{E}_{P_{\mathcal{D}}(\cdot|s_t, a_{t:t+h}^+)} \left[\hat{V}_{\text{ac}}^+(s_{t+h}) - V^*(s_{t+h}) \right].
 \end{aligned} \tag{199}$$

2553 Let

$$\Delta(s_t) := V^*(s_t) - Q^*(s_t, a_t^+). \tag{200}$$

$$\hat{\Delta}(s_t) := \hat{V}_{\text{ac}}^+(s_t) - Q^*(s_t, a_t^+). \tag{201}$$

2558 From the inequalities above, we have

$$\hat{\Delta}(s_t) \leq \vartheta_h^L + \gamma^h \sup_{s_{t+h}} \left[\hat{\Delta}(s_{t+h}) - \Delta(s_{t+h}) \right], \tag{202}$$

$$0 \leq \Delta(s_t) \leq \frac{\vartheta_h^G}{1 - \gamma^h} + \hat{\Delta}(s_t), \tag{203}$$

$$\hat{\Delta}(s_t) - \Delta(s_t) \leq \min \left\{ \frac{\vartheta_h^G}{1 - \gamma^h}, \hat{\Delta}(s_t) \right\}. \tag{204}$$

2567 The minimum operator allows us to obtain two upper-bounds on Δ :

$$\Delta(s_t) \leq \vartheta_h^L + \frac{(1 + \gamma^h)\vartheta_h^G}{1 - \gamma^h}, \tag{205}$$

$$\Delta(s_t) \leq \frac{\vartheta_h^G}{1 - \gamma^h} + \hat{\Delta}(s_t) \leq \frac{\vartheta_h^L + \vartheta_h^G}{1 - \gamma^h}. \tag{206}$$

2574 Finally, combining these two upper-bounds together and recursively applying the inequality yields
 2575 our desired results:

$$V^*(s_t) - Q^*(s_t, a_t^+) \leq \frac{\vartheta_h^L}{1 - \gamma} + \frac{\vartheta_h^L}{(1 - \gamma)(1 - \gamma^h)} + \frac{\gamma^h \min(\vartheta_h^G, \vartheta_h^L)}{(1 - \gamma)(1 - \gamma^h)}. \tag{207}$$

2579 \square

2580
 2581
 2582
 2583
 2584
 2585
 2586
 2587
 2588
 2589
 2590
 2591

2592 G.11 PROOF OF THEOREM F.4
2593

2594 **Theorem F.4** (Worst-case Closed-loop AC Policy under BOV). *For any $\gamma \in (0, 1)$, $\vartheta_h^G, \vartheta_h^L \in$
2595 $\left(0, \frac{\gamma - \gamma^h}{4(1-\gamma)}\right]$, $c \in \left[0, \frac{\gamma - \gamma^h}{4(1-\gamma^h)}\right)$, $\sigma \in \left(0, \frac{\min(\vartheta_h^G, \vartheta_h^L)}{1-\gamma}\right)$, there exists \mathcal{M} and \mathcal{D} satisfying the mixture
2596 assumption in Theorem 4.11 such that there exists $s_t \in \text{supp}(P_{\mathcal{D}^*}(s_t))$, where*

$$2598 V^*(s_t) - V^*(s_t) = \frac{\vartheta_h^L}{1-\gamma} + \frac{\vartheta_h^G + \gamma^h \min(\vartheta_h^L, \vartheta_h^G)}{(1-\gamma)(1-\gamma^h)} - \sigma, \quad V^*(s_t) - V_{\text{ac}}^*(s_t) \geq \frac{c}{1-\gamma} \quad (38)$$

2600 To show that our upper-bound is achievable, we need to carefully design both the MDP and the data
2601 distribution. For clarity of the proof, we divide up the construction into two parts. The first part
2602 (Lemma G.9) focuses on designing part of the MDP and two data distributions \mathcal{D}^* and \mathcal{D}^\diamond such that
2603 any action chunk that has a value bigger than $V^* - \frac{\vartheta_h^G}{1-\gamma^h}$ is preferred over the action chunks in \mathcal{D}^*
2604 and \mathcal{D}^\diamond . The second part (Lemma G.10) focuses on constructing the remaining MDP and the \mathcal{D}^\triangle
2605 that contains the action chunk that π_{ac}^+ picks where \hat{V}_{ac}^+ overestimates the value of this action chunk
2606 by $\vartheta_h^L + \frac{\gamma^h \min(\vartheta_h^L, \vartheta_h^G)}{1-\gamma^h}$. Finally, we assemble these two results (combining \mathcal{D}^* , \mathcal{D}^\diamond , \mathcal{D}^\triangle) to show
2607 that the MDP and the mixture data achieve our upper-bound *exactly*.
2608

2609 **Lemma G.9** (“The Castle”). *For $\delta \in (0, 1)$, $\vartheta_h^G < \frac{\gamma - \gamma^h}{2(1-\gamma)}$, consider a 2-state, 2-action MDP in
2610 Figure 10. Let there be two data distributions, \mathcal{D}^* and \mathcal{D}^\diamond . \mathcal{D}^* is collected by the following optimal
2611 closed-loop policy from X and Y :*

$$2613 \pi^*(X) = 0, \pi^*(Y) = 1. \quad (208)$$

2614 *\mathcal{D}^\diamond is collected by the following optimal closed-loop policy from X and Y :*

$$2615 \pi^\diamond(X) = 1, \pi^\diamond(Y) = 0. \quad (209)$$

2616 *Let \mathcal{D} be a mixture of \mathcal{D}^* and \mathcal{D}^\diamond with*

$$2618 P_{\mathcal{D}} = (1 - \varsigma)P_{\mathcal{D}^*} + \varsigma P_{\mathcal{D}^\diamond}. \quad (210)$$

2619 *There exists $c_1 \in (0, 1/2)$ such that*

- 2621 1. \mathcal{D}^* and \mathcal{D}^\diamond both individually exhibits 0-variability in optimality conditioned on s_t, a_t for all
2622 $s_t, a_t \in \text{supp}(P_{\mathcal{D}}(s_t, a_t))$,
- 2623 2. \mathcal{D} exhibits ϑ_h^G -variability in optimality conditioned on $s_t, a_{t:t+h}$ for all $s_t, a_{t:t+h} \in$
2624 $\text{supp}(P_{\mathcal{D}}(s_t, a_{t:t+h}))$,

2625 *and*

$$2627 \hat{V}_{\text{ac}}^+(X) = \hat{V}_{\text{ac}}^+(Y) = \frac{1 - \gamma + \varsigma(\gamma - \gamma^h)}{2(1 - \gamma^h)(1 - \gamma)} - \frac{\varsigma \vartheta_h^G}{1 - \gamma^h}. \quad (211)$$

2630 *Proof.* Set

$$2632 c_1 = \frac{(1 - \gamma)\vartheta_h^G}{\gamma - \gamma^h}. \quad (212)$$

2633 We first check whether $c_1 \in (0, 1/2)$. For the upper-bound, it is clear that $c_1 < 1/2$ because
2634 $\vartheta_h^G < \frac{\gamma - \gamma^h}{2(1-\gamma)}$. For the lower-bound, $c > 0$ because all terms in the fraction are positive.
2635

2636 We now check the two optimality variability conditions. The first (local) one is trivial because π^*
2637 always receives $r = 1/2 - c_1$ and π^* always receives $r = 1/2$, and the optimal value for X and Y
2638 are both $V^*(X) = V^*(Y) = \frac{1}{2(1-\gamma)}$.
2639

2640 Next, we check the second (global) condition by analyzing all possible states and action chunks in \mathcal{D} .
2641 We observe that for any $a_{t:t+h}$ that starts with $a_t = 0$, we have

$$2642 \tilde{Q}_{\min}(X, a_{t:t+h}) = \frac{1 - 2c_1(\gamma - \gamma^h)}{2(1 - \gamma)}, \quad (213)$$

$$2644 \tilde{Q}_{\max}(X, a_{t:t+h}) = \frac{1}{2(1 - \gamma)}, \quad (214)$$

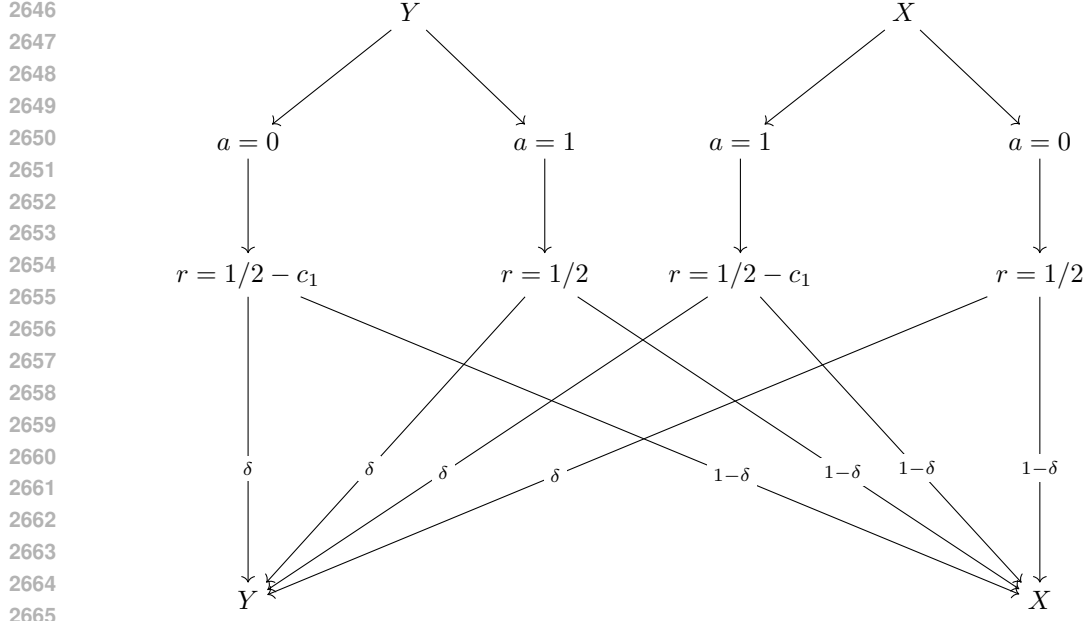


Figure 10: **MDP construction Part 1 for Theorem F.4 (“the castle”)**. This diagram describes state X and Y and how actions $a = 0$ and $a = 1$ transition between them. The main purpose of this construction is to make $\hat{V}_{ac}^+(X)$ underestimate V^* by exactly $\vartheta_h^G/(1 - \gamma^h)$. This allows the action chunk that appears in the second part of the construction to be preferred (by π_{ac}^+) over the action chunks that start with $a = 0$ or $a = 1$.

which gives

$$\tilde{Q}_{\max}(X, a_{t:t+h}) - \tilde{Q}_{\min}(X, a_{t:t+h}) = \vartheta_h^G. \quad (215)$$

By symmetry, we also have

$$\tilde{Q}_{\max}(Y, a_{t:t+h}) - \tilde{Q}_{\min}(Y, a_{t:t+h}) = \vartheta_h^G. \quad (216)$$

for all $a_{t:t+h}$ that starts with $a_t = 1$.

Now, for any $a_{t:t+h}$ that starts with $a_t = 1$, we have

$$\tilde{Q}_{\min}(X, a_{t:t+h}) = \frac{\gamma - 2c_1(\gamma - \gamma^h)}{2(1 - \gamma)}, \quad (217)$$

$$\tilde{Q}_{\max}(X, a_{t:t+h}) = \frac{\gamma}{2(1 - \gamma)}, \quad (218)$$

which admits the same gap as the case when $a_t = 0$. The same also holds for Y with $a_t = 1$. Thus, \mathcal{D} exhibits ϑ_h^G -variability in optimality conditioned on $s_t, a_{t:t+h}$ for all $s_t, a_{t:t+h} \in \text{supp}(P_{\mathcal{D}}(s_t, a_{t:t+h}))$.

Finally, we check for the value,

$$\begin{aligned} \hat{V}_{ac}^+(X) &= \hat{V}_{ac}^+(Y) = (1 - \varsigma)/2 + \varsigma(1/2 + (1 - 2c_1)\frac{\gamma - \gamma^h}{2(1 - \gamma)}) \\ &= \frac{1}{1 - \gamma^h} \left[1/2 + \varsigma \frac{(1 - 2c_1)(\gamma - \gamma^h)}{2(1 - \gamma)} \right] \\ &= \frac{1}{2(1 - \gamma^h)} \left[1 + \varsigma \frac{\gamma - \gamma^h - 2(1 - \gamma)\vartheta_h^G}{1 - \gamma} \right] \\ &= \frac{1 - \gamma + \varsigma(\gamma - \gamma^h)}{2(1 - \gamma^h)(1 - \gamma)} - \frac{\varsigma\vartheta_h^G}{1 - \gamma^h}, \end{aligned} \quad (219)$$

as desired. \square

2700 **Lemma G.10** (“The Flower”). Assume $\vartheta_h^G \in \left(0, \frac{1-\gamma^h}{8}\right]$, $\vartheta_h^L \in \left(0, \frac{\gamma-\gamma^h}{4(1-\gamma)}\right]$, $\gamma \in (0, 1)$, and
 2701 Consider a 5-state, 3-action MDP in Figure 11 building on top of the transitions that already in
 2702 Figure 10. Let \mathcal{D}^Δ be a data distribution induced by a cycling, time-dependent (with a time cycle
 2703 length of h) policy π^Δ (we use the subscript to indicate the time step from 0 to $h-1$):
 2704

$$\pi_0^\Delta(s_t = X) = \pi_0^\Delta(s_t = \tilde{X}) = 2, \quad (220)$$

$$\pi_0^\Delta(s_t = Y) = 3 \quad (221)$$

$$\pi_k^\Delta(s_{t+k} = \tilde{C}) = \pi_k^\Delta(s_{t+k} = \tilde{D}) = 2, \quad \forall k \in \{1, 2, \dots, h-2\}, \quad (222)$$

$$\pi_k^\Delta(s_{t+h-1} = \tilde{C}) = \pi_k^\Delta(s_{t+h-1} = \tilde{D}) = 0, \quad (223)$$

$$\pi_k^\Delta(s_{t+k} = X) = 0, \quad \forall k \in \{1, 2, \dots, h-1\}, \quad (224)$$

$$\pi_k^\Delta(s_{t+k} = Y) = 1, \quad \forall k \in \{1, 2, \dots, h-1\}. \quad (225)$$

2714 Let \hat{V}_{ac}^+ be the nominal value of the action chunking policy π_{ac}^+ learned from \mathcal{D}^Δ and let
 2715

$$\Delta = \vartheta_h^L + \frac{\vartheta_h^G}{1-\gamma^h} + \frac{\gamma^h \min(\vartheta_h^G, \vartheta_h^L)}{1-\gamma^h}. \quad (226)$$

2719 For any $c \in \left[0, \frac{\gamma-\gamma^h}{4(1-\gamma^h)}\right)$, there exists some $0 < c_2 \leq 1/2$, $0 < c_3 \leq 1/2$, $\delta, \delta_2 \in (0, 1)$, such that
 2720 for every $0 < \tilde{\Delta} < \min\left(\Delta, \frac{2\vartheta_h^G}{1-\gamma^h}\right)$,
 2721

- 2723 1. \mathcal{D}^Δ exhibits 0-variability in optimality conditioned on $s_t, a_{t:t+h}$ for all $s_t, a_{t:t+h} \in$
 2724 $\text{supp}(P_{\mathcal{D}^\Delta}(s_t, a_{t:t+h}))$,
- 2726 2. \mathcal{D}^Δ exhibits ϑ_h^L -variability in optimality conditioned on s_t, a_t for all $s_t, a_t \in$
 2727 $\text{supp}(P_{\mathcal{D}^\Delta}(s_t, a_t))$,

2728 and

$$\hat{V}_{\text{ac}}^+(X) = \frac{1}{2(1-\gamma)} - \frac{\vartheta_h^G}{1-\gamma^h} + \tilde{\Delta}, \quad (227)$$

$$V^*(X) - V^*(X) = \frac{\Delta - \tilde{\Delta}}{1-\gamma}, \quad (228)$$

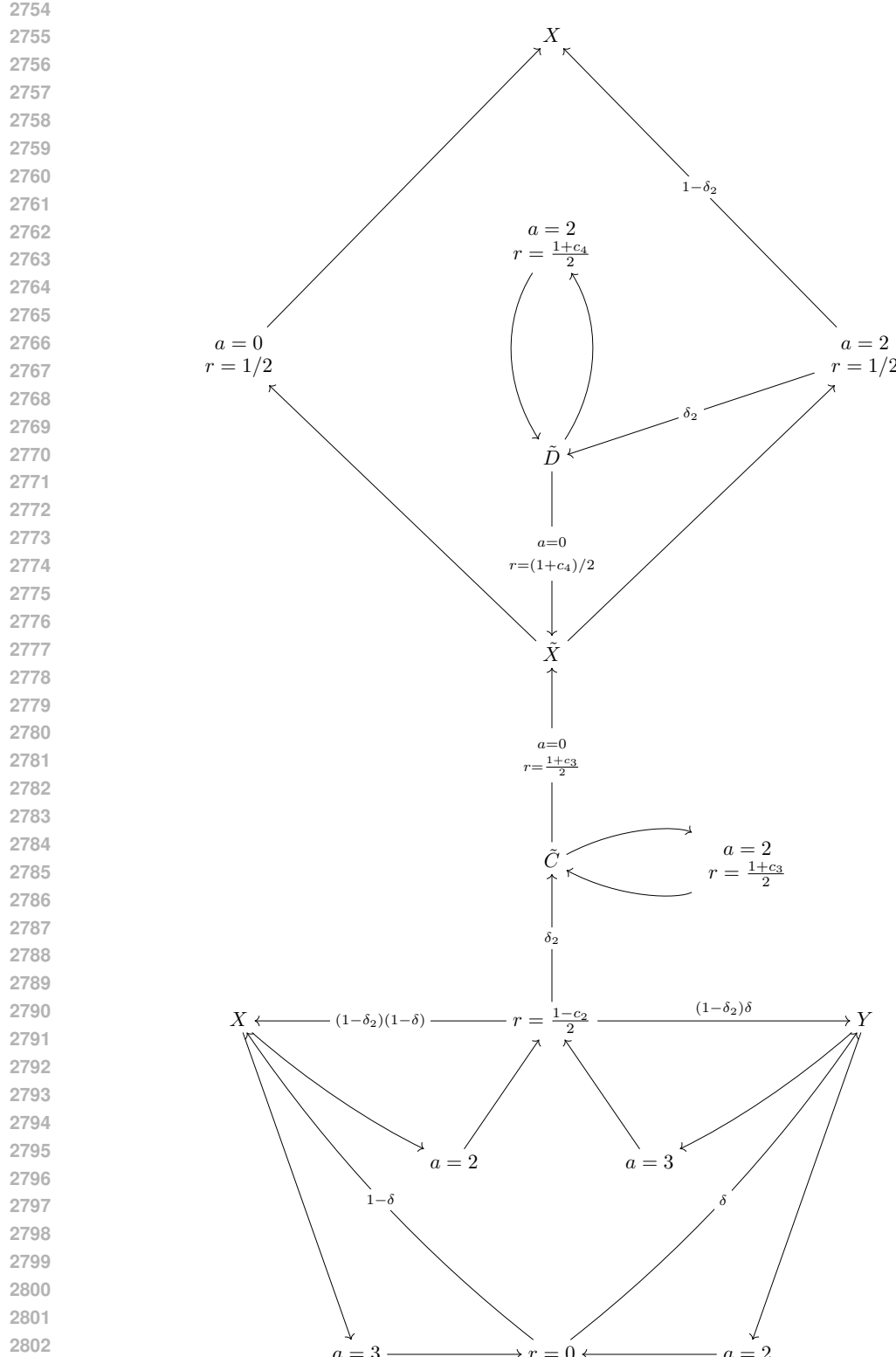
$$V^*(X) - V_{\text{ac}}^+(X) \geq \frac{c}{1-\gamma}, \quad (229)$$

$$V^*(X) - V_{\text{ac}}^*(X) \geq \frac{c}{1-\gamma}. \quad (230)$$

2740 *Proof.* Without the loss of generality, we assume we always start from state X . Due to symmetry,
 2741 the same analysis applies to state Y (with the first action being $a_t = 3$ rather than $a_t = 2$).
 2742

2743 Due to cycling nature of the data collection policy, we observe that all action chunks starting from
 2744 X are in the form of $a_{t:t+h} = (2, \underbrace{\dots}_{0\text{'s and }1\text{'s}})$ or $a_{t:t+h} = (2, 2, \dots, 2, 0)$. These two possibilities
 2745 correspond to two different paths that the data collection policy takes:
 2746

- 2748 • $a_{t:t+h}^o = (2, \underbrace{\dots}_{0\text{'s and }1\text{'s}})$: Stay in either X or Y . The agent going on this path receives a
 2749 constant reward of $1/2$ except the first step where it receives a reward of $(1 - c_2)/2$.
- 2751 • $a_{t:t+h}^\Delta = (2, 2, \dots, 2, 0)$: Visit \tilde{C} and then stays there for $h-1$ until it goes out with $a=0$
 2752 to visit \tilde{X} . The agent going on this path receives a constant reward of $(1 + c_3)/2$ except the
 2753 first step where it receives a reward of $(1 - c_2)/2$.



2804: Figure 11: **MDP construction Part 2 for Theorem E.4 (“the flower”)**. This diagram describes the remaining
2805: states \tilde{C} , \tilde{D} and \tilde{X} , and what actions $a = 2$ and $a = 3$ do in state X and Y . The main purpose of this
2806: construction is to make $\hat{V}_{ac}^+(X)$ overestimate the optimal value of the action chunks that $\pi_{ac}^+, Q^*(X, a_t^+)$, by
2807: exactly $\vartheta_h^L + \gamma^h \min(\vartheta_h^L, \vartheta_h^G)/(1 - \gamma^h)$.

2808 Similarly, all action chunks starting from \tilde{X} are in the form of $a_{t:t+h} = (2, \underbrace{\dots}_{0\text{'s and }1\text{'s}})$ or $a_{t:t+h} =$
 2809
 2810 $(2, 2, \dots, 2, 0)$. These two possibilities correspond to two different paths that the data collection
 2811 policy takes:
 2812

2813 • $a_{t:t+h}^o = (2, \underbrace{\dots}_{0\text{'s and }1\text{'s}})$: Stay in either X or Y . The agent going on this path receives a
 2814 constant reward of $1/2$.
 2815

2816 • $a_{t:t+h}^\Delta = (2, 2, \dots, 2, 0)$: Visit \tilde{C} and then stays there for $h-1$ until it goes out with $a=0$
 2817 to visit \tilde{X} . The agent going on this path receives a constant reward of $(1+c_4)/2$ except the
 2818 first step where it receives a reward of $1/2$.
 2819

2820 Now, we divide up the problem into two cases depending on the relative values of ϑ_h^L and ϑ_h^G .
 2821

2822 1. Case $\vartheta_h^L \geq \vartheta_h^G$:

2823 Set

2824

$$c_2 = 2 \left[\vartheta_h^L + \frac{(1+\gamma^h)\vartheta_h^G}{1-\gamma^h} \right] - 2\tilde{\Delta} > 0, \quad (231)$$

2825

$$c_3 = \frac{2(1-\gamma)\vartheta_h^L}{\gamma-\gamma^h} > 0, \quad (232)$$

2826

$$c_4 = \frac{2(1-\gamma)\vartheta_h^G}{\gamma-\gamma^h} > 0. \quad (233)$$

2827 Next, we check that $c_2, c_3, c_4 \leq 1/2$.

2828 We first observe that

2829

$$(1-\gamma)(1-\gamma^h) - 2(\gamma-\gamma^h) = 1 - 3\gamma + \gamma^h(\gamma+1) \leq 1 - 3\gamma + \gamma(\gamma+1) = (1-\gamma)^2 \geq 0. \quad (234)$$

2830 Dividing both sides by $8(1-\gamma)$ yields

2831

$$\frac{1-\gamma^h}{8} \geq \frac{\gamma-\gamma^h}{4(1-\gamma)} \geq \vartheta_h^L \geq \vartheta_h^G. \quad (235)$$

2832 Now, using the inequality above, we have

2833

$$\begin{aligned} c_2 &= 2 \left[\vartheta_h^L + \frac{(1+\gamma^h)\vartheta_h^G}{1-\gamma^h} \right] - 2\tilde{\Delta} \\ &\leq 2 \left[\vartheta_h^L + \frac{(1+\gamma^h)\vartheta_h^L}{1-\gamma^h} \right] \\ &\leq \frac{4\vartheta_h^L}{1-\gamma^h} \\ &\leq 1/2. \end{aligned} \quad (236)$$

2834 Furthermore,

2835

$$c_4 \leq c_3 = \frac{2(1-\gamma)\vartheta_h^L}{\gamma-\gamma^h} \leq 1/2. \quad (237)$$

2836 Next, we check the data distribution \mathcal{D}^Δ satisfies both optimality variability conditions. We first
 2837 note that we only need to check for $s_t \in \{X, \tilde{X}\}$ because all other states are out of the support due
 2838 to the cycling nature of the data collection policies. The first (global) optimality condition is trivial
 2839 because the h -step reward received is deterministic conditioned on $a_{t:t+h} \in \{a_{t:t+h}^o, a_{t:t+h}^\Delta\}$, and
 2840 the optimal value of $V^*(s_{t+h})$ is always $\frac{1}{2(1-\gamma)}$. This leads to 0-variability in optimality conditioned

on $s_t, a_{t:t+h}$. For the second (local) optimality condition, we check the difference in optimality for two paths from $s_t, a_t = 2$ for both $s_t = X$ and $s_t = \tilde{X}$.

For $s_t = X$, the optimality gap is

$$c_3 \frac{\gamma - \gamma^h}{2(1 - \gamma^h)} = \vartheta_h^L. \quad (238)$$

For $s_t = \tilde{X}$, the optimality gap is

$$c_4 \frac{\gamma - \gamma^h}{2(1 - \gamma^h)} = \vartheta_h^G \leq \vartheta_h^L. \quad (239)$$

This concludes that the second (local) optimality condition is also satisfied.

Next, we first analyze which action chunk π_{ac}^+ prefers by computing \hat{Q}_{ac}^+ 's:

$$\hat{Q}_{ac}^+(X, a_{t:t+h}^o) = \frac{1}{2} \left[(1 - c_2) + \frac{\gamma - \gamma^h}{1 - \gamma} \right] + \gamma^h \hat{V}_{ac}^+(X), \quad (240)$$

$$\hat{Q}_{ac}^+(X, a_{t:t+h}^\Delta) = \frac{1}{2} \left[(1 - c_2) + (1 + c_3) \frac{\gamma - \gamma^h}{1 - \gamma} \right] + \gamma^h \hat{V}_{ac}^+(\tilde{X}), \quad (241)$$

$$\hat{Q}_{ac}^+(\tilde{X}, a_{t:t+h}^o) = \frac{1}{2} \left[\frac{1 - \gamma^h}{1 - \gamma} \right] + \gamma^h \hat{V}_{ac}^+(X), \quad (242)$$

$$\hat{Q}_{ac}^+(\tilde{X}, a_{t:t+h}^\Delta) = \frac{1}{2} \left[1 + (1 + c_4) \frac{\gamma - \gamma^h}{1 - \gamma} \right] + \gamma^h \hat{V}_{ac}^+(\tilde{X}). \quad (243)$$

We first observe that

$$\begin{aligned} \hat{Q}_{ac}^+(\tilde{X}, a_{t:t+h}^\Delta) - \hat{Q}_{ac}^+(X, a_{t:t+h}^\Delta) &= \frac{1}{2} \left[c_2 - (c_3 - c_4) \frac{\gamma - \gamma^h}{1 - \gamma} \right] \\ &= \vartheta_h^L + \frac{(1 + \gamma^h) \vartheta_h^G}{1 - \gamma^h} - \vartheta_h^L + \vartheta_h^G - \tilde{\Delta} \\ &= \frac{2\vartheta_h^G}{1 - \gamma^h} - \tilde{\Delta} \\ &> 0. \end{aligned} \quad (244)$$

Also,

$$\hat{Q}_{ac}^+(\tilde{X}, a_{t:t+h}^o) - \hat{Q}_{ac}^+(X, a_{t:t+h}^o) = c_2 > 0 \quad (245)$$

Therefore,

$$\begin{aligned} \hat{V}_{ac}^+(X) &= \max(\hat{Q}_{ac}^+(X, a_{t:t+h}^o), \hat{Q}_{ac}^+(X, a_{t:t+h}^\Delta)) \\ &< \max(\hat{Q}_{ac}^+(\tilde{X}, a_{t:t+h}^o), \hat{Q}_{ac}^+(\tilde{X}, a_{t:t+h}^\Delta)) \\ &= \hat{V}_{ac}^+(\tilde{X}). \end{aligned} \quad (246)$$

Now, we can compare the values for the action chunks for X and \tilde{X} :

$$\hat{Q}_{ac}^+(X, a_{t:t+h}^\Delta) - \hat{Q}_{ac}^+(X, a_{t:t+h}^o) = c_3 \frac{\gamma - \gamma^h}{2(1 - \gamma)} + \gamma^h (\hat{V}_{ac}^+(\tilde{X}) - \hat{V}_{ac}^+(X)) > 0, \quad (247)$$

$$\hat{Q}_{ac}^+(\tilde{X}, a_{t:t+h}^\Delta) - \hat{Q}_{ac}^+(\tilde{X}, a_{t:t+h}^o) = c_4 \frac{\gamma - \gamma^h}{2(1 - \gamma)} + \gamma^h (\hat{V}_{ac}^+(\tilde{X}) - \hat{V}_{ac}^+(X)) > 0, \quad (248)$$

since $c_3, c_4 > 0$ and $h > 1, 0 < \gamma < 1$ (and thus $\frac{\gamma - \gamma^h}{1 - \gamma} > 0$).

This concludes that $\pi_{ac}^+(X) = \pi_{ac}^+(\tilde{X}) = a_{t:t+h}^\Delta = (2, 2, \dots, 2, 0)$ and thus

$$\hat{V}_{ac}^+(\tilde{X}) = \frac{1 - \gamma + (\gamma - \gamma^h)(1 + c_4)}{2(1 - \gamma^h)(1 - \gamma)}, \quad (249)$$

2916 and

$$\begin{aligned} \hat{V}_{\text{ac}}^+(X) &= \frac{1}{2} \left[(1 - c_2) + (1 + c_3) \frac{\gamma - \gamma^h}{1 - \gamma} \right] + \frac{\gamma^h}{1 - \gamma^h} \hat{V}_{\text{ac}}^+(\tilde{X}) \\ &= \frac{1}{2(1 - \gamma)} - \frac{\vartheta_h^G}{1 - \gamma^h} + \frac{\tilde{\Delta}}{2}. \end{aligned} \quad (250)$$

2922 We can now compute the remaining values as follows:

$$V^*(X) = \frac{1}{2(1 - \gamma)}, \quad (251)$$

$$Q^*(X, a = 2) = \frac{(1 - c_2)(1 - \gamma) + \gamma}{2(1 - \gamma)}, \quad (252)$$

$$Q^*(X, a = 2) = \frac{1 - c_2}{2(1 - \gamma)}. \quad (253)$$

2931 Substituting the value of c_2 yields

$$V^*(X) - V^*(X) = \frac{\vartheta_h^L}{1 - \gamma} + \frac{(1 + \gamma^h)\vartheta_h^G}{(1 - \gamma)(1 - \gamma^h)} - \frac{\tilde{\Delta}}{2(1 - \gamma)}. \quad (254)$$

2936 2. Case $\vartheta_h^L < \vartheta_h^G$:

2937 Set

$$\Delta = 2 \left[\frac{\vartheta_h^L + \vartheta_h^G}{1 - \gamma^h} \right] \quad (255)$$

$$c_2 = 2 \left[\frac{\vartheta_h^L + \vartheta_h^G}{1 - \gamma^h} \right] - \tilde{\Delta} > 0, \quad (256)$$

$$c_3 = c_4 = \frac{2(1 - \gamma)\vartheta_h^L}{\gamma - \gamma^h} > 0 \quad (257)$$

2946 where again $\tilde{\Delta}$ is any value that satisfies $0 < \tilde{\Delta} \leq \Delta$.2948 From the definitions above and the value range of ϑ_h^G ($\vartheta_h^G \leq \frac{1 - \gamma^h}{4}$), it is clear that

$$c_3 = c_4 < c_2 \leq \frac{4\vartheta_h^G}{1 - \gamma^h} \leq \frac{2(1 - \gamma)}{\gamma - \gamma^h} \leq 1/2. \quad (258)$$

2952 Next, we check the data distribution \mathcal{D}^Δ satisfies both optimality variability conditions. With the same argument as the previous case, we can quickly conclude that the global optimality condition is satisfied. We just need to show the remaining local optimality condition. We repeat the procedure from the previous case.2957 For $s_t = X$, the local optimality gap is

$$c_3 \frac{\gamma - \gamma^h}{2(1 - \gamma^h)} = \vartheta_h^L. \quad (259)$$

2961 For $s_t = \tilde{X}$ the local optimality gap is the same because $c_4 = c_3$:

$$c_4 \frac{\gamma - \gamma^h}{2(1 - \gamma^h)} = \vartheta_h^L. \quad (260)$$

2965 This concludes that the second (local) optimality condition is also satisfied for the second case.

2967 Now, we can follow the same procedure as the previous case to show that $\hat{Q}_{\text{ac}}^+(X, a_{t:t+h}^\Delta) - \hat{Q}_{\text{ac}}^+(X, a_{t:t+h}^o) > 0$ and $\hat{Q}_{\text{ac}}^+(\tilde{X}, a_{t:t+h}^\Delta) - \hat{Q}_{\text{ac}}^+(\tilde{X}, a_{t:t+h}^o) > 0$.2969 This concludes that $\pi_{\text{ac}}^+(X) = \pi_{\text{ac}}^+(\tilde{X}) = a_{t:t+h}^\Delta = (2, 2, \dots, 2, 0)$, and thus

2970

2971

$$\hat{V}_{\text{ac}}^+(\tilde{X}) = \frac{1}{2} \left[\frac{1 - \gamma + (1 + c_3)(\gamma - \gamma^h)}{(1 - \gamma)(1 - \gamma^h)} \right], \quad (261)$$

2974
and

$$\begin{aligned} \hat{V}_{\text{ac}}^+(X) &= \frac{1}{2} \left[(1 - c_2) + (1 + c_3) \frac{\gamma - \gamma^h}{1 - \gamma} \right] + \frac{\gamma^h}{1 - \gamma^h} \hat{V}_{\text{ac}}^+(\tilde{X}) \\ &= \frac{1}{2(1 - \gamma)} - \frac{\vartheta_h^G}{1 - \gamma^h} + \frac{\tilde{\Delta}}{2}. \end{aligned} \quad (262)$$

2980
Repeating the same procedure as the previous case, we obtain

$$V^*(X) - Q^*(X, a = 2) = \frac{\vartheta_h^L + \vartheta_h^G}{1 - \gamma^h} - \tilde{\Delta}, \quad (263)$$

2985
resulting in an optimality of

$$V^*(X) - V^*(X) = \frac{\vartheta_h^L + \vartheta_h^G}{(1 - \gamma)(1 - \gamma^h)} - \frac{\tilde{\Delta}}{1 - \gamma}. \quad (264)$$

2989
3. Sub-optimality of V_{ac}^+ :2991
Finally, we can use a pretty crude upper-bound on the actual value of the action chunking policy π_{ac}^+
2992 (reparameterizing $\tilde{\delta}_2 = 1 - (1 - \delta_2)^h$):
2993

$$V_{\text{ac}}^+(X) \leq (1 - \tilde{\delta}_2) \left[(1 - c_2)/2 + \frac{\delta(\gamma - \gamma^h)}{2(1 - \gamma)} + \gamma^h V_{\text{ac}}^+(X) \right] + \frac{\tilde{\delta}_2}{1 - \gamma} \quad (265)$$

$$\leq \frac{1 - \tilde{\delta}_2}{2(1 - \gamma^h)(1 - \gamma)} [1 - \gamma + \delta(\gamma - \gamma^h)] + \frac{\tilde{\delta}_2}{1 - \gamma}. \quad (266)$$

2999
Set $\delta = 1/2$, we have

$$V_{\text{ac}}^+(X) \leq \frac{1 - \tilde{\delta}_2}{2(1 - \gamma^h)(1 - \gamma)} [1 - \gamma/2 - \gamma^h/2] + \frac{\tilde{\delta}_2}{1 - \gamma}. \quad (267)$$

3004
We set

$$\delta_2 = 1 - \left[1 - \frac{\gamma - \gamma^h - 4c(1 - \gamma^h)}{2 - 3\gamma^h + \gamma} \right]^{1/h}, \quad (268)$$

3008
which results in

$$\tilde{\delta}_2 = \frac{\gamma - \gamma^h - 4c(1 - \gamma^h)}{2 - 3\gamma^h + \gamma}. \quad (269)$$

3013
It is clear that $0 < \delta_2 < 1$ because $c < \frac{\gamma - \gamma^h}{4(1 - \gamma^h)}$ and $\frac{\gamma - \gamma^h}{2 - 3\gamma^h + \gamma} < 1$.3014
Substituting $\tilde{\delta}_2$ in the bound of $V_{\text{ac}}^+(X)$ above, we obtain

$$V^*(X) - V_{\text{ac}}^+(X) \geq \frac{c}{1 - \gamma}. \quad (270)$$

3018
3019
3020
3021
□3022
3023
Proof of Theorem F.4. Let

$$\Delta = \vartheta_h^L + \frac{\vartheta_h^G}{1 - \gamma^h} + \frac{\gamma^h \min(\vartheta_h^G, \vartheta_h^L)}{1 - \gamma^h}. \quad (271)$$

3024 Consider the 5-state, 3-action MDP constructed in Lemma G.9 and Lemma G.10 and a data distribution
 3025 consisting of a mixture of three data distributions \mathcal{D}^* , \mathcal{D}^\diamond (from Lemma G.9) and \mathcal{D}^Δ (from
 3026 Lemma G.10):
 3027

$$P_{\mathcal{D}} = \alpha(1 - \varsigma)P_{\mathcal{D}^*} + \varsigma P_{\mathcal{D}^\diamond} + (1 - \alpha)P_{\mathcal{D}^\Delta}. \quad (272)$$

3029 We set α to be any value between 0 and 1 (non-inclusive) and set ς as any positive value such that
 3030

$$\varsigma < \frac{(\gamma - \gamma^h) - 2\vartheta_h^G(1 - \gamma) + 2\tilde{\Delta}(1 - \gamma)(1 - \gamma^h)}{(\gamma - \gamma^h) - 2\vartheta_h^G(1 - \gamma)}, \quad (273)$$

3033 where $\tilde{\Delta} = \sigma(1 - \gamma) < \min(\vartheta_h^L, \vartheta_h^G) < \min(\Delta, \frac{2\vartheta_h^G}{1 - \gamma^h})$ (satisfying the condition for $\tilde{\Delta}$ in
 3034 Lemma G.10).
 3035

3036 The numerator and the denominator are both positive:
 3037

$$(\gamma - \gamma^h) - 2\vartheta_h^G(1 - \gamma) + 2\tilde{\Delta}(1 - \gamma)(1 - \gamma^h) > (\gamma - \gamma^h) - 2\vartheta_h^G(1 - \gamma) > 0, \quad (274)$$

3039 meaning such ς always exists.
 3040

3041 Substituting the inequality to the result of Lemma G.9 results in
 3042

$$\frac{1 - \gamma + \varsigma(\gamma - \gamma^h)}{2(1 - \gamma^h)(1 - \gamma)} - \frac{\varsigma\vartheta_h^G}{1 - \gamma^h} < \frac{1}{2(1 - \gamma)} - \frac{\vartheta_h^G}{1 - \gamma^h} + \tilde{\Delta}, \quad (275)$$

3045 which shows that π_{ac}^+ will always prefer $a_{t:t+h}^\Delta$ over action chunks in \mathcal{D}^* and \mathcal{D}^\diamond .
 3046

3047 This means that the value \hat{V}_{ac}^+ and the action chunking policy π_{ac}^+ we learn from \mathcal{D} coincides with
 3048 these of \mathcal{D}^Δ , allowing us to directly use the results of Lemma G.10.
 3049

3050 Thus, we can conclude that
 3051

$$V^*(s_t) - V_{ac}^+(s_t) \geq \frac{c}{1 - \gamma}, \quad (276)$$

3052 and
 3053

$$V^*(X) - V^*(X) = \frac{\Delta - \tilde{\Delta}}{1 - \gamma} = \frac{\vartheta_h^L}{1 - \gamma} + \frac{\vartheta_h^G}{(1 - \gamma)(1 - \gamma^h)} + \frac{\gamma^h \min(\vartheta_h^L, \vartheta_h^G)}{(1 - \gamma)(1 - \gamma^h)} - \sigma, \quad (277)$$

3054 as desired.
 3055 \square
 3056

3060
 3061
 3062
 3063
 3064
 3065
 3066
 3067
 3068
 3069
 3070
 3071
 3072
 3073
 3074
 3075
 3076
 3077

3078 G.12 PROOF OF PROPOSITION F.6
3079

3080 **Proposition F.6** (Deterministic Dynamics are Weakly Open-loop Consistent). *If a transition dynamics*
 3081 *\mathcal{M} is ε -deterministic, then any data \mathcal{D} collected from \mathcal{M} is weakly ε_h -open-loop consistent with*
 3082 *respect to \mathcal{M} for any $h \in \mathbb{N}^+$ as long as $\varepsilon_h \geq 3(1 - (1 - \varepsilon)^{h-1})$.*

3083
 3084 *Proof.* Since T is ε -deterministic, it can be represented as $T(\cdot | s, a) = (1 - \varepsilon)\delta_{f(s, a)} + \varepsilon\tilde{T}(\cdot | s, a)$
 3085 for some $f : \mathcal{S} \times \mathcal{A} \rightarrow \mathcal{S}$ and $\tilde{T} : \mathcal{S} \times \mathcal{A} \rightarrow \Delta_{\mathcal{S}}$. Let $f(s, a_1, \dots, a_h) = f(\dots f(f(s, a_1), a_2) \dots a_h)$
 3086
 3087 Let $I \in \{0, 1\}$ a binary indicator variable that is 1 if and only if

$$3088 s_{t+k+1} = f(s_{t+k}, a_{t+k}), \forall k \in \{0, 1, 2, \dots, h-1\} \quad (278)$$

3089 Intuitively $I = 1$ when the trajectory is generated deterministically until but not including the last
 3090 state s_h in the trajectory chunk.
 3091

3092 From the fact that T is ε -deterministic, we know that

$$3093 P_{\mathcal{D}}(I_h = 1) \geq (1 - \varepsilon)^{h-1} \quad (279)$$

3094 We also have
 3095

$$3096 P_{\mathcal{D}}(a_{t:t+h} | s_t) = P_{\mathcal{D}}(I_h = 1)P_{\mathcal{D}}(a_{t:t+h} | s_t, I_h = 1) + P_{\mathcal{D}}(I_h = 0)P_{\mathcal{D}}(a_{t:t+h} | s_t, I_h = 0) \quad (280)$$

3098 Then we have
 3099

$$3100 D_{\text{TV}}(P_{\mathcal{D}}(a_{t:t+h} | s_t) \| P_{\mathcal{D}}(a_{t:t+h} | s_t, I_h = 1)) \leq (1 - (1 - \varepsilon)^{h-1}) \quad (281)$$

3101 If we transform each distribution of $a_{t:t+h}$ deterministically by $f(s_t, \cdot)$, by data processing inequality
 3102 (DPI; Lemma G.4), we have

$$3103 D_{\text{TV}}(\mathbb{E}_{a_{t:t+h} \sim P_{\mathcal{D}}(\cdot | s_t)} [\delta_{f(s_t, a_{t:t+h})}] \| \mathbb{E}_{a_{t:t+h} \sim P_{\mathcal{D}}(\cdot | s_t, I_h = 1)} [\delta_{f(s_t, a_{t:t+h})}]) \leq (1 - (1 - \varepsilon)^{h-1}) \quad (282)$$

3106 Similarly, we have
 3107

$$3108 D_{\text{TV}}(P_{\mathcal{D}}(a_{t:t+h+1} | s_t) \| P_{\mathcal{D}}(a_{t:t+h+1} | s_t, I_{h+1} = 1)) \leq (1 - (1 - \varepsilon)^h) \quad (283)$$

3109 which can be also deterministically transformed by taking $a_{t:t+h+1} \mapsto (f(s_t, \cdot), a_{t+h})$ (again with
 3110 DPI, Lemma G.4) to obtain

$$3111 D_{\text{TV}}\left(\mathbb{E}_{a_{t:t+h} \sim P_{\mathcal{D}}(\cdot | s_t)} [\pi_{\mathcal{D}}^{\circ}(a_{t+h} | s_t, a_{t:t+h}) \mathbb{I}_{f(s_t, a_{t:t+h})}] \| \right. \\ 3112 \left. \mathbb{E}_{a_{t:t+h} \sim P_{\mathcal{D}}(\cdot | s_t, I_{h+1} = 1)} [\pi_{\mathcal{D}}^{\circ}(a_{t+h} | s_t, a_{t:t+h}, I_{h+1} = 1) \mathbb{I}_{f(s_t, a_{t:t+h})}] \right) \leq (1 - (1 - \varepsilon)^h) \quad (284)$$

3115 Now, if we analyze the distribution of s_{t+h} subject to the open-loop execution of the action sequence
 3116 from $P_{\mathcal{D}}(\cdot | s_t)$ and break it up into the deterministic and the non-deterministic case, we get
 3117

$$3118 \mathbb{E}_{a_{t:t+h} \sim P_{\mathcal{D}}(\cdot | s_t)} [T_{a_{t:t+h}}(\cdot | s_t)] = P_T(I = 1) \mathbb{E}_{a_{t:t+h} \sim P_{\mathcal{D}}(\cdot | s_t)} [\delta_{f(s_t, a_{t:t+h})}] + \\ 3119 P_T(I = 0) \mathbb{E}_{a_{t:t+h} \sim P_{\mathcal{D}}(\cdot | s_t)} [T_{a_{t:t+h}}(\cdot | s_t, I_h = 0)] \quad (285)$$

3121 Note that $P_T(I = 1)$ denotes the probability that an open-loop executed trajectory using $a_{t:t+h} \sim$
 3122 $P_{\mathcal{D}}(\cdot | s_t)$ is deterministic. This is different from $P_{\mathcal{D}}(I_h = 1)$ because the latter is based on
 3123 $P_{\mathcal{D}}(s_{t:t+h+1}, a_{t:t+h})$ whereas $P_T(I_h = 1)$ is based on the open-loop trajectory distribution: $P_{\mathcal{D}}(\cdot |$
 3124 $s_t) \prod_{k=0}^{h-1} T(s_{t+k} | s_t, a_{t:t+k})$. They both admit the same lower bound of $2(1 - (1 - \varepsilon)^{h-1})$.

3125 Therefore,

$$3126 D_{\text{TV}}(\mathbb{E}_{a_{t:t+h} \sim P_{\mathcal{D}}(\cdot | s_t)} [T_{a_{t:t+h}}(\cdot | s_t)] \| \mathbb{E}_{a_{t:t+h} \sim P_{\mathcal{D}}(\cdot | s_t)} [\delta_{f(s_t, a_{t:t+h})}]) \leq (1 - (1 - \varepsilon)^{h-1}) \quad (286)$$

3129 Similarly for the state-action case, we can multiply both side by the same conditional distribution
 3130 $\pi_{\mathcal{D}}^{\circ}(a_{t+h} | s_t, a_{t:t+h})$ which preserves the TV bound. For the left-hand side, we have
 3131

$$P_{\mathcal{D}}^{\circ}(s_{t+h}, a_{t+h} | s_t) = \mathbb{E}_{a_{t:t+h} \sim P_{\mathcal{D}}(\cdot | s_t)} [\pi_{\mathcal{D}}^{\circ}(a_{t+h} | s_t, a_{t:t+h}) T_{a_{t:t+h}}(s_{t+h} | s_t)] \quad (287)$$

3132 Therefore, we get

$$\begin{aligned} D_{\text{TV}}(P_{\mathcal{D}}^{\circ}(s_{t+h}, a_{t+h} | s_t) \| \mathbb{E}_{a_{t:t+h} \sim P_{\mathcal{D}}(\cdot | s_t)} [\pi_{\mathcal{D}}^{\circ}(a_{t+h} | s_t, a_{t:t+h}) \mathbb{I}_{f(s_t, a_{t:t+h})}]) \\ \leq (1 - (1 - \varepsilon)^{h-1}) \end{aligned} \quad (288)$$

3136 We also have

$$P_{\mathcal{D}}(s_{t+h} | s_t) = (1 - \varepsilon)^{h-1} P_{\mathcal{D}}(s_{t+h} | s_t, I = 1) + (1 - (1 - \varepsilon)^{h-1}) P_{\mathcal{D}}(s_{t+h} | s_t, I_h = 0) \quad (289)$$

3137 Similarly, we have

$$\begin{aligned} D_{\text{TV}}(P_{\mathcal{D}}(s_{t+h} | s_t) \| P_{\mathcal{D}}(s_{t+h} | s_t, I_h = 1)) \\ = D_{\text{TV}}(P_{\mathcal{D}}(s_{t+h} | s_t) \| \mathbb{E}_{a_{t:t+h} \sim P_{\mathcal{D}}(\cdot | s_t, I_h = 1)} [\delta_{f(s_t, a_{t:t+h})}]) \leq (1 - (1 - \varepsilon)^{h-1}) \end{aligned} \quad (290)$$

3138 For state-action, we can also get

$$\begin{aligned} P_{\mathcal{D}}(s_{t+h}, a_{t+h} | s_t) = (1 - \varepsilon)^h P_{\mathcal{D}}(s_{t+h}, a_{t+h} | s_t, I_{h+1} = 1) \\ + (1 - (1 - \varepsilon)^h) P_{\mathcal{D}}(s_{t+h}, a_{t+h} | s_t, I_{h+1} = 0) \end{aligned} \quad (291)$$

3139 which can be turned into the TV distance bound:

$$\begin{aligned} D_{\text{TV}}(P_{\mathcal{D}}(s_{t+h}, a_{t+h} | s_t) \| P_{\mathcal{D}}(s_{t+h}, a_{t+h} | s_t, I_{h+1} = 1)) \\ = D_{\text{TV}}(P_{\mathcal{D}}(s_{t+h}, a_{t+h} | s_t) \| \mathbb{E}_{a_{t:t+h} \sim P_{\mathcal{D}}(\cdot | s_t, I_{h+1} = 1)} [\pi_{\mathcal{D}}^{\circ}(a_{t+h} | s_t, a_{t:t+h}, I_{h+1} = 1) \mathbb{I}_{f(s_t, a_{t:t+h})}]) \\ \leq (1 - (1 - \varepsilon)^h) \end{aligned} \quad (292)$$

3140 Connecting all three total variation inequality (Equations (282), (286) and (290)) together, we get

$$D_{\text{TV}}(P_{\mathcal{D}}(s_{t+h} | s_t) \| \mathbb{E}_{a_{t:t+h} \sim P_{\mathcal{D}}(\cdot | s_t)} [T_{a_{t:t+h}}(\cdot | s_t)]) \leq 3(1 - (1 - \varepsilon)^{h-1}) \leq \varepsilon_h \quad (293)$$

3141 Connecting all three total variable inequality for state-action (Equations (284), (287) and (292)) together, we get

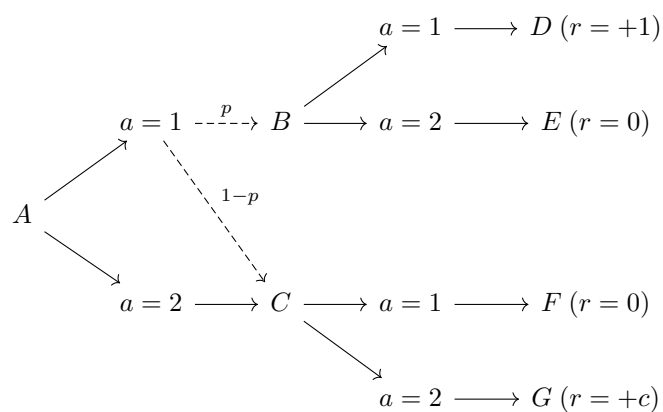
$$\begin{aligned} D_{\text{TV}}(P_{\mathcal{D}}^{\circ}(s_{t+h-1}, a_{t+h-1} | s_t) \| P_{\mathcal{D}}(s_{t+h}, a_{t+h} | s_t)) \leq 3 - 2(1 - \varepsilon)^{h-1} - (1 - \varepsilon)^{h-2} \\ \leq 3(1 - (1 - \varepsilon)^{h-1}) \\ \leq \varepsilon_h \end{aligned} \quad (294)$$

3142 Therefore, \mathcal{D} is ε_h -open-loop consistent as desired. \square

3143 H A PATHOLOGICAL FAILURE OF ACTION CHUNKING POLICIES WITHOUT THE 3144 STRONG OPEN-LOOP CONSISTENCY ASSUMPTION

3145 In this section, we show an example where the optimal action chunking policy defined in Equation (17)
3146 can be highly suboptimal in the absence of the strong open-loop consistency condition.

3147 We define an MDP as follows. Let $\mathcal{S} = \{A, B, C, D, E, F, G\}$ and $\mathcal{A} = \{1, 2\}$. Define the transition
3148 dynamics and reward function as shown in the diagram below:



3186 where $p, c \in (0, 1)$ are real numbers and dotted lines denote stochastic transitions. For simplicity,
 3187 assume that the MDP has a length-2 finite horizon with $\gamma = 1$, and the reward function depends only
 3188 on states $r(A) = r(B) = r(C) = r(E) = r(F) = 0$, $r(D) = 1$, and $r(G) = c$. Assume that the
 3189 dataset is collected by a policy $\pi_{\mathcal{D}}$ defined as $\pi_{\mathcal{D}}(A) = 1$ (with probability 0.5) or 2 (with probability
 3190 0.5), $\pi_{\mathcal{D}}(B) = 1$ (with probability 1), and $\pi_{\mathcal{D}}(C) = 2$ (with probability 1).

3191 Then, we have the following:
 3192

$$P_{\mathcal{D}}(A, (1, 1)) = D, R(A, (1, 1)) = 1, \quad (295)$$

$$P_{\mathcal{D}}(A, (1, 2)) = G, R(A, (1, 2)) = c, \quad (296)$$

$$P_{\mathcal{D}}(A, (2, 2)) = G, R(A, (2, 2)) = c, \quad (297)$$

3193 where we denote action chunks as a tuple and slightly abuse notation to denote deterministic outputs
 3194 of $P_{\mathcal{D}}(\cdot | s_0, a_{0:2})$ (e.g., $P_{\mathcal{D}}(A, (1, 1)) = D$ indicates that all length-2 trajectories in \mathcal{D} from state A
 3195 with $a_0 = a_1 = 1$ have $s_2 = D$ with probability 1). From this, we can compute \hat{Q}_{ac}^+ as follows:
 3196

$$\hat{Q}_{\text{ac}}^+(A, (1, 1)) = 1, \quad (298)$$

$$\hat{Q}_{\text{ac}}^+(A, (1, 2)) = c, \quad (299)$$

$$\hat{Q}_{\text{ac}}^+(A, (2, 2)) = c. \quad (300)$$

3200 Then, assuming the missing data has a Q-value of 0 (i.e., $\hat{Q}_{\text{ac}}^+(A, (2, 1)) = 0$), the optimal action
 3201 chunking policy is defined as $\hat{\pi}_{\text{ac}}^+(A) = (1, 1)$ (Equation (17)).
 3202

3203 The true value of this action chunking policy is p . However, if p is small enough and c is large enough,
 3204 the optimal strategy in this MDP is to always choose $(a_0, a_1) = (2, 2)$, in which case the agent
 3205 receives a constant return of c . The suboptimality in this example is therefore $c - p$, which can be
 3206 made arbitrarily close to 1 (the maximum possible regret in any finite, length-2 sparse-reward MDP
 3207 with a terminal reward bounded by $[0, 1]$). This shows a pathological failure of an action chunking
 3208 policy without the strong open-loop consistency assumption.
 3209

I ADDITIONAL RELATED WORK ON HIERARCHICAL REINFORCEMENT LEARNING

3210 Hierarchical reinforcement learning methods (Dayan & Hinton, 1992; Dietterich, 2000; Peng et al.,
 3211 2017; Riedmiller et al., 2018; Shankar & Gupta, 2020; Pertsch et al., 2021; Gehring et al., 2021; Xie
 3212 et al., 2021) solve tasks by typically leveraging a bi-level structure: a set of low-level/skill policies that
 3213 directly interact with the environment and a high-level policy that selects among low-level policies.
 3214 The low-level policies can also be learned via online RL (Kulkarni et al., 2016; Vezhnevets et al.,
 3215 2016; 2017; Nachum et al., 2018) or offline pre-training on a prior dataset (Paraschos et al., 2013;
 3216 Merel et al., 2018; Ajay et al., 2021; Pertsch et al., 2021; Touati et al., 2022; Nasiriany et al., 2022;
 3217 Hu et al., 2023; Frans et al., 2024; Chen et al., 2024; Park et al., 2024b). In the options framework,
 3218 these low-level policies are often additionally associated with initiation and termination conditions
 3219 that specify when and for how long these actions can be used (Sutton et al., 1999; Menache et al.,
 3220 2002; Chentanez et al., 2004; Şimşek & Barto, 2007; Konidaris, 2011; Daniel et al., 2016; Srinivas
 3221 et al., 2016; Fox et al., 2017; Bacon et al., 2017; Bagaria & Konidaris, 2019; Bagaria et al., 2024;
 3222 de Mello Koch et al., 2025). A long-lasting challenge in HRL is optimization stability because the
 3223 high-level policy needs to optimize for an objective that is shaped by the constantly changing low-
 3224 level policies (Nachum et al., 2018). Prior work (Ajay et al., 2021; Pertsch et al., 2021; Wilcoxson
 3225 et al., 2024) avoided this by first pre-train low-level policies and then keep them frozen during the
 3226 optimization of the high-level policy. Macro-actions (McGovern & Sutton, 1998; Durugkar et al.,
 3227 2016), or action chunking (Zhao et al., 2023) is another form of temporally extended action, a special
 3228 case of the low-level policies often considered in HRL, options literature, where a short horizon of
 3229 actions are predicted all at once and executed in open loop. Such approach collapses the bi-level
 3230 structure, conveniently side stepping optimization instability, and when combined with Q-learning,
 3231 has shown great empirical successes in offline-to-online RL setting (Seo et al., 2024; Li et al., 2025b).
 3232 Action chunking policies need to predict multiple actions open-loop, which can be difficult to learn
 3233 and sacrifice reactivity. Our approach regains policy reactivity by predicting and executing only a
 3234 partial action chunk, while still learning with the fully chunked critic for TD-backup. This design
 3235

3240 preserves the value propagation benefits of chunked critic without relying on fully open-loop action
 3241 chunking policies, allowing our approach to work well on a wider range of tasks.
 3242

3243 J INTUITION BEHIND OPTIMALITY VARIABILITY

3244 In this section, we provide more intuition on the definition of optimality variability. With Definition 4.10, if we pick X to be the current state and the current action (i.e., s_t, a_t), a bounded optimality
 3245 variability subject to such conditioning means that as long as we observe the initial action (e.g., picking up the cube), the optimality of the outcome after h -steps does not vary too much (e.g., does not
 3246 misdrop the object that fails the task immediately). It turns out that if (1) the data distribution is a
 3247 mixture of a bunch of data sources where the optimality variability conditioned on the *current actions*
 3248 is bounded within each data source, and additionally (2) the optimality variability conditioned on the
 3249 *current action chunks* is bounded globally across mixture, we can form a much stronger bound on the
 3250 optimality of π^* . It is worth noting that the second optimality variability condition is *much weaker*
 3251 than the first one because it is conditioned on the event where we observe the state s_t and the entire
 3252 action chunk $a_{t:t+h}$ (rather than the first action a_t). For example, for data mixture where each pair of
 3253 data distributions has non-overlapping support on the action chunks, the second condition is trivially
 3254 implied by the first condition.
 3255

3256
 3257
 3258
 3259
 3260
 3261
 3262
 3263
 3264
 3265
 3266
 3267
 3268
 3269
 3270
 3271
 3272
 3273
 3274
 3275
 3276
 3277
 3278
 3279
 3280
 3281
 3282
 3283
 3284
 3285
 3286
 3287
 3288
 3289
 3290
 3291
 3292
 3293